# Functional characterization of a seven-WD40 repeat protein Rak1 in *Ustilago maydis*

**Dissertation**

zur
Erlangung des Doktorgrades
der Naturwissenschaften
(Dr. rer. nat.)

dem Fachbereich Biologie
der Philipps-Universität Marburg
vorgelegt von

**Lei Wang**
aus Shandong/China

Marburg/Lahn 2011

# Functional characterization of a seven-WD40 repeat protein Rak1 in *Ustilago maydis*

**Dissertation**

zur
Erlangung des Doktorgrades
der Naturwissenschaften
(Dr. rer. nat.)

dem Fachbereich Biologie
der Philipps-Universität Marburg
vorgelegt von

**Lei Wang**
aus Shandong/China

Marburg/Lahn 2011

Die Untersuchungen zur vorliegenden Arbeit wurden unter der Betreuung von Frau Prof. Dr. Regine Kahmann von Oktober 2007 bis Dezember 2010 am Max-Planck-Institut für Terrestrische Mikrobiologie in der Abteilung für Organismische Interaktionen durchgeführt.

vom Fachbereich Biologie
der Philipps-Universität Marburg als Dissertation
angenommen am: 19.05.2011
Erstgutachter: Frau Prof. Dr. Regine Kahmann
Zweitgutachter: Herr Prof. Michael Bölker
Tag der mündlichen Prüfung am: 14.06.2011

Wang, L., Berndt, P., Xia, X., Kahmann, R. Rak1, a seven-WD40 repeat protein related to human RACK1, regulates mating and pathogenicity in *Ustilago maydis*. (In preparation)

## Declaration

I hereby declare that the dissertation entitled "**Functional characterization of a seven-WD40 repeat protein Rak1 in *Ustilago maydis***" submitted to the Department of Biology, Philipps-Universität Marburg, is the original and independent work carried out by me under the guidance of the PhD committee, and the dissertation is not formed previously on the basis of any award of Degree, Diploma or other similar titles.

(Ort, Datum) Lei Wang

## Summary

In the phytopathogenic smut fungus *Ustilago maydis* cell fusion of compatible haploid cells is controlled by a pheromone/receptor system. The pheromone signal is transmitted via a conserved MAP kinase module that activates Prf1, an essential regulator of sexual and pathogenic development. To find additional components in MAP kinase signaling, *U. maydis* Rak1, a seven-WD40 repeat motif protein that is orthologous to mammalian RACK1 was studied. *rak1* gene was constitutively expressed and Rak1 protein localized in the cytoplasm as well as in the membrane fraction. In *U. maydis* Rak1 was found to affect cell wall synthesis and cell growth and could partially complement the growth phenotype of *Saccharomyces cerevisiae asc1* mutant at elevated temperature. Deletion of *rak1* strongly attenuated conjugation tube formation in haploid cells resulting in poor mating ability. This defect could be traced back to reduced expression of the pheromone and pheromone-receptor genes. With the genetic activation of the MAP kinase module, the formation of conjugation tubes of FB1Δrak1 could be rescued. Furthermore, the defect of FB1Δrak1 in conjugation tube formation could be restored by the constitutive expression of the pheromone receptor gene *pra1* or the pheromone response transcription factor *prf1* upon pheromone stimulation. In solopathogenic strain the deletion of *rak1* led to attenuated filamentation and pathogenicity, which could be rescued by the constitutive expression of an active *bE/bW* heterodimer. This analysis made it likely that *rak1* controls the expression of *prf1*.

By microarray analysis, 201 genes were identified to be differentially regulated in the *rak1* deletion strain. 163 up-regulated genes showed a significant enrichment in the functional categories like metabolism, energy, virulence and stress and toxin resistance. 38 down-regulated genes showed a significant enrichment in lipid metabolism, fermentation and a MAPK signaling-dependent pathway. Among the down-regulated genes in FB1Δrak1, *rop1*, a direct positive transcriptional regulator of *prf1*, was detected. The constitutive expression of *rop1* in FB1Δrak1 could induce the expression of *mfa1* as well as conjugation tube formation in response to pheromone stimulation. Collectively, *rak1* functions as a novel regulator of *rop1* and consequently of *prf1* gene expression during mating and pathogenic development.

## Zusammenfassung

In dem pflanzenpathogenen Brandpilz *Ustilago maydis* wird die Paarungsreaktion zweier kompatibler Zellen durch ein Pheromon/Rezeptor System koordiniert. Der Pheromon Stimulus wird dabei über ein konserviertes MAP Kinase Modul übermittelt was zur Aktivierung von Prf1 führt, einem essentiellen Regulator für sexuelle und pathogene Entwicklung. Um zusätzliche Komponenten des MAP kinase Signalwegs zu finden, wurde *U. maydis* Rak1, ein sieben-WD40-Domänen Protein, ein Ortholog von RACK1 in Säugerzellen, untersucht. In *U. maydis* wird *rak1* konstitutiv exprimiert und lokalisiert im Zytoplasma und in der Membran. Rak1 spielt eine Rolle in der Aufrechterhaltung der Zellwandintegrität und in der Regulation des Zellwachstums und konnte den bei erhöhten Temperaturen auftretenden Wachstumsphänotyp von *Saccharomyces cerevisiae asc1* Mutanten komplementieren. Die Deletion von rak1 führte zu einer deutlichen Reduktion der Bildung von Konjugationshyphen und resultierte damit in dramatisch reduzierter Paarungseffizienz. Dieser Effekt konnte auf die reduzierte Expression des Pheromon- und des Pheromonrezeptor-Gens zurückgeführt werden. Durch die genetische Aktivierung des MAP kinase Moduls konnte die Bildung von Konjugationshyphen in FB1Δrak1 wieder hergestellt werden. Weiterhin konnte die Konjugationshyphenbildung durch konstitutive Expression des Pheromonrezeptor Gens *pra1* oder des Pheromon aktivierten Transkriptionsfaktors *prf1* und gleichzeitiger Gabe von kompatiblem Pheromon wiederhergestellt werden. In solopathogenen Stämmen führte die Deletion von *rak1* zu abgeschwächter Filamentbildung sowie Pathogenität, was durch Expression des kompatiblen *bE/bW* Heterodimers komplementiert werden konnte. Diese Analyse erlaubte es *rak1* genetisch oberhalb von *prf1* zu platzieren.

Durch Mikroarray-Analyse konnten 201 Gene identifiziert werden, die in dem *rak1* Deletionsstamm differenziell reguliert sind. 163 induzierte Gene zeigten eine signifikante Anreicherung in den funktionellen Kategorien Metabolismus, Energie, Virulenz und Stress- bzw. Toxinresistenz. Die 38 reprimierten Gene zeigten eine signifikante Anreicherung im Lipidstoffwechsel, Fermentation und einem MAPK abhängigen Signalweg. Unter den reprimierten Genen in FB1Δrak1 wurde *rop1* gefunden, ein direkter positiver transkriptioneller Regulator von *prf1*. Die konstitutive Expression von *rop1* in FB1Δrak1 führte zur Induktion der Expression von *mfa1* und der Pheromon-abhängigen Konjugationshyphenbildung. Zusammenfassend wirkt Rak1

als neuartiger Regulator der *rop1* und dadurch *prf1* Genexpression während der Kreuzungsreaktion und der pathogenen Entwicklung.

# Abbreviations

| | |
|---|---|
| A | Adenine |
| aa | amino acid |
| Amp | Ampicillin |
| APS | Ammonium persulfate |
| Ara | Arabinose |
| AMP | Adenosine monophosphate |
| bp | base pair |
| C | Cytosine |
| cAMP | cyclic adenosine monophosphate |
| CBX | Carboxin |
| cDNA | complementary DNA |
| CM | Complete medium |
| C-terminal | Carboxyl-terminal |
| C-terminus | Carboxy-terminus |
| DAPI | 4',6-diamidino-2-phenylindole |
| DIC | Differential interference contrast |
| DMSO | Dimethyl sulphoxide |
| eGFP | Enhanced green fluorescence protein |
| f.c. | Final concentration |
| G | Guanine |
| GDP | Guanosine diphosphate |
| GTP | Guanosine triphosphate |
| HA | Hemagglutinin |
| IB | Immunoblotting |
| IP | Immunoprecipitation |
| kb | kilobase |
| kDa | kilodalton |
| LC-MS | Liquid chromatography-mass spectrometry |
| MAPK | Mitogen Activated Protein Kinase |
| MAPKK | MAPK kinase |
| MAPKKK | MAPKK kinase |
| mRNA | Messager RNA |
| MOPS | 3-(N-morpholino) propanesulfonic acid |
| Nat | Nourseothricin |
| $OD_{600}$ | Optical density at 600 nm |
| ORF | Open reading frame |
| PCR | Polymerase chain reaction |
| PD | Potato dextrose |
| PEG | Polyethylene glycol |
| PKA | Protein kinase A |
| RT-PCR | Real time PCR or reverse transcription PCR |
| RNA | Ribonucleic acid |
| rRNA | Ribosomal RNA |
| RA | Ras associated |
| SDS-PAGE | Sodium dodecyl sulfate polyacrylamide gel electrophoresis |
| T | Thymine |
| TCA | Trichloroacetic acid |
| SH3 | Src Homolog 3 |
| WD | tryptophan-aspartic acid |

# Contents

# 1 Introduction

## 1.1 *Ustilago maydis* as a model organism

*Ustilago maydis*, a facultative biotrophic basidiomycete fungus, has a very narrow host range and induces smut disease in maize and its progenitor teosinte. In recent years, *U. maydis* has emerged as one of the most important fungal models for the study of dimorphism, mating, signaling and plant-pathogen interactions (Bolker, 2001; Kamper *et al.*, 2006; Klosterman *et al.*, 2007; Martinez-Espinoza *et al.*, 2002; Perez-Martin *et al.*, 2006). A number of molecular tools and cell biological approaches have been developed to study all phases of its development (Basse and Steinberg, 2004; Kahmann and Kamper, 2004; Steinberg and Perez-Martin, 2008), such as high efficiency transformation, inducible promoters and GFP fusion protein technique and life imaging. In 2006, the genome sequence of *U. maydis* was published, with a genome size of 20.5 Mb corresponding to 23 chromosomes, the genome is highly compact and codes for approximately 6,900 proteins (Kamper *et al*., 2006). Currently, the MIPS *Ustilago maydis* database (MUMDB; http://mips.gsf.de/genre/proj/ustilago/) lists 6902 gene models. Custom-made Affymetrix arrays exist for the analysis of genome-wide transcriptome profiles (Eichhorn *et al*., 2006; Heimel *et al*., 2010a; Zahiri *et al*., 2010; Zarnack *et al*., 2008). More recently, the FLP-mediated recombination system has been adopted, which paves the way for analysis of multi-gene families with redundant functions (Khrunyk *et al*., 2010).

## 1.2 Life cycle of *U. maydis*

*U. maydis* cells exist both as a haploid form and as a filamentous dikaryotic form (Fig. 1). Haploid cells display yeast-like growth and divide by budding; they are saprophytic and can grow on non-living matter. Therefore, haploid cells can be propagated and genetically modified under laboratory conditions. After fusion of compatible haploid cells, dikaryotic filaments are formed. These are parasitic and able to infect maize plant. On leaf surface, the dikaryotic filament develops infection structure appressorium by sensing the presence of hydroxy-fatty acids and hydrophobicity (Mendoza-Mendoza *et al.*, 2009a). The appressorium could penetrate into host tissue. After penetration, *U. maydis* grows intracellular and the hyphae pass from one cell to another and are surrounded by the host plasma membrane and establish a biotrophic interaction. On

charcoal-containing plates the dikaryotic filaments can be recognized by their white fuzziness. This phenomenon can be used to test the mating ability of haploid cells. The most dramatic symptom in the *U. maydis*-maize interaction is the induction of large tumors. Such tumors can develop on all green parts of the plants, including stems, leaves, tassels and ears. Within the tumors, the fungal mycelium proliferates and branches. This is followed by karyogamy, hyphal filamentation and spore differentiation. Pathogenic development is completed by the release of large quantities of highly melanized, diploid telispores (Fig. 1). These spores are distributed by wind and rain and can germinate under favourable conditions. During germination, meiosis occurs and results in the production of haploid cells. Under laboratory conditions the completion of life cycle in young plants takes 3-4 weeks. *U. maydis* is completely dependent on its host maize to complete life cycle because it is incapable of ex planta sporulation (Banuett, 1995; Bolker, 2001; Brefort *et al.*, 2009; Klosterman *et al.*, 2007).

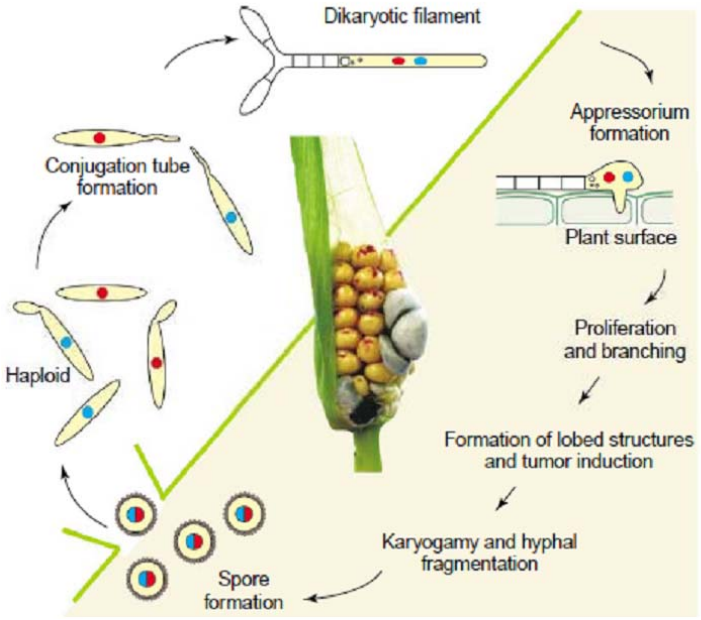


Figure 1 Life cycle of *U. maydis*. The processes indicated below the green line are absolutely dependent on maize plant. The blue and red nuclei indicate that haploid cells have compatible mating types. The central part of the figure shows tumor formation on maize and the lower part is the release of black teliospores. Under suitable conditions, the diploid spores germinate, undergo meiosis and produce haploid sporidia. Taken from Feldbrugge *et al.* (2004).

## 1.3 The *a* and *b* loci

In *U.* maydis, two loci (the incompatibility or mating type loci), *a* and *b*, control cell fusion of compatible mating type cells, filamentation and pathogenic development (Banuett, 1995; Wahl *et al.*, 2010).

### 1.3.1 The *a* locus

The *a* locus has two alleles, *a1* and *a2*, coding for lipopeptide pheromone precursor (*mfa*) and pheromone receptor (*pra*) genes, which control cell recognition and fusion of compatible mating type cells. The pheromone receptor Pra1/2 can recognize the pheromone secreted by the compatible mating type cells. The binding of pheromone to the pheromone receptor leads to a morphological transition from yeast-like cells to conjugation tube formation (Bolker *et al*., 1992; Spellig *et al*., 1994). Mature lipopeptide pheromones Mfa1 and Mfa2 consist of 13 and 9 amino acids, respectively. Both are post-translationally modified at their C-terminal cysteines by farnesylation and carboxyl methyl esterification (Spellig *et al*., 1994). The pheromone receptors (Pra1/2) belong to the family of seven transmembrane proteins that are coupled to heterotrimeric G proteins. In the absence of pheromone, the pheromone receptor is constitutively endocytosed from the plasma membrane and degraded in the vacuole. After pheromone binding, formation of conjugation tubes is initiated and pheromone receptor localizes to the tip of conjugation tubes (Fuchs *et al*., 2006). The *a2* locus has two additional genes, *lga2* and *rga2*, which locate between *mfa2* and *pra2* and direct uniparental mitochondrial DNA inheritance and constrain mitochondrial DNA recombination during sexual development (Fedler *et al*., 2009).

### 1.3.2 The *b* locus

The multiallelic *b* mating type locus is required for filamentous growth and pathogenic development in *U. maydis*. The *b* locus codes for bE and bW homeodomain proteins that are involved in intracellular recognition through combinatorial interactions (Gillissen *et al*., 1992; Kronstad and Leong, 1990). The bE and bW polypeptides encoded by the same allele are unable to interact, whereas the bE and bW encoded by different alleles can dimerize and form an active heterodimer. Dimerization involves interaction in the N-terminal variable domains (Kamper *et al.*, 1995). Th bE/bW heterodimer functions as a transcription factor, which directly and indirectly regulates expression of genes involved in filamentous growth and establishment of the biotrophic stage (Brachmann *et al.*, 2001; Heimel *et al.*, 2010b; Scherer *et al.*, 2006; Wahl *et al.*, 2010). Moreover, the expression of *mfa* and *pra* in the *a* locus is down-regulated by the

active bE/bW heterodimer (Urban *et al.*, 1996), which could explain the attenuation of fusion in strains expressing an active bE/bW heterodimer (Laity *et al*., 1995). The replacement of of *bW1* by *bW2* and the introduction of *mfa2* into the *a1b1* background strain produced a solopathogenic strain SG200, which is haploid but can filament and induce tumor formation without prior cell fusion (Bolker *et al.*, 1995).

## 1.4 Pheromone signaling pathways in *U. maydis*

Under low-nutrient conditions, *U. maydis* haploid cells can secrete lipopeptide pheromone which can be perceived by the pheromone receptor Pra of compatible mating type cells (Bolker *et al*., 1992; Spellig *et al*., 1994). The pheromone signal is transmitted by two conserved signaling cascades (Fig. 2): the cAMP-dependent protein kinase A (PKA) pathway and the mitogen-activated protein kinase (MAPK) signaling pathway (Kruger *et al.*, 1998; Muller *et al.*, 1999; Muller *et al.*, 2003b). Pheromone stimulated cells transiently arrest at the $G_2$ stage of the cell cycle (Garcia-Muse *et al*., 2003).

### 1.4.1 Components of cyclic AMP signaling pathway

The cAMP signaling pathway (Fig. 2) is composed of the heterotrimeric G protein α subunit Gpa3 and β subunit Bpp1, adenylyl cyclase Uac1, and protein kinase A (PKA) consisting of regulatory subunit Ubc1 (*Ustilago bypass of cyclase 1*) and the major catalytic subunit Adr1 (Gold *et al.*, 1994; Gold *et al.*, 1997; Muller *et al.*, 2004; Regenfelder *et al.*, 1997). The GTP-bound form of Gpa3 mediates the activation of Uac1 which catalyzes the transition of ATP into cAMP (Kruger *et al.*, 1998; Regenfelder *et al.*, 1997). Subsequently, cAMP binds to Ubc1, leading to the dissociation of Adr1 from Ubc1 (Durrenberger *et al*., 1998).

When the components of the cAMP signaling pathway are disrupted, the cell morphology and expression of *mfa1* are affected. Δgpa3, Δbpp1 and Δuac1 strains display a constitutively filamentous phenotype and strongly reduced expression of *mfa1*, indicating that cAMP signaling represses filamentous growth of *U. maydis* (Gold *et al.*, 1997; Muller *et al.*, 2004; Regenfelder *et al.*, 1997). Deletion of *ubc1* results in a multiple-budding phenotype and the up-regulation of *mfa1* expression (Gold *et al.*, 1994; Hartmann *et al.*, 1999). The up-regulation of *mfa1* expression was also found in strains harboring a constitutively active version Ras1QL, which suggests that Ras1 also

acts as one component of the cAMP signaling pathway (Muller *et al*., 2003a). Furthermore, several downstream targets of the cAMP signaling have been identified. One target is the widely studied transcription factor Prf1, which will be discussed in the following section. Ukb1, a predicted Ser/Thr protein kinase with 30 putative PKA phosphorylation sites, is proposed to be one PKA target. Ukb1 plays a role in lateral budding and filamentous growth. The *ukb1* deletion strains fail to induce tumors and are unable to complete sexual development (Abramovitch *et al*., 2002). Another direct target of PKA Hgl1, which acts as a regulator for the switch between budding and filamentous growth and is required for teliospore formation during infection (Durrenberger *et al.*, 2001). Recently, nine genes representing two high-affinity iron uptake systems were identified as the Adr1 targets using whole genome microarrys (Eichhorn *et al*., 2006). Calcineurin (CN), a protein phosphatase, was shown to be an antagonist of PKA. The deletion of CN catalytic subunit *ucn1* leads to a dramatic multiple-budding phenotype and reduced mating ability (Egan *et al.*, 2009). By deleting the compounds of cAMP signaling in solopathogenic strain, it was demonstrated that the regulated expression of these genes is crucial for pathogenic development (Regenfelder *et al.*, 1997).

### 1.4.2 Components of MAP kinase signaling pathway

The MAP kinase module (Fig. 2) consists of Kpp4/Ubc4, Fuz7/Ubc5 and three MAP kinases Kpp2/Ubc3, Kpp6 and Crk1 (Banuett and Herskowitz, 1994; Brachmann *et al.*, 2003; Garrido *et al.*, 2004; Mayorga and Gold, 1999; Muller *et al.*, 1999; Muller *et al.*, 2003b). Ubc2 acts as an adaptor protein that interacts with Kpp4/Ubc4 through its SAM domain (Klosterman *et al*., 2008; Mayorga and Gold, 2001). This MAP kinase module is necessary for conjugation tube formation and pathogenic development. Except for Kpp6, disruption of any component of the MAP kinase module displays a severe mating defect, inability to form appressoria and the abolishment of pathogenicity (Mendoza-Mendoza *et al.*, 2009a; Muller *et al.*, 2003b). Kpp6 is required for the appressorial penetration step (Brachmann *et al*., 2003). Rok1, the putative dual specificity phosphatase, was found to negatively regulate the phosphorylation status of the MAP kinase Kpp2 as well as the MAP kinase Kpp6. When *rok1* is deleted, increased filamentation and hypervirulence are observed (Di Stasio *et al*., 2009). More recently, Sho1 and Msb2-like proteins were identified to act upstream of the MAP kinases Kpp2

and Kpp6 and to play a key role during surface sensing and appressorium differentiation in *U. maydis* (Lanver *et al.*, 2010).

### 1.4.3 Crosstalk between cAMP and MAP kinase signaling pathways

In *U. maydis*, cAMP and MAPK signalling pathways are tightly interconnected. For example, PKA signaling enhances the expression of pheromone and pheromone receptor (Hartmann *et al.*, 1999; Kruger *et al.*, 1998). The deletion of individual component of MAPK module or *ubc2* suppresses the filamentous growth phenotype of *uac1* deletion mutant (Andrews *et al.*, 2000; Kruger *et al.*, 1998; Mayorga and Gold, 2001). In addition, the deletion of *gpa3* or *uac1* increases the expression of *crk1* (Garrido and Perez-Martin, 2003). Upon pheromone stimulation, cAMP and MAPK signalling pathways are activated (Muller *et al.*, 2003b). One point of crosstalk between cAMP and MAPK signaling is the pheromone response factor Prf1 (Fig. 2). Both Adr1 and Kpp2 can interact with Prf1 *in vivo* (Kaffarnik *et al*., 2003). Cyclic AMP activated PKA leads to phosphorylation of Prf1, resulting in transcriptional activation of the *a* genes. This pheromone-induced *mfa1* expression is dependent on the intact PKA sites in Prf1. Activated-MAP kinase Kpp2 also phosphorylates Prf1 at distinct MAPK sites. The dual phosphorylation of Prf1 by Adr1 and Kpp2 triggers the expression of *b* genes (Kaffarnik *et al*., 2003; Zarnack *et al*., 2008).

Prf1 is an HMG (high-mobility-group) domain transcriptional factor that regulates the expression of *a* and *b* genes through binding to the pheromone response elements (Hartmann *et al*., 1996). Its transcription is regulated by the MAP kinase Kpp2 as well as the MAP kinase Crk1 through a complex interplay of at least three transcriptional factors that bind to three different *cis*-regulatory elements in the *prf1* promoter. Prf1 itself binds to two PREs conferring to autoregulation; Rop1 binds to three RRSs (Rop1 response element) and Hap2 binds to CCAAT motif (Brefort *et al.*, 2005; Garrido *et al.*, 2004; Kaffarnik *et al.*, 2003; Mendoza-Mendoza *et al.*, 2009b). In addition, the UAS (Upstream Activating Sequence) locates between position -1594 bp to -1509 bp upsteam of the *prf1* gene integrates various nutritional inputs (Hartmann *et al.*, 1999). The deletion of *prf1* impaires expression of the *a* and *b* genes and conjugation tube formation as well as pathogenicity (Hartmann *et al*., 1996). However, *prf1* deletion mutants constitutively expressing the pheromone receptor can form conjugation tubes when stimulated by compatible pheromone, indicating that Prf1 is dispensable for

conjugation tube formation and there must exist another branch pathway that regulates the morphological reprogramming (Muller *et al.*, 2003b).

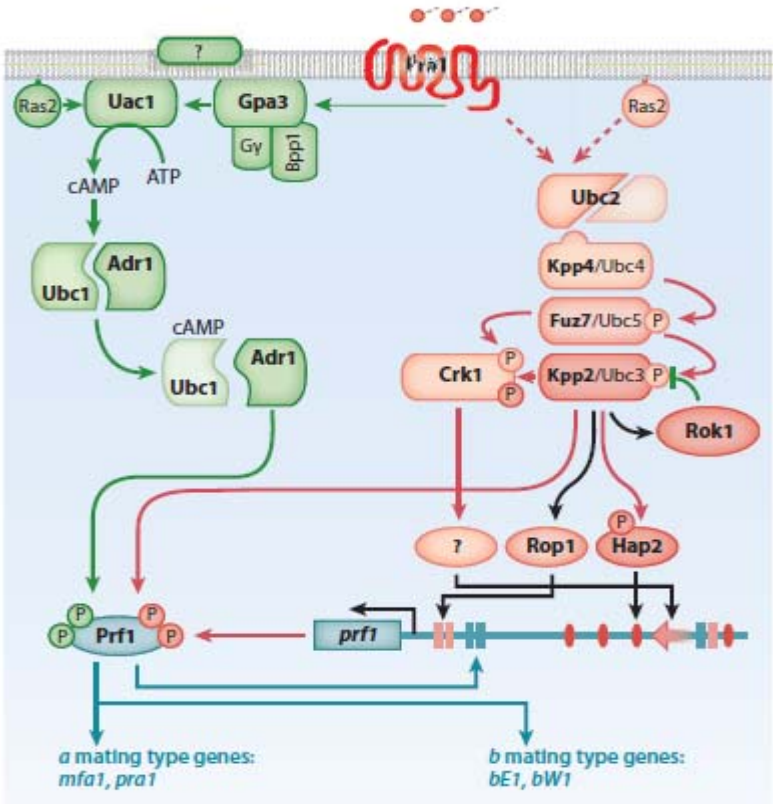


Figure 2 Pheromone signaling pathways in *U. maydis*. Components of the cAMP (green) and MAPK (red) signaling pathways and targets are indicated (green or red arrows, respectively). Phosphorylation is indicated by small circles labeled with P. Transcriptional activation is indicated by black and blue arrows. Postulated interactions and unknown components are indicated by question marks. Taken from Brefort *et al.* (2009).

## 1.5 RACK1, a conserved seven-WD40 repeat protein

RACK1 was initially identified as an intracellular Receptor for Activated protein Kinase C (PKC) (Ron *et al.*, 1994). It is a member of the Trp-Asp (WD) repeat protein family, which can fold into a seven-bladed β-propeller structure. The WD repeat sequence of RACK1 is highly conserved in all eukaryotic species (McCahill *et al.*, 2002; Sengupta *et al.*, 2004). In recent years, accumulated data have shown that RACK1 plays pivotal roles in various biological processes, such as signal transduction and protein translation (Shor *et al.*, 2003; Vomastek *et al.*, 2007).

### 1.5.1 RACK1 functions as a scaffold in signaling pathways

The function of RACK1 as a scaffold protein in signaling pathways has been widely demonstrated. RACK1 interacts with the cytoplasmic domains of transmembrane proteins as well as with soluble signaling proteins (Table 1). At least two domains that allow proteins to interact with RACK1 have been identified: SH2 domains (Chang *et al.*, 2001; Chang *et al.*, 1998) and pleckstrin homology (PH) domains (Koehler and Moran, 2001; Rodriguez *et al.*, 1999). RACK1 functions as an intracellular receptor for several isoforms of activated protein kinase C, including β, ε, δ and μ (Hermanto *et al.*, 2002; Pass *et al.*, 2001; Ron *et al.*, 1994; Rosdahl *et al.*, 2002). The binding of RACK1 to PKC leads to an increase in kinase activity and movement of activated PKC to proper sites (Ron *et al.*, 1999). RACK1 also regulates tyrosine kinase-mediated signaling by interacting with the Src kinase and inhibiting its tyrosine kinase activity at G1 stage of colon cell cycle (Chang *et al.*, 1998; Mamidipudi and Cartwright, 2006). RACK1 mediates the recruitment of STAT3 to IR and IGF-1R specifically to allow activation (Zhang *et al.*, 2006). In the integrin-activated ERK pathway, RACK1 functions as a scaffold protein that associates with Raf, MEK and ERK, and targets active ERK to focal adhesions. When the expression of *RACK1* is attenuated, the ERK activity in response to adhesion is reduced (Vomastek *et al.*, 2007).

**Table 1 RACK1 interacting proteins**

| Interactors | references |
|---|---|
| Receptors | |
| integrin β subunit | (Liliental and Chang, 1998) |
| human Type I IFN receptor | (Croze *et al.*, 2000) |
| Adiponectin receptor 1 | (Xu *et al.*, 2009) |
| alpha chain of the type I IFNR, IL-2R β chain | (Usacheva *et al.*, 2003) |
| insulin-like growth factor 1, receptor (IGF-1R) | (Hermanto *et al.*, 2002) |
| Insulin receptor (IR) | (Zhang *et al.*, 2006) |
| Cytoplasmic signaling proteins | |
| several isoforms of activated protein kinase C, including β, ε, δ and μ | (Hermanto *et al.*, 2002; Pass *et al.*, 2001; Ron *et al.*, 1994; Rosdahl *et al.*, 2002) |
| Src kinase | (Chang *et al.*, 1998; Mamidipudi and Cartwright, 2006) |
| Jak1 and Tyk2 | (Usacheva *et al.*, 2003) |
| Raf, MEK and ERK | (Vomastek *et al.*, 2007) |
| STAT3 | (Zhang *et al.*, 2006) |
| Phosphodiesterase PDE4D5 isoform | (Yarwood *et al.*, 1999) |
| Protein phosphatase 2A (PP2A) | (Kiely *et al.*, 2006) |
| Smad3 | (Okano *et al.*, 2006) |
| Androgen receptor | (Rigas *et al.*, 2003) |

| | |
|---|---|
| JNK1 and JNK2 | (Lopez-Bergami *et al.*, 2005) |
| Fyn tyrosine kinase | (Yaka *et al.*, 2002) |
| Gpa1, Gpg1 and Gpg2 | (Palmer *et al.*, 2006) |
| Gpa2 | (Zeller *et al.*, 2007) |
| | Ion channel |
| $Na^+/H^+$ exchanger isoform 5 (NHE5) | (Onishi *et al.*, 2007) |
| 1,4,5-trisphosphate receptor | (Patterson *et al.*, 2004) |
| Multidrug resistance protein 3 (MDR3/ABCB4) | (Ikebuchi *et al.*, 2009) |
| *N*-methyl D-aspartate (NMDA) receptor | (Yaka *et al.*, 2002) |
| large conductance calcium-activated potassium channel | (Isacson *et al.*, 2007) |

### 1.5.2 RACK1 acts as a component of the ribosomes

Asc1p, a homolog of mammalian RACK1, was identified using mass spectrometry to be part of the small ribosomal subunit in *Saccharomyces cerevisiae* (Link *et al*., 1999). Cryo-electron microscopy (cryo-EM) study revealed that Asc1p locates at the back of the 40S subunit head region in the vicinity of the mRNA exit channel (Nilsson *et al.*, 2004; Sengupta *et al.*, 2004). Recently, conserved charged amino acids on one side of the β-propeller structure of Asc1p were found to confer most of the 40S subunit binding affinity (Coyle *et al.*, 2009). The deletion of *asc1* increases levels of specific proteins *in vivo* and the purified Asc1p deficient ribosome increases the translational activity in *vitro* (Gerbasi *et al.*, 2004). In fast-growing *S. cerevisiae* cells, nearly all Asc1p is tightly bound to ribosomes, but there exists also a ribosome-free form depending on growth conditions. The ribosome-associated Asc1p interacts with Scp160p which connects specific mRNAs, ribosomes and a translation factor with an adaptor for signaling molecules (Baum *et al.*, 2004). The presence of RACK1 homologs in ribosomes was also demonstrated in *Schizosaccharomyces pombe*, *Trypanosoma brucei* and human (Ceci *et al.*, 2003; Regmi *et al.*, 2008; Shor *et al.*, 2003). In *S. pombe* Cpc2, a homolog of RACK1, is associated with the ribosome. Its disruption leads to a decrease in 80S monosomes and polysomes and a deficiency in a subset of highly expressed cellular proteins, such as methionine synthase and homocysteine synthase (Shor *et al.*, 2003). In *T. brucei* TbRACK1 interacts with monosomes and polysomes and forms a complex with eukaryotic elongation factor 1a (eEF1A). The knockdown of *Tbrack1* disrupts the initiation of translation and phosphorylation of a 30 kDa ribosomal protein (Regmi *et al.*, 2008). In human cells, the presence of RACK1 provides a physical and functional link between PKC signaling and ribosome activation. RACK1 recruits

activated protein kinase C to the ribosome, which leads to the stimulation of translation through the phosphorylation of initiation factor 6 and, potential mRNA-associated proteins (Ceci *et al.*, 2003). The binding of RACK1 to the 40S subunit of ribosome is crucial for nascent peptide-dependent translation arrest that is induced by basic amino acid sequences, leading to endonucleotic cleavage of the mRNA as well as to co-translational protein degradation (Kuroha *et al.*, 2010).

### 1.5.3 RACK1 functions as a Gβ subunit

RACK1 is structurally similar to heterotrimeric G protein β subunits with 7 WD40 repeats (Ullah *et al.*, 2008). Gib2, a novel Gβ-like/RACK1 homolog of the human fungal pathogen *Cryptococcus neoformans*, was found to function as a Gβ subunit in cAMP signaling pathway. Yeast two hybrid and pulldown assays showed that Gib2 interacts with the Gα subunit Gpa1 acting in the cAMP signaling pathway. Additional yeast two hybrid assays demonstrated an interaction between Gib2 and two Gγ subunits Gpg1 and Gpg2 (Palmer *et al.*, 2006). In *S. cerevisiae* Asc1p was also shown to function as a Gβ subunit for the Gα subunit Gpa1 in cAMP pathway. Asc1p interacts directly and preferentially with the inactive form of Gpa1p, and inhibits Gpa1p guanine nucleotide exchange activity. In addition, Asc1p was shown to bind adenylyl cyclase Cyr1p and to diminish the production of cAMP in response to glucose stimulation (Zeller *et al.*, 2007).

### 1.5.4 Other roles of RACK1

In addition to the above-mentioned roles, a lot of other functions of RACK1 also have been identified (Table 1). These include the regulation of protein degradation (Liu *et al*., 2007; Zhang *et al*., 2008) and an involvement in ion channel activity regulation (Isacson *et al.*, 2007; Patterson *et al.*, 2004). In cancer cells, RACK1 interacts with DLC1, upon paclitaxel treatment, RACK1, DLC1 and CIS mediates the degradation of BimEL through ElonginB/C-Cullin2-CIS E3 ligase complex (Zhang *et al.*, 2008). In HEK293 cell, RACK1 competes with HSP90 for binding to HIF-1α, links HIF-1α to Elongin-C, and promotes HIF-1α degradation (Liu *et al.*, 2007). Furthermore, RACK1 was also found to regulate protein trafficking. The overexpression of RACK1 inhibits the internalization and down-regulation of the M2 muscarinic acetylcholine receptor in a receptor subtype-specific manner. Decreased expression of RACK1 increases the rate of agonist internalization of the M2 muscarinic acetylcholine receptor, indicating that

RACK1 may both interfere with agonist-induced sequestration and be required for subsequent targeting of internalized M2 receptors to the degradative pathway (Reiner *et al.*, 2010).

## 1.6 Aim of this study

In *U. maydis*, the pheromone MAPK signaling pathway is essential for cell recognition, cell fusion, filamentation and pathogenic development. Many components of this signaling pathway have been identified, such as the 7-transmembrane receptors Pra1/2, the MAPK cascasde including MAPKK kinase Kpp4, MAPK kinase Fuz7 and MAP kinases Crk1, Kpp2 and Kpp6, and downstream target Prf1. However, there are still significant gaps in understanding of the mode of signal transmission from the receptor to the downstream MAPK cascade. In particular, in the majority of MAP kinase modules scaffold proteins like Ste5p of *S. cerevisiae* have not yet been identified in *U. maydis*. In mammals RACK1 functions as a scaffold in signaling pathways. It was interesting to study if Rak1, the homolog of mammalian RACK1, also functions as a scaffold regulating the pheromone-responsive MAPK signaling pathway in *U. maydis*. The main emphasis in this study was 1) to test if *U. maydis* Rak1 functions as a component of the pheromone signaling pathway, 2) to study the role of Rak1 during vegetative growth and morphological transition as well as pathogenic development, 3) to examine how Rak1 regulates conjugation tube formation and mating.

# 2 Results

## 2.1 Rak1, a conserved seven-WD40 repeat protein

### 2.1.1 Rak1 has seven WD40 repeat motifs

The 313 aa protein Um10146 shares 68% amino acid identity with mammalian RACK1 (Receptor for Activated Protein C Kinase), and is predicted to have seven WD40 repeat motifs (Fig. 3A). Hereafter, *um10146* was designated *rak1*. The *rak1* gene was predicted to contain 2 introns. Through SWISS Model (Arnold *et al.*, 2006), Rak1 protein could be modelled to exhibit a seven-bladed β-propeller-like structure using *Homo sapiens* RACK1 as a template (Fig. 3B).

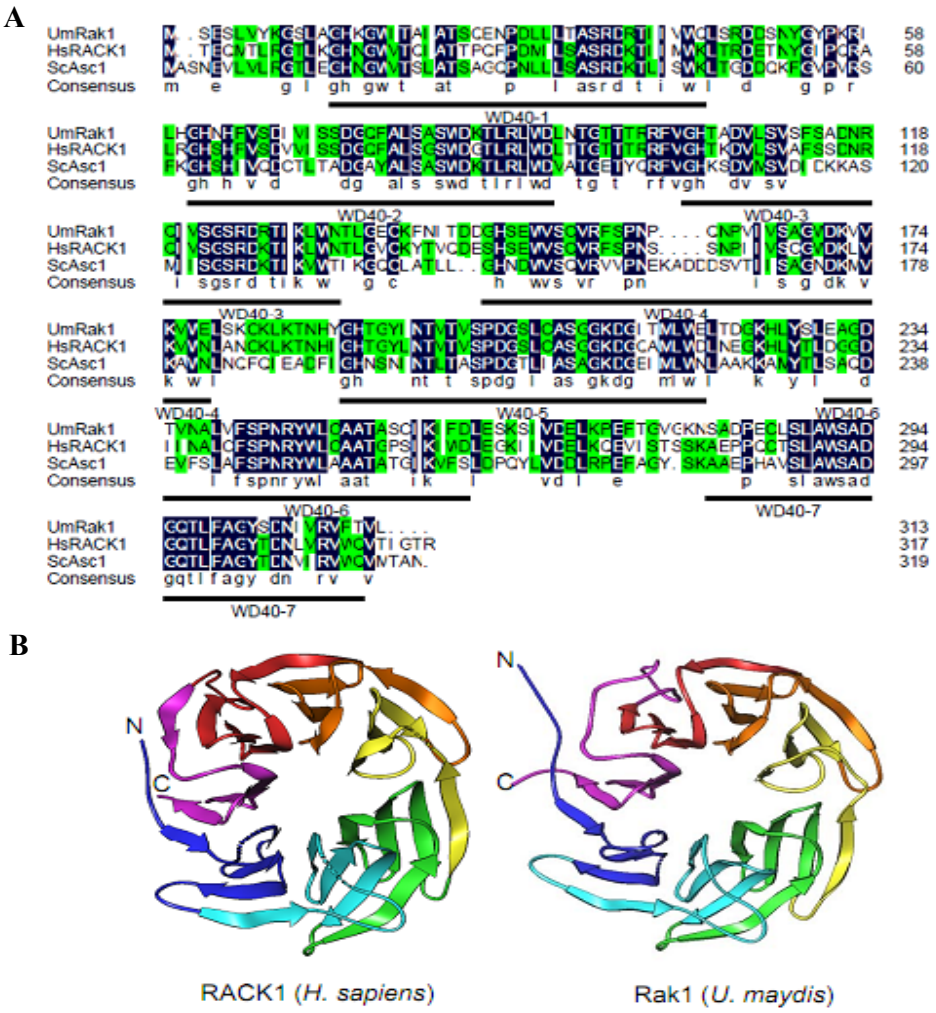


Figure 3 Amino acid sequence alignments of Rak1 related proteins and structure model. (A) Conserved and similar amino acids are colored with black and green respectively. Organism sources and NCBI accession numbers are *Homo sapiens* RACK1 (NP_006089) and *S. cerevisiae* Asc1p (NP_013834.1). The 7 WD40 consensus motif regions are indicated by a thick line below amino acid sequences. The amino acid identity between UmRak1 and HsRACK1 is 68% and the amino acid identity between UmRak1 and ScAsc1 is 51%. (B) *Homo sapiens* RACK1 was used as a template to predict the 3-dimensional structure of Rak1.

### 2.1.2 Rak1 can partially complement the growth defect of an *asc1* mutant of *S. cerevisiae*

Rak1 and *S. cerevisiae* Asc1p show 51% amino acid identity (Fig. 3A). *S. cerevisiae asc1* deletion mutant shows growth defect at elevated temperature (Gerbasi *et al.*, 2004). To test if Rak1 and Asc1p are genetically orthologous, BY47471 and BY47471asc1Δ were transformed with an empty expression vector (pYES2), or pYES2-rak1HA encoding the *rak1* C-terminally fused to an HA tag, individually. Western blotting analysis showed that Rak1 was expressed in the *asc1* mutants (Fig. 4A). Transformants of BY4741asc1Δ with pYES2 showed growth sensitivity towards high temperature. The introduction of Rak1 in BY4741asc1Δ partially enhanced the ability to grow at 37°C (Fig. 4B). This data indicates that Rak1 can to some extent replace some function of Asc1p in *S. cerevisiae*.

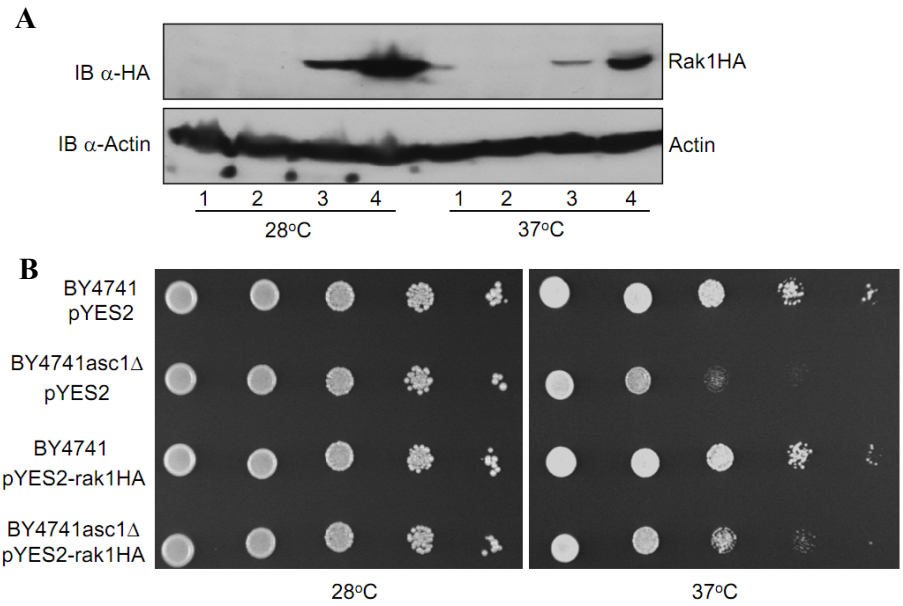


Figure 4 Complementation assay of the temperature-sensitive growth defect in the *S. cerevisiae asc1* mutant by *rak1*. (A) Western blotting analysis of extracts with anti-HA (upper panel) and anti-Actin (bottom panel). Lane 1: BY4741pYES2; lane 2: BY4741asc1ΔpYES2; lane 3: BY4741pYES2-rak1HA; lane 4: BY4741asc1ΔpYES2-rak1HA. The probing with anti-Actin served as a loading control. (B) The indicated strains were grown to log phase in liquid medium, diluted and spotted onto SD-Ura plates, grown at 28°C and 37°C individually for 3 d and photographed.

## 2.2 *rak1* regulates cell growth and stress response

To study the function of *rak1* in *U. maydis*, deletion mutants were generated in the compatible strains FB1 and FB2 as well as in the haploid solopathogenic strain SG200 by replacing the entire *rak1* ORF with a hygromycin resistance cassette.

The colonies of FB1Δrak1 were dramatically smaller than colonies of FB1 on agar plate. In addition, colonies of FB1Δrak1 were donut-shaped compared to dome-shaped colonies of FB1 (Fig. 5A). Donut-shaped colonies were previously reported to be indicative for a cell separation defect (Weinzierl *et al.*, 2002). Microscopic analysis revealed that in FB1Δrak1, the donut-shaped colony morphology is not assignable to a cell morphology phenotype or separation defect (Fig. 5C). In liquid medium, the doubling time of FB1Δrak1 was 3.3±0.4 h compared to FB1 with a doubling time of 2.6±0.2 h (Fig. 5B). These data indicate that *rak1* has a role in regulation of colony morphology and cell growth. In the strain FB1Δrak1-rak1 reintroduction of *rak1* complemented the growth phenotype (Figs. 5A and 5B).

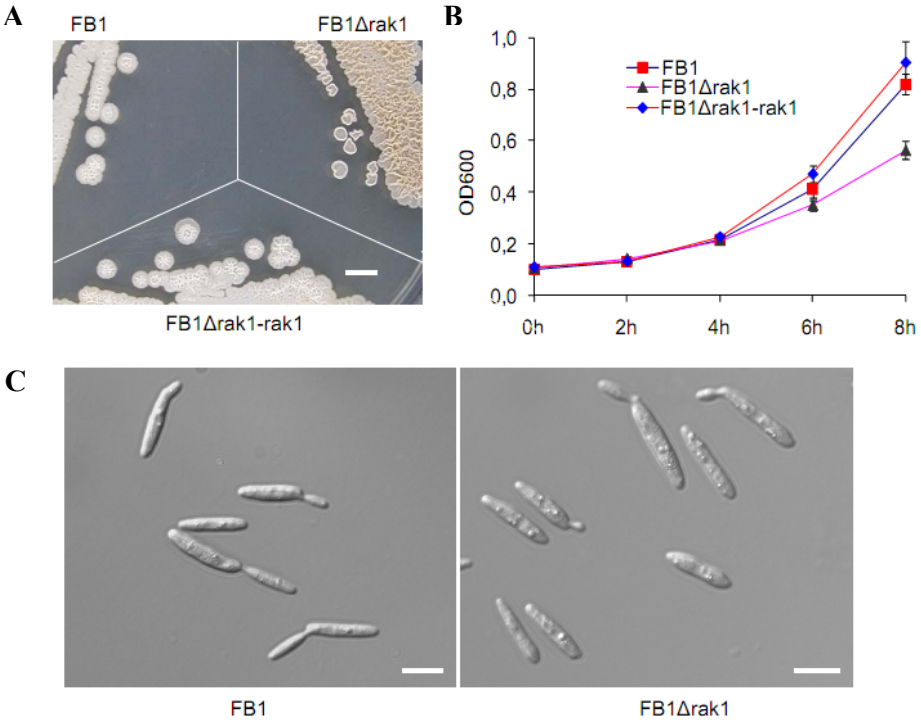


Figure 5 *rak1* deletion mutants show reduced cell growth phenotype. (A) Indicated strains were streaked on PD plates and incubated at 28°C for 4 d. FB1 and FB1Δrak1-rak1 colonies are dome-shaped, while FB1Δrak1 colonies are donut-shaped. Bar, 5 mm. (B) Indicated strains were grown in CM medium with 1% glucose and $OD_{600}$ was measured at different time points. Error bars represent the standard deviation. (C) Deletion of *rak1* does not affect the cell morphology of *U. maydis*. FB1 and FB1Δrak1 were grown in CM medium with 1% glucose at 28°C. Bars, 10 µm.

To determine whether *U. maydis rak1* plays a role under stress conditions, the response of SG200Δrak1 to the cell wall stressing agents calcofluor white and Congo red, the osmotic stressors sorbitol and sodium chloride were assayed. SG200Δrak1 showed increased sensitivity to cell wall stressors calcofluor white and Congo red (Fig. 6).

These defects can be rescued by the introduction of single copy of the *rak1* ORF. The deletion of *rak1* did not affect the sensitivity towards the osmotic stressors. These results suggest that *rak1* is involved in cell wall biosynthesis.

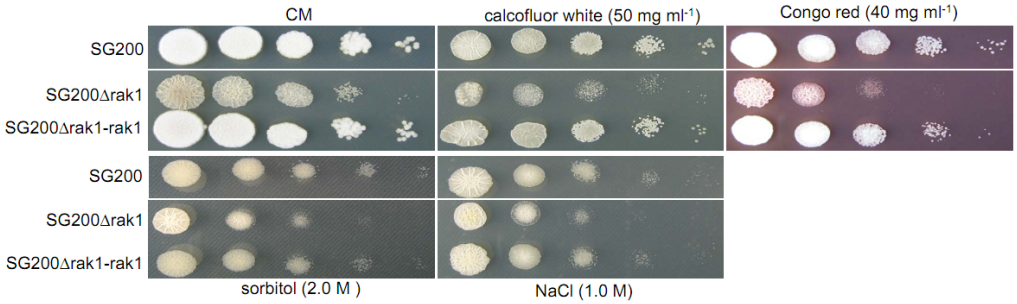


Figure 6 *rak1* is involved in cell wall biosynthesis. Serial dilutions (tenfold) of strains indicated on the left were spotted on CM plates with different stressors, calcofluor white, Congo red, sorbitol and NaCl. Photos were taken after 2-3 d incubation at 28°C.

## 2.3 *rak1* is required for conjugation tube formation, mating and post-fusion development

In mating assays on charcoal-containing plates, the successful fusion of compatible haploid *U. maydis* cells results in the formation of the filamentous dikaryon, which appears as white fuzziness covering the colonies (Banuett and Herskowitz, 1989). In this assay, *rak1* deletion strains displayed a strong reduction in the dikaryon formation when compatible *rak1* deletion strains were co-spotted (Fig. 7A). When FB1Δrak1 and FB2 were co-spotted, the fuzzy reaction was more severely attenuated compared to the combination between FB1 and FB2Δrak1. This may be due to the non-isogenetic backgrounds (Fig. 7A). Solopathogenic haploid strain SG200 exhibits white fuzziness on charcoal-containing plates without prior cell fusion (Bolker *et al.*, 1995). SG200Δrak1 showed a strong reduction in filamentation, which could not be rescued by the addition of synthetic a2 pheromone (Fig. 7B). These findings indicate that *rak*1 is involved in cell fusion and has an additional role during post-fusion development.

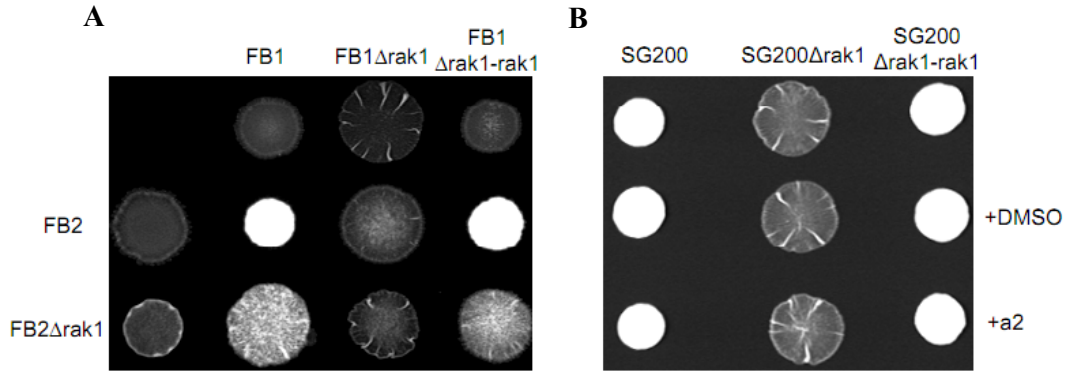


Figure 7 The deletion of *rak1* reduces mating and filamentous growth. (A) Mating between compatible strains. The strains indicated on top were spotted alone and in combination with the strains indicated on the left on charcoal-containing PD plates. Dikaryotic filaments display white fuzziness. (B) Filamentation assay of solopathogenic strains. The strains indicated on top were spotted on charcoal-containing PD plates. Middle: strains were stimulated with DMSO for 1 h before spotting. Bottom: strains were stimulated with synthetic a2 pheromone in DMSO for 1 h before spotting.

To investigate the mating defect of *rak1* deletion strains in more detail, FB1, FB1Δrak1 and FB1Δrak1-rak1 strains were stimulated with synthetic a2 pheromone. Upon pheromone stimulation for 5 h, 0.5±0.4% of FB1Δrak1 formed conjugation tubes compared to 94.3±3.4% of FB1 and 91.2±8.5% of FB1Δrak1-rak1 (Figs. 8A and 8B). This data shows that *rak1* is essential for the morphological response to pheromone stimulation.

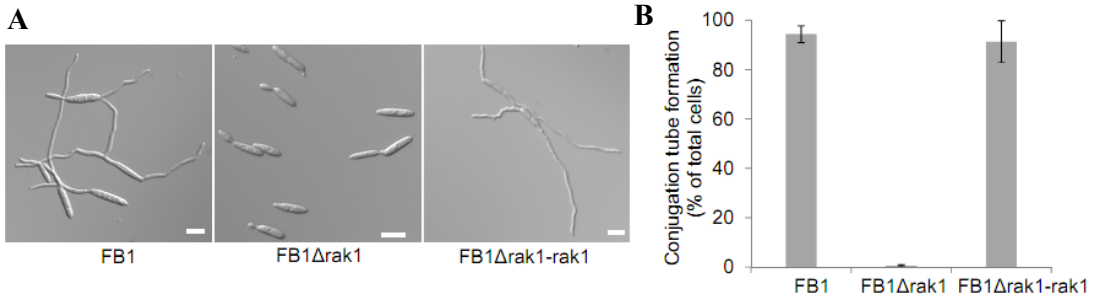


Figure 8 The *rak1* deletion abolishes conjugation tube formation. The indicated strains were stimulated with synthetic a2 pheromone at 28°C for 5 h. Bars, 10 µm. (B) Quantification of conjugation tube formation. Strains were treated with synthetic a2 pheromone as in (A). The percentage of cells that had formed conjugation tubes were determined, more than 600 cells were analyzed in three independent experiments. Error bars represent the standard deviation.

In all cases the observed phenotypes corresponding *rak1* deletion strains can be complemented by reintroduction of *rak1* into these strains (Figs. 7 and 8).

## 2.4 *rak1* plays a role during pathogenic development

### 2.4.1 The deletion of *rak1* abolishes tumor formation

To study whether *rak1* plays a role during pathogenic development, maize seedlings were infected with mixtures of compatible *rak1* deletion strains or with wild type strains. 17% of plants infected by *rak1* deletion strains formed tumors compared to 79% of plants infected by wild type strains showed tumors (Fig. 9). To exclude that the reduction in tumor formation is caused by the cell fusion defect of compatible *rak1* deletion strains, plant infections were performed with the solopathogenic strain SG200 and its derivative SG200Δrak1. Upon infection with SG200, 85% of plants showed tumor formation, while no tumors could be observed in SG200Δrak1 infected plants (Fig. 9). Introduction of single copy of *rak1* ORF into the *ip* locus of SG200Δrak1 could restore tumor formation, indicating successful complementation (Fig. 9).

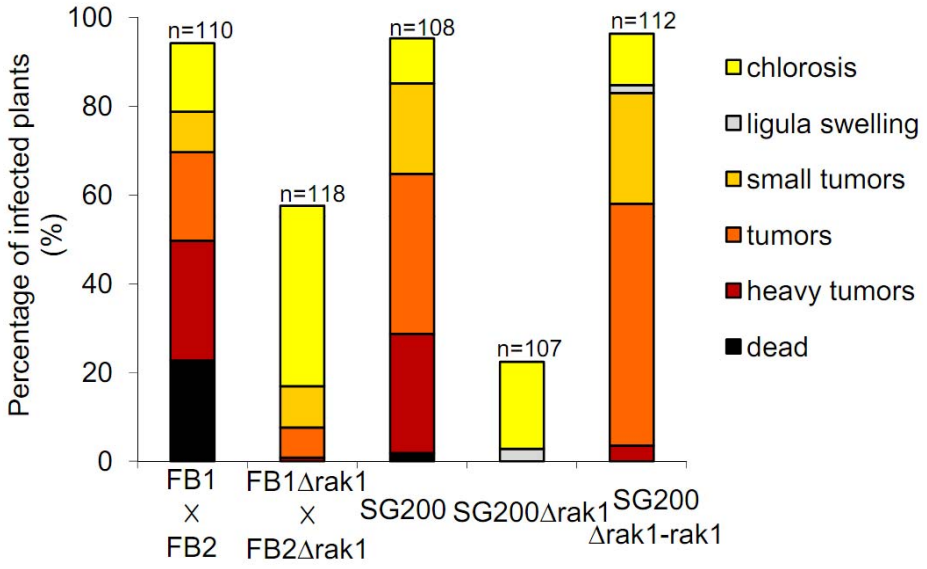


Figure 9 The deletion of *rak1* attenuates pathogenicity. Plant infections with the indicated strains were performed in three replicates, each replicate with at least 35 plants. Symptoms were scored 12 days after infection following the scheme developed by Kamper *et al.* (2006) indicated on the right. Numbers on top of bars represent the number of infected plants.

To determine at which stage pathogenic development is impaired in *rak1* deletion strain, SG200AM1 and the derivative SG200AM1Δrak1 were used. SG200AM1 is a solopathogenic strain harboring an appressorial marker fused to eGFP which is expressed specifically in hyphal tips forming an appressorium, both *in vivo* and *in vitro* (Mendoza-Mendoza *et al.*, 2009a). Under *in vitro* inducing conditions, 78±1.8% of SG200AM1 cells showed filamentation and 22±1.3% of those cells formed appressoria (Figs. 10A and 10B), while SG200AM1Δrak1 showed a strong reduction of

filamentation (17±2.4%) and no appressoria formation was detectable (Figs. 10A and 10B), indicating impairment in perception or integration of these stimuli in the *rak1* deletion strain. This finding is in line with the previously observed severely attenuated filamentation and loss of pathogenicity in the *rak1* deletion strain.

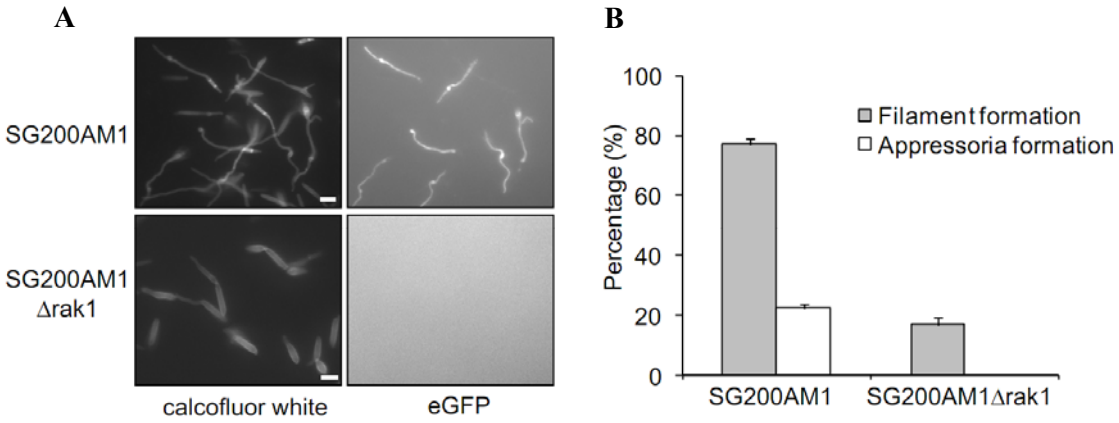


Figure 10 *rak1* deletion mutants are attenuated in filamentation and appressoria formation. (A) Microscopic observation of filamentation and appressoria formation. The indicated strains were sprayed on Parafilm with 100 µM of 16-hydroxyhexadecanoic acid. After 18 h of incubation at 28°C, cells were stained with calcofluor white (left panel) and analyzed for appressorial marker gene (AM1) expression by eGFP signal emission (right panel). Bars, 10µm. (B) Quantification of filament and appressoria formation of indicated strains. The bars represent results of three independent experiments, more than 300 filaments per sample were scored. Error bars represent the standard deviation.

### 2.4.2 Expression of the *b* heterodimer partially rescues the pathogenicity of *rak1* deletion mutant

The *b* heterodimer regulates filamentation and pathogenic development in *U. maydis* (Kamper *et al.*, 1995). To investigate whether a constitutively expressed *b* heterodimer can rescue the virulence defect of the *rak1* deletion strain, *rak1* was deleted in HA103 strain which constitutively expresses a bE1/bW2 heterodimer (Hartmann *et al*., 1996). On charcoal-containing plates HA103Δrak1 showed filamentation which was as strong as observed in HA103 (Fig. 11A). Moreover, 57% of plants infected by HA103Δrak1 formed tumors compared to 80% tumor rate in HA103 (Fig. 11B). These findings indicate that the severely reduced virulence of the *rak1* deletion strain results from a defect in the expression of *b* genes.

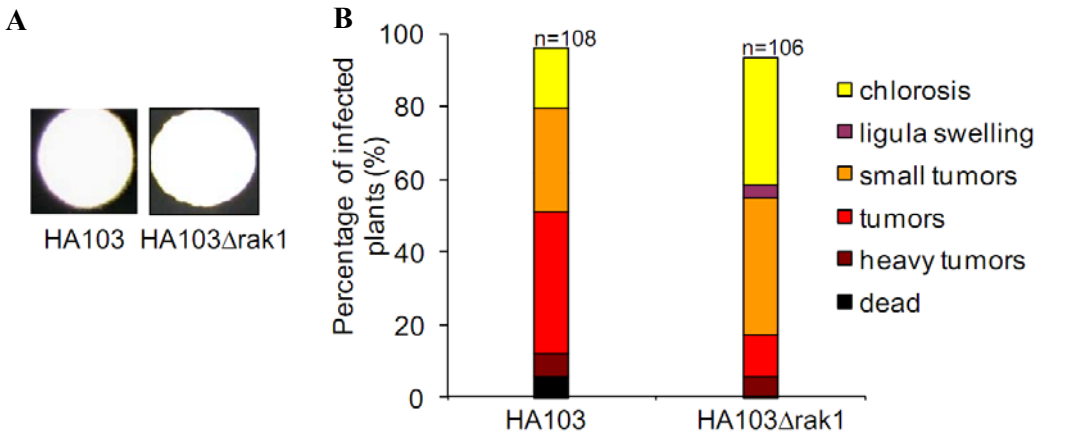


Figure 11 Constitutively expressed *b* heterodimer partially rescues filamentation and pathogenicity of *rak1* deletion strain. (A) Filamentation assay of HA103 and HA103Δrak1. The indicated strains were spotted on charcoal-containing plates and incubated for 48 h at 28°C. (B) Pathogenicity assay of HA103 and HA103Δrak1 was done as described in the legend of Figure 10. Numbers on top of bars represent the number of infected plants.

## 2.5 The localization of Rak1

To gain insight into the localization of Rak1, a *rak1-eGFP* fusion construct was generated and used to replace *rak1* in FB1 (Fig. 12A). Western blotting analysis showed that Rak1-eGFP fusion protein was expressed and had the expected size of 62.5 kDa (Fig. 12B). To test whether the eGFP tagged Rak1 is functional, the FB1rak1-eGFP strain was stimulated with synthetic a2 pheromone. Upon pheromone stimulation for 5 h, the majority of cells formed conjugation tubes (Fig. 12C and data not shown). Rak1-eGFP localized in the cytoplasm of haploid cells and conjugation tubes excluding the nuclei (Fig. 12C). Protein fractionation detected Rak1 protein in the cytosol as well as in the membrane fraction (Fig. 12D). Sho1-Flag fusion protein acted as a marker for membrane proteins (Lanver *et al.*, 2010).

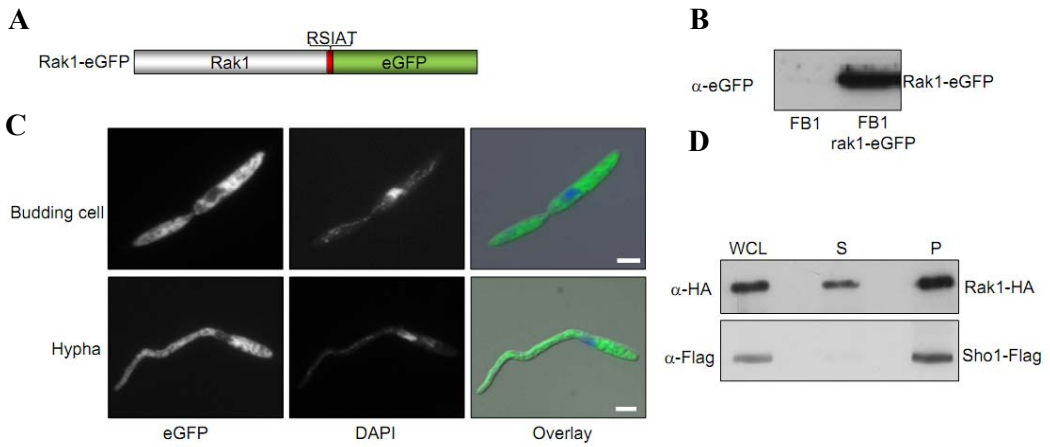


Figure 12 Localization of Rak1-eGFP in *U. maydis*. (A) Schematic representation of Rak1-eGFP fusion protein. eGFP was fused to the C-terminus of Rak1 with a short RSIAT linker. (B) Rak1-eGFP fusion protein was expressed in haploid cells. Indicated strains were grown in CM medium with 1% glucose, proteins were prepared, separated by SDS-PAGE and detected with eGFP antibody. (C) Rak1-eGFP localizes in the cytoplasm excluding the nucleus. With synthetic a2 pheromone stimulation for 5 h, FB1rak1-eGFP formed conjugation tube. Top panel: budding cell; bottom panel: hypha showing conjugation tube. Cells were fixed with formaldehyde, DAPI was used to stain nuclei. The fluorescent signals corresponding to eGFP (left column) and DAPI (middle column) were merged (right column). Bars, 5 µm. (D) Analysis of Rak1 localization after cell fractionation. WCL: whole cell lysate, S: cytoplasmic fraction; P: membrane fraction. Sho1-Flag acts as a marker for membrane proteins. After differential centrifugation, fractionations were separated by SDS-PAGE. Rak1-HA was detected with HA antibody (top panel), Sho1-Flag was detected with Flag antibody (bottom panel).

## 2.6 *rak1* is involved in regulation of pheromone responsive gene expression

### 2.6.1 *rak1* is required for the expression of the pheromone responsive genes

The finding that the morphological response to pheromone is abolished in *rak1* deletion strain led me to investigate the transcriptional response to pheromone. In *U. maydis*, *rak1* was expressed in sporidia and its expression was not induced further upon pheromone stimulation (Fig. 13). The expression of the pheromone responsive genes in the *a* locus (*mfa1* and *pra1*) and *b* locus (*bE1* and *bW1*) in FB1Δrak1 was analyzed. A low basal expression of *mfa1* and strongly increased expression of all four genes after pheromone stimulation for 5 h was detected in FB1 (Müller *et al*., 2003b and Fig. 13). In FB1Δrak1 the basal expression of *mfa1* was undetectable and after pheromone stimulation except for a weak induction of *mfa1* expression, the expression of *pra1*, *bE1* and *bW1* was undetectable (Fig. 13). This finding indicates that *rak1* is required for the expression of *a* and *b* genes.

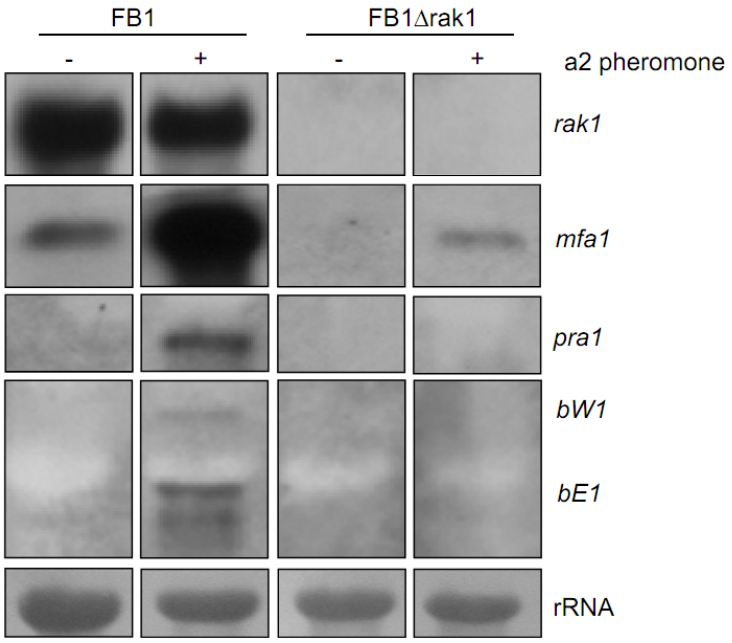


Figure 13 The deletion of *rak1* affects the expression of pheromone responsive genes. After synthetic a2 pheromone (+) or DMSO (-) treatment for 5 h, RNA was prepared from the indicated strains, 10 µg of total RNA was loaded in each lane. The rRNA was stained with methylene blue as a loading control at the bottom. The blot was hybridized successively with probes indicated on the right.

As a more sensitive assay for pheromone production in the *rak1* deletion strain, the pheromone tester strain FBD12-17 (*a2a2b1b2*) was used. This diploid strain develops white fuzziness when exposed to a1 pheromone secreted by FB1 on charcoal-containing plates (Spellig *et al.*, 1994). When a mixture of FB1Δrak1 and FBD12-17 was spotted, white fuzziness was induced, which was comparable to the mixture of FB1 and FBD12-17 (Fig. 14). This suggests that the *rak1* deletion strain expresses low level of pheromone gene which could not be detected by Northern blotting analysis.

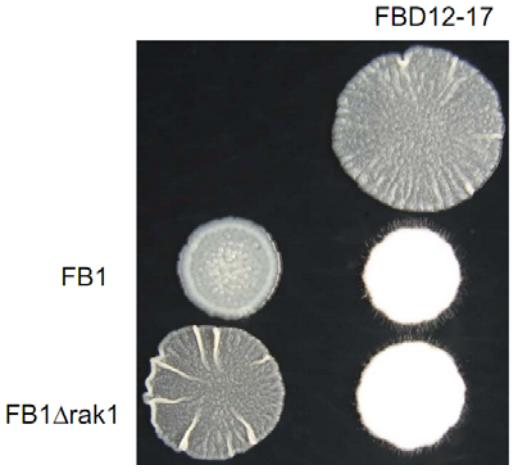


Figure 14 FB1Δrak1 induces filamentation in FBD12-17. The indicated strains were spotted alone and in the indicated combinations on charcoal-containing PD plates. The white fuzziness indicates the formation of aerial hyphae by FBD12-17 in response to a1 pheromone secreted by FB1 and FB1Δrak1. The photo was taken after 48 h incubation at 28°C.

### 2.6.2 *rak1* is required for the basal expression of *prf1*

The expression of *a* and *b* genes is dependent on the transcription factor Prf1 which is transcriptionally regulated by MAP kinase signaling (Hartmann *et al*., 1996; Kaffarnik *et al*., 2003). To this end, the *rak1* gene under the control of *otef* promoter was integrated into the *ip* locus in FB1. Northern blotting revealed that in FB1 *prf1* showed a low basal expression (Hartmann *et al.*, 1999 and Fig. 15) which was undetectable in FB1Δrak1; the expression of *prf1* in FB1rak1$^{con}$ was twofold increased compared to its expression in FB1 (Fig. 15). Subsequently, in FB1rak1$^{con}$ the expression of *mfa1* was found twentyfold higher than in FB1 (Fig. 15). This data indicates that the defect in *mfa1* expression is due to the abolishment of basal expression of *prf1*.

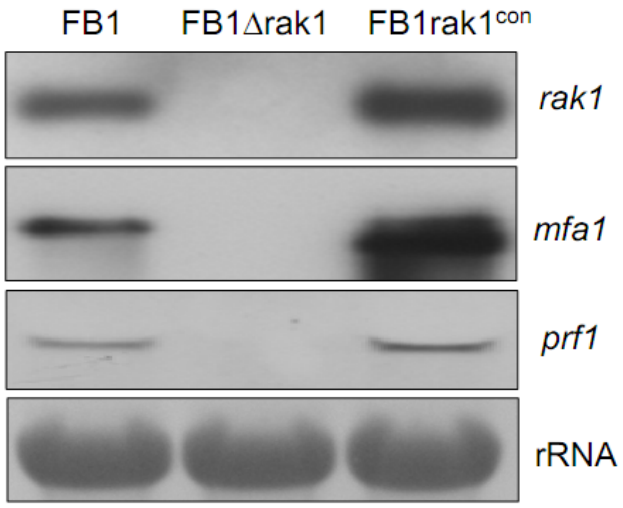


Figure 15 *rak1* is essential for the expression of *prf1* and *mfa1*. *rak1* gene under the control of *otef* promoter was integrated into the *ip* locus in FB1. The indicated strains were grown in CM medium with 1% glucose, total RNA was prepared, 10 µg of total RNA was loaded in each lane and rRNA was stained with methylene blue as a loading control. The blot was hybridized successively with probes indicated on the right.

### 2.6.3 *rak1* does not affect the *crk1* expression

Crk1, the MAP kinase, has been shown to regulate the expression of *prf1* and its transcription is negatively regulated by cAMP signaling pathway (Garrido and Perez-Martin, 2003; Garrido *et al.*, 2004). To test if the defect of *prf1* expression in *rak1* deletion strain is due to defect in *crk1* expression, the *crk1* transcript was detected in FB1Δrak1 and FB1rak1$^{con}$. The level of *crk1* expression was not altered in the absence of *rak1* or overexpression conditions of *rak1* (Fig. 16). This indicates that *rak1* is dispensable for the expression of *crk1*.

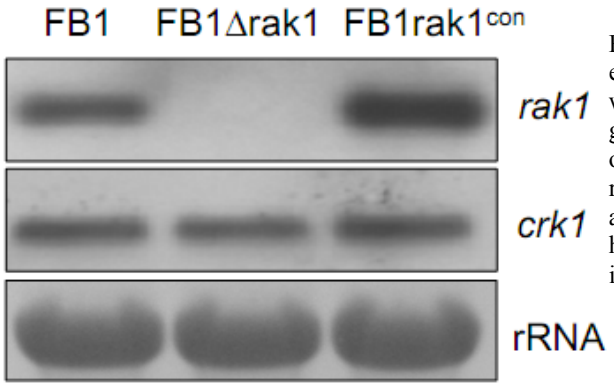


Figure 16 *rak1* is not required for the expression of *crk1*. The indicated strains were grown in CM medium with 1% glucose. Total RNA was prepared, 10 µg of RNA was loaded in each lane and rRNA was stained with methylene blue as a loading control. The blot was hybridized successively with probes indicated on the right.

## 2.7 Activation of the mating MAPK pathway rescues conjugation tube formation in *rak1* deletion mutant

In *U. maydis* conjugation tube formation is regulated by the pheromone-induced MAP kinase module consisting of Kpp4, Fuz7 and Kpp2 (Muller *et al.*, 2003b). Given the failure of *rak1* deletion strain to respond to pheromone, genetic epistasis analysis was used to test whether Rak1 functions upstream or downstream of this module. To this end, the FB1$P_{crg1}$:fuz7DD harboring a constitutively active allele of the MAPKK Fuz7 (Fuz7DD) under the control of an arabinose inducible and glucose repressible promoter (Muller *et al.*, 2003b) was used. The derivative strain FB1$P_{crg1}$:fuz7DDΔrak1 was generated in which *rak1* was deleted. Under repressing condition, both strains FB1$P_{crg1}$:fuz7DD and FB1$P_{crg1}$:fuz7DDΔrak1 were morphologically identical (data not shown). After transfer to arabinose-containing medium for 5 h, both strains formed conjugation tube-like structures (Fig. 17A). Furthermore, at the Fuz7DD induction, the expression of *mfa1* was detected in the *rak1* deletion strain, and the expression level of *mfa1* was comparable to the level in FB1$P_{crg1}$:fuz7DD (Fig. 17B).

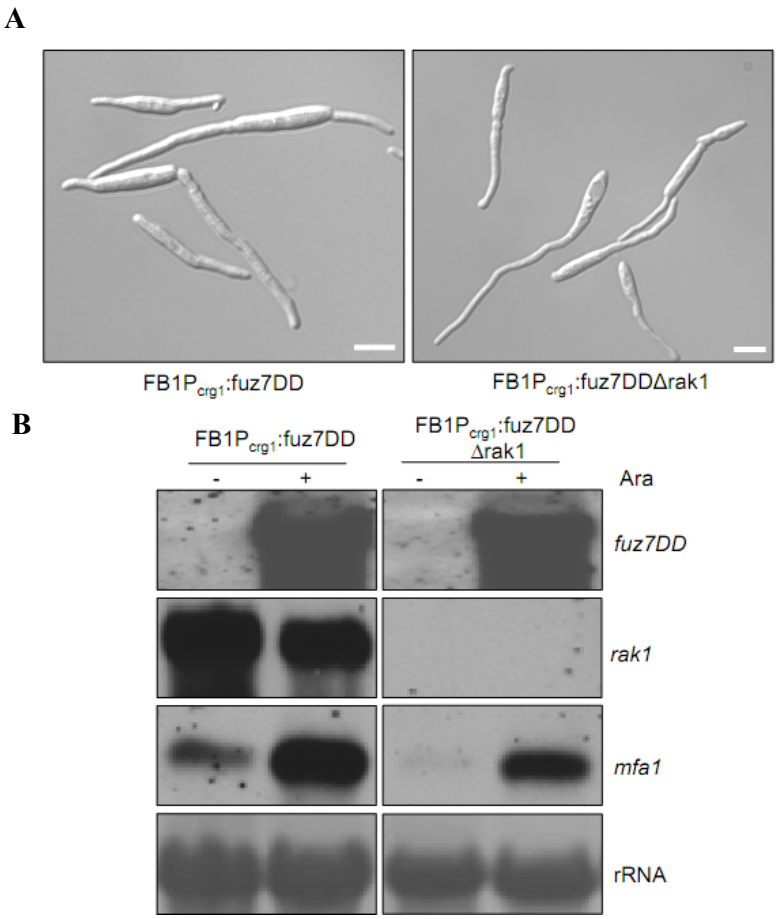


Figure 17 The induction of Fuz7DD bypasses the need for *rak1*. (A) FB1P$_{crg1}$:fuz7DD and FB1P$_{crg1}$:fuz7DDΔrak1 were transferred from CM medium with 1% glucose to CM medium with 1% arabinose and incubated for 5 h at 28°C. Bars, 10 µm. (B) Strains indicated on top were incubated in CM medium with 1% glucose (-) or transferred to CM medium with 1% arabinose (+) for 5 h. RNA was prepared from the indicated strains and 10 µg of total RNA was loaded in each lane. The rRNA was stained with methylene blue as a loading control. The blot was hybridized successively with probes indicated on the right.

As *rak1* deletion mutant fails to express the pheromone receptor gene *pra1*, I considered the possibility that their mating defect could result from the inability to sense pheromone and hence reduce the activation of the pheromone responsive MAPK cascade. To this end, *rak1* deletion strains that either express the pheromone receptor gene *pra1* (FB1Δrak1pra1$^{con}$) or the pheromone response factor gene *prf1* (FB1Δrak1prf1$^{con}$) under the control of *otef* promoter were generated. Upon pheromone stimulation FB1Δrak1pra1$^{con}$ and FB1Δrak1prf1$^{con}$ formed conjugation tubes in contrast to the yeast-like FB1Δrak1 (Fig. 18A). Upon pheromone stimulation the expression of *prf1* and *mfa1* was highly induced in FB1Δrak1pra1$^{con}$ (Fig. 18B). This suggests that

FB1Δrak1 fails to perceive pheromone because they do not express sufficient levels of pheromone receptor in a Prf1-dependent manner.

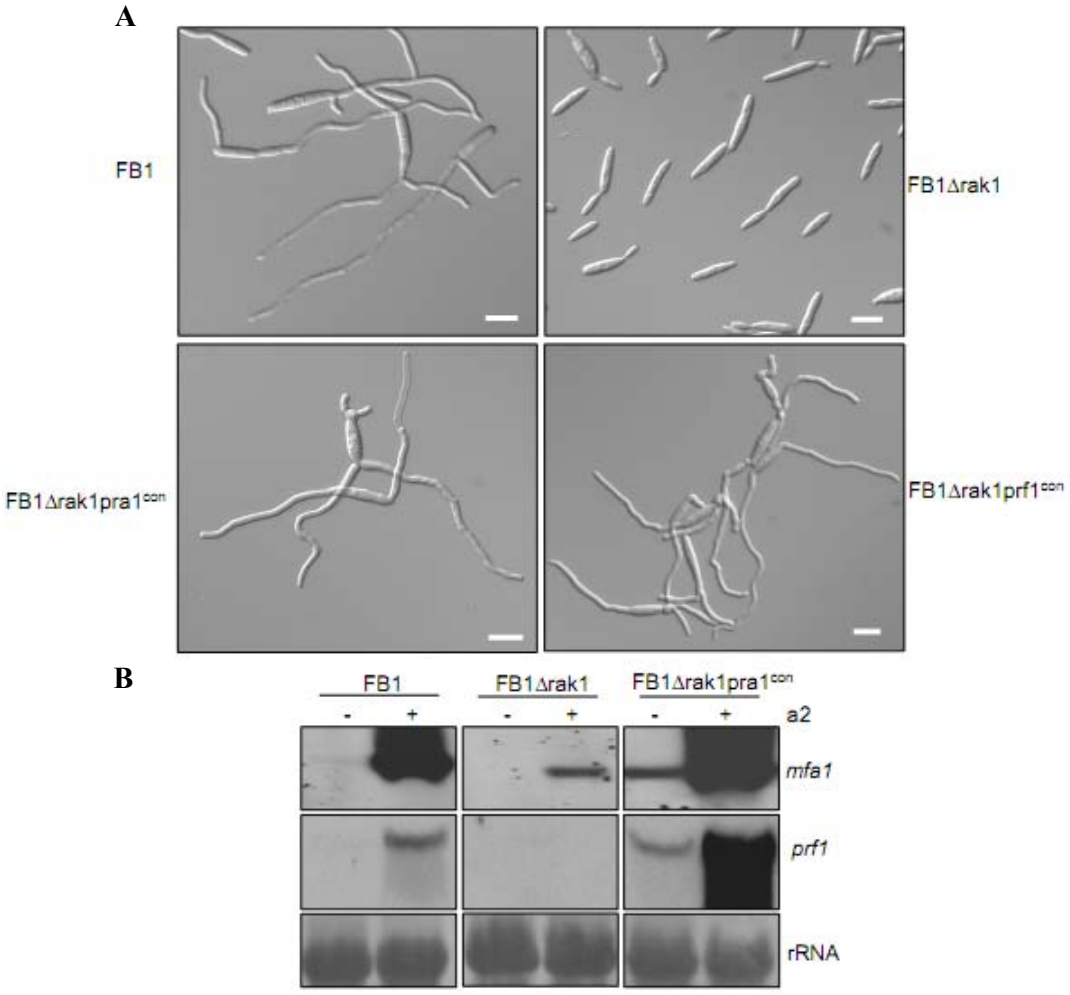


Figure 18 The constitutive expression of *pra1* or *prf1* induces conjugation tube formation in FB1Δrak1 with pheromone stimulation. (A) *pra1 or prf1* was individually integrated into the *ip* locus under the control of *otef* promoter in FB1Δrak1. Cell morphology was scored after synthetic a2 pheromone stimulation for 5 h. Bars, 10μm. (B) Strains were treated with a2 pheromone (+) as in (A) or DMSO (-). RNA was prepared from the indicate strains, 10 μg of total RNA was loaded in each lane. The rRNA was stained with methylene blue as a loading control. The blot was successively hybridized with probes indicated on the right.

## 2.8 Is *rak1* involved in the cAMP signaling pathway?

### 2.8.1 Addition of cAMP partially rescues the expression of *mfa1* in *rak1* deletion mutant

In *U. maydis*, cAMP signaling pathway regulates the expression of *prf1* and *a* genes (Hartmann *et al.*, 1999; Kruger *et al.*, 1998). To study whether *rak1* affects the expression of *mfa1* via the cAMP signaling, mating as well as the expression of *mfa1* in the *rak1* deletion strain was analyzed after application of exogenous cAMP. When a

mixture of FB1Δrak1 and FB2Δrak1 was spotted on charcoal-containing PD plates with 6 mM cAMP, the fuzzy reaction was partially restored (Fig. 19A). To test whether the application of exogenous cAMP could rescue the expression of *mfa1*, FB1Δrak1 was treated with different concentrations of cAMP for 5 h. In FB1 15 mM cAMP strongly increased the expression level of *mfa1* (Kruger *et al.* 1998; Fig. 19B). In FB1Δrak1, at low cAMP levels the expression of *mfa1* was undetectable and was induced at 15 mM cAMP. However, compared to stimulation in FB1 the induction of *mfa1* in FB1Δrak1 was fivefold lower (Fig. 19B).

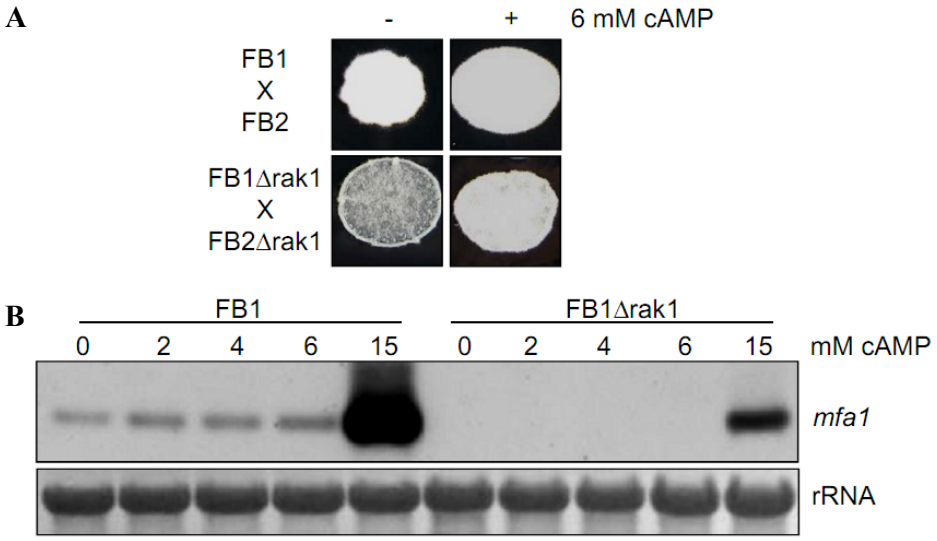


Figure 19 Cyclic AMP partially rescues the mating defect and *mfa1* expression of Δrak1 strains. (A) Mating assay on charcoal-containing PD plates without (-) or with (+) 6 mM cAMP for 48 h. The strains combinations indicated on the left were spotted. Dikaryotic filaments display white fuzziness. (B) FB1 and FB1Δrak1 were grown in CM medium with 1% glucose supplemented with the indicated concentrations of cAMP for 5 h. RNA was prepared from the indicated strains, 10 µg of total RNA was loaded in each lane and rRNA was stained with methylene blue as a loading control. The blot was hybridized with *mfa1* probe.

### 2.8.2 Specificity of *rak1* function

To test if *rak1* specifically regulates the expression of *mfa1* via *prf1*, expression of *fer2* and *frb34* was analyzed in FB1Δrak1. Both genes have the same expression patterns as *mfa1* and are positively regulated by cAMP signaling (Brachmann *et al*., 2001; Eichhorn *et al*., 2006). As previously described (Brachmann *et al*., 2001; Eichhorn *et al*., 2006), the deletion of *gpa3* or *uac1* severely reduced the expression of *fer2*, *frb34* and *mfa1*, while the deletion of *ubc1* dramatically enhanced the expression of these genes (Fig. 20). In FB1Δrak1, *mfa1* expression was abolished, *fer2* expression was not

affected and *frb34* expression was strongly increased relative to FB1 (Fig. 20). These data suggest that *rak1* differentially regulates the expression of *frb34* and *mfa1*.

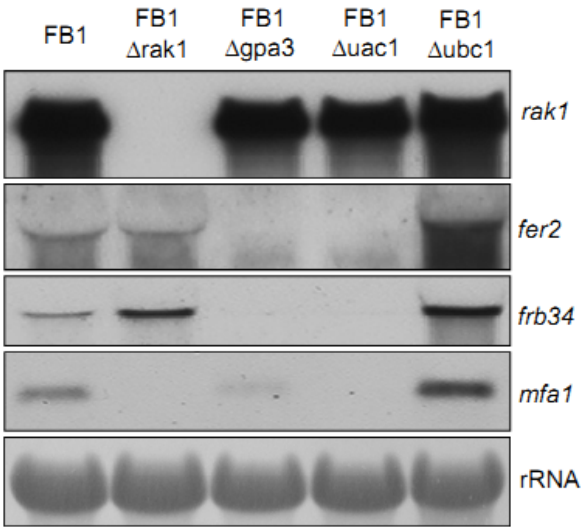


Figure 20 *rak1* differentially regulates the expression of *mfa1* and *frb34*, but is dispensable for *fer2* expression. RNA was prepared from the indicated strains, 10 µg of total RNA was loaded in each lane and rRNA was stained with methylene blue as a loading control. The blot was hybridized successively with probes indicated on the right.

In wild type cells, overexpression of PKA catalytic subunit Adr1 leads to the highly induced transcript levels of *mfa1* (Eichhorn *et al.*, 2006). To analyze whether this induction requires *rak1*, *adr1* was integrated into the *ip* locus of FB1Δrak1 under the control of *crg1* promoter. Under repressing condition, both strains FB1$P_{crg1}$:adr1 and FB1Δrak1$P_{crg1}$:adr1 were morphologically identical to FB1 and 5 h after transfer to arabinose-containing medium, both strains displayed a multiple-budding phenotype (data not shown). In FB1Δrak1$P_{crg1}$:adr1 the expression of *mfa1* was undetectable with arabinose induction compared to strongly induced expression in FB1$P_{crg1}$:adr1 (Fig. 21). This data shows that the regulation of *mfa1* expression by Adr1 is dependent on the presence of *rak1*.

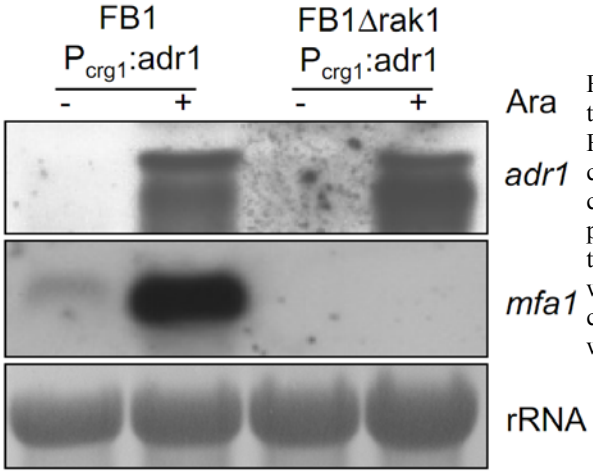


Figure 21 *mfa1* induction by Adr1 requires the presence of *rak1*. FB1$P_{crg1}$:adr1 and FB1Δrak1$P_{crg1}$:adr1 were grown in glucose-containing CM medium (-) or arabinose-containing CM medium (+) for 5 h. RNA was prepared from the indicated strains, 10 µg of total RNA was loaded in each lane and rRNA was stained with methylene blue as a loading control. The blot was hybridized successively with probes indicated on the right.

### 2.8.3 *rak1* does not affect the multiple-budding phenotype caused by the inhibitor of calcineurin

Calcineurin is a protein phosphatase, which was shown to be an antagonist to PKA phosphorylation. CsA is an inhibitor of calcineurin and its application to *U. maydis* can mimic the deletion of the catalytic subunit of calcineurin *ucn1* and results in a multiple-budding phenotype (Egan *et al.*, 2009). To test if *rak1* affects the phosphorylation of some PKA downstream targets, FB1 and FB1Δrak1 were treated with CsA. With CsA treatment, FB1Δrak1 displayed a multiple-budding phenotype, which was comparable to that of FB1 (Fig. 22). When the response to CsA and synthetic a2 pheromone was assayed, FB lost cell polarity and appeared as chains of round cells. However, FB1Δrak1 displayed the multiple-budding phenotype. Convincingly, FB1Δrak1pra1$^{con}$ behaved like FB1 (Fig. 22). This data suggests that Rak1 does not affect the phosphorylation status of PKA downstream targets. The formation of chains of round cells must result from the pheromone-induced activation of the MAPK pathway in the absence of calcineurin.

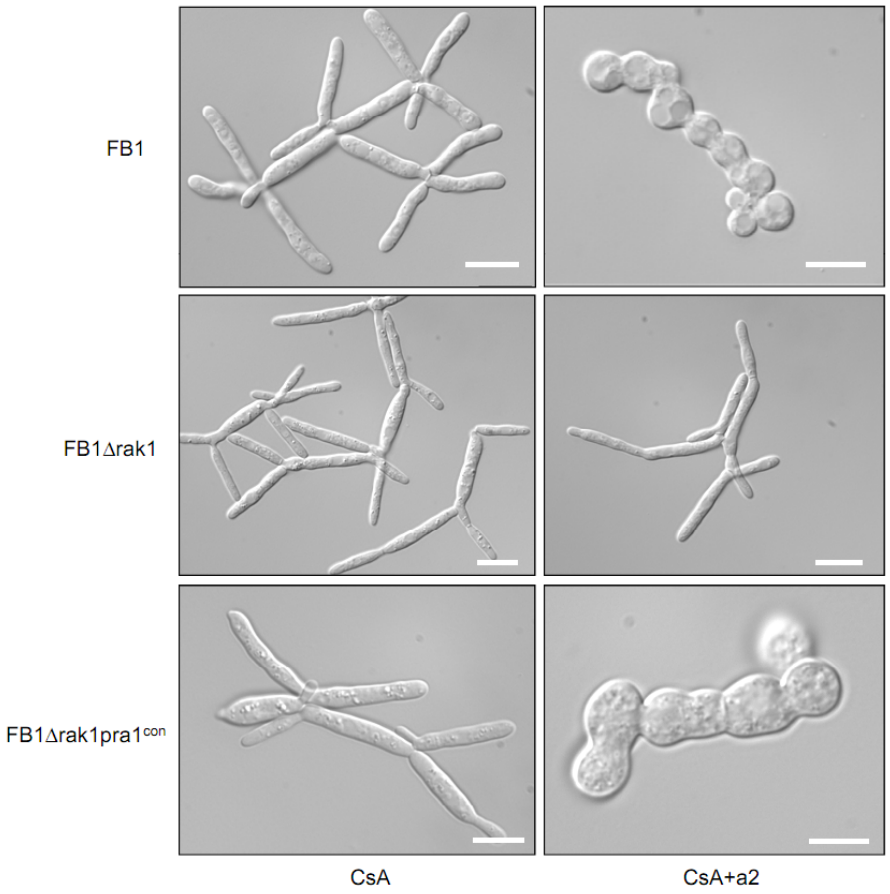


Figure 22 *rak1* does not affect the multiple-budding phenotype caused by the inhibitor of calcineurin. FB1, FB1Δrak1 and FB1Δrak1pra1$^{con}$ were treated with 10 μg ml$^{-1}$ of CsA (left column) or CsA+a2 pheromone (right column) in CM medium with 1% glucose overnight. Bars, 10 μm.

### 2.8.4 Does Rak1 function as a non-conventional Gβ subunit?

Gib2 and Asc1p, homologs of Rak1, have shown to be non-conventional Gβ subunits that interact with Gα subunits (Palmer *et al.*, 2006; Zeller *et al.*, 2007). To test if Rak1 could act as a Gβ subunit in *U. maydis*, its interactions with all Gα subunits, Gpa1, Gpa2, Gpa3 and Gpa4, and Gγ subunit Gpg1 (Um11209) were analyzed in yeast two hybrid assays. In these assays, *rak1* gene was inserted into pGBKT7, the Gα and Gγ genes were individually inserted into pGADT7. Protein expression was detected by Western blotting and proteins with the expected sizes were produced (Fig. 23B). However, none of the strains expressing the combination of Rak1 and the Gα or Gγ could grow on SD medium without Leu/Trp/His with 3 mM 3-AT (Fig. 23A), indicating that Rak1 does not directly interact with any of respective proteins.

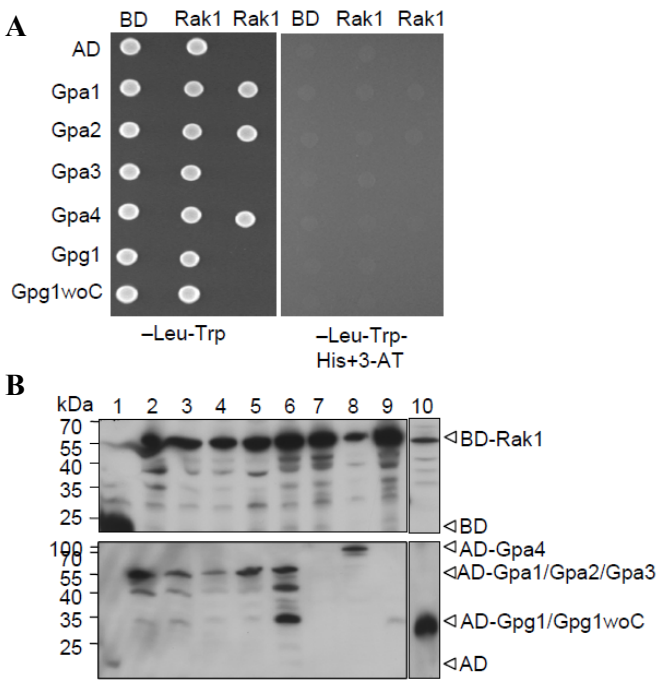


Figure 23 Yeast two hybrid assay for analyzing the interaction between Rak1 and Gα or Gγ subunits. (A) After co-transforming pGBKT7 or pGBKT7-Rak1 (indicated on top) and pGADT7 derivatives (indicated on the left) in *S. cerevisiae* AH109. The indicated strains were grown in SD-Leu-Trp medium overnight. Cells were spotted on selective plates (-Leu-Trp) and on medium stringency plates (-Leu-Trp-His+3mM 3-AT) and incubated for 3-5 d at 28°C. (B) Western blotting analysis for protein expression in yeast. Lane 1: AH109 co-transformed with control vectors. Lanes 2 and 3: AH109 co-transformed with pGBKT7-Rak1 and pGADT7-Gpa1. Lanes 4 and 5: AH109 co-transformed with pGBKT7-Rak1 and pGADT7-Gpa2. Lane 6: AH109 co-transformed with pGBKT7-Rak1 and pGADT7-Gpa3. Lanes 7 and 8: AH109 co-transformed with pGBKT7-Rak1 and pGADT7-Gpa4. Lane 9: AH109 co-transformed with pGBKT7-Rak1 and pGADT7-Gpg1. Lane 10: AH109 co-transformed with pGBKT7-Rak1 and pGADT7-Gpg1woC lacking the CAAX motif. Protein expression was detected with antibodies against the Gal4 binding domain (top panel) and against the Gal4 activation domain (bottom panel). Except for the strain in lane 7 which does not express the AD-Gpa4 fusion protein, all other strains expressed both fusion proteins. The fusion proteins are indicated by arrowheads on the right. The molecular weight marker is depicted on the left.

To analyze if there is an interaction between Rak1 and Gpa3 by a different techinque, coimmunoprecipitation was performed. HA-Gpa3 and myc-Rak1 were individually translated from TNT T7 Coupled Reticulocyte lysate system (Promega). HA-Gpa3 could be precipitated by anti-HA affinity matrix from the protein mixture of HA-Gpa3 and myc-Rak1. However, myc-Rak1 could not be co-precipitated (Fig. 24). As yeast two hybrid assay, no direct interaction between Rak1 and Gpa3 was identified.

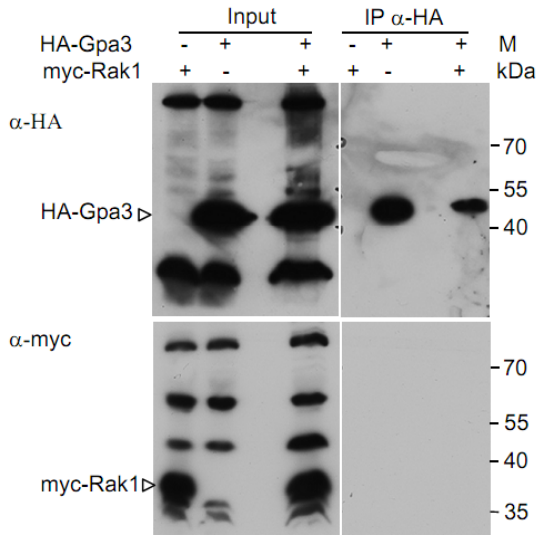


Figure 24 Coimmunoprecipitation of Rak1 and Gpa3. HA-Gpa3 and myc-Rak1 fusion proteins were individually translated from TNT T7 Coupled Reticulocyte lysate system (Promega). Anti-HA affinity matrix, 10 µM GDP and HA-Gpa3 protein were mixed with or without myc-Rak1 protein, washed, eluted with SDS-PAGE sample buffer and analyzed by SDS-PAGE and immunoblotting. Proteins were detected with antibodies against HA (top panel) and against myc (bottom panel). The molecular weight marker is depicted on the right.

## 2.9 Analysis of the transcriptome in the *rak1* deletion mutant

To analyze the effect of *rak1* on the transcriptome, DNA microarray analysis was performed. Custom-made Affymetrix arrays representing 93% of all *U. maydis* genes were used (Kamper *et al*. 2006 and Methods). FB1 and FB1Δrak1 were grown to log phase ($OD_{600}$=0.5) in CM medium with 1% glucose. Cells were harvested and RNA was prepared. The analysis was performed in biological triplicates. The transcription profiles showed that transcripts of 201 genes (3.24% of 6,200 genes represented on the microarray) changed at least twofold ($p < 0.05$) in FB1Δrak1 compared to FB1. 164 genes were up-regulated and 37 genes were down-regulated relative to FB1 (Table 2). To obtain a better understanding of the processes affected by the deletion of *rak1*, these genes were grouped into functional categories using the FunCatDB (Ruepp *et al*., 2004). This analysis revealed that among the up-regulated genes, there was a significant enrichment ($P \leq 0.05$) in several key categories like metabolism, energy, virulence and resistance (Supplementary Table 1). Among the up-regulated genes in the microarray analysis, three genes encoding non-secreted enzymes were identified, which might play a role in modification of the fungal cell wall (Table 2), two putative chitin deacetylases (*um11922*, *um02019*) and one putative chitinase Cts1 (*um10419*).

The down-regulated genes showed a significant enrichment in lipid metabolism, alcohol fermentation and a MAPK signaling-dependent pathway (Supplementary Table 2). Among the genes in the MAPK signaling-dependent pathway category, *prf1*, *mfa1* and *pra1* were found to be down-regulated in FB1Δrak1, which was consistent with the

Northern blotting results (Figs. 13 and 15) and validated the quality of the data set. Interestingly, the second most differentially regulated gene was *rop1*, its expression was found to be fortyfold reduced in FB1Δrak1 compared to FB1 (Table 2). Rop1 is a direct positive regulator of *prf1* expression (Brefort *et al*., 2005). To confirm the array data, Northern blotting analysis was performed. As shown previously (Brefort *et al*., 2005), in FB1 the basal expression of *rop1* with three transcripts of different sizes was detected (Fig. 25A). In line with the microarray data, the *rak1* deletion abolished the expression of *rop1* (Fig. 25A).

**Table 2 List of differentially expressed genes in FB1Δrak1/FB1 strains identified by microarray analysis**

| probe set | um-number* | annotation* | Log2 Fold change |
|---|---|---|---|
| CLUSTER64_RC | um01612 | conserved hypothetical protein | 1.01 |
| W30um229G | um01891 | probable GUF1 - GTP-binding protein | 1.01 |
| W190um119G | um01705 | conserved hypothetical protein | 1.02 |
| C85um027G | um04224 | related to Myosin-like protein NUF2 | 1.02 |
| C52um065G | um04145 | conserved hypothetical Ustilago-specific protein | 1.02 |
| W90um156G | um10419 | Cts1 chitinase | 1.03 |
| C110um027G | um04219 | conserved hypothetical protein | 1.04 |
| C165um056G | um01859 | related to ribitol kinase | 1.05 |
| W70um195G | um01837 | conserved hypothetical protein | 1.05 |
| C80um025G | um04127 | probable ERG26 - C-3 sterol dehydrogenase (C-4 decarboxylase) | 1.05 |
| CLUSTER20_RC | um01613 | related to AUR1 - inositol phosphorylceramide synthase | 1.05 |
| UG24-1e11-47a7_RC | um01458 | probable DNA polymerase delta catalytic subunit | 1.06 |
| W70um156G | um10423 | conserved hypothetical protein | 1.06 |
| W10um012G | um02103 | probable RRD2 - Activator of the phosphotyrosyl phosphatase activity of PP2A | 1.06 |
| C55um074G | um01824 | conserved hypothetical protein | 1.07 |
| C85um089G | um10820 | probable nadh-ubiquinone oxidoreductase 10.5 kDa subunit | 1.07 |
| C65um135G | um12161 | related to lipase family | 1.07 |
| C95um158G | um01755 | putative protein | 1.09 |
| W235um074G | um01785 | putative protein | 1.09 |
| W96um135G | um01650 | conserved hypothetical protein | 1.09 |
| C16um003G | um01979 | related to MTQ2 - Putative S-adenosylmethionine-dependent methyltransferase | 1.10 |
| C5um103G | um01994 | conserved hypothetical protein | 1.10 |
| C30um032G | um11767 | conserved hypothetical protein | 1.10 |
| W45um159G | um15073 | conserved hypothetical protein | 1.11 |
| C175um027G | um11130 | conserved hypothetical protein | 1.11 |
| W70um158G | um01761 | conserved hypothetical protein | 1.11 |
| C35um228G | um10451 | related to cytochrome c oxidase subunit I | 1.11 |
| W110um119G | um01724 | conserved hypothetical protein | 1.11 |
| W115um074G | um01812 | conserved hypothetical protein | 1.12 |
| C40um025G | um04134 | probable methionine synthase, vitamin-b12 independent | 1.12 |

| | | | |
|---|---|---|---|
| W55um178G | um02019 | probable Chitin deacetylase | 1.12 |
| C95um013G | um11099 | mes1 probable MES1 - methionyl-tRNA synthetase | 1.13 |
| W170um119G | um01709 | conserved hypothetical protein | 1.14 |
| W190um010G | um01242 | related to SRP101 - signal recognition particle receptor, alpha chain | 1.14 |
| EST01um234 | um03396 | conserved hypothetical protein | 1.14 |
| C145um119G | um01714 | probable monooxygenase | 1.14 |
| C75um066G | um04182 | probable TYR1 - prephenate dehydrogenase (NADP+) | 1.14 |
| C91um074G | um01817 | conserved hypothetical protein | 1.16 |
| W95um074G | um01816 | related to TRM7 - tRNA 2`-O-ribose methyltransferase | 1.16 |
| W90um167G | um04242 | conserved hypothetical protein | 1.16 |
| C15um003G | um01980 | related to Cytochrome P450 4F8 | 1.16 |
| C30um056G | um12172 | conserved hypothetical protein | 1.17 |
| C45um089G | um01553 | conserved hypothetical protein | 1.17 |
| C110um087G | um05857 | conserved hypothetical protein | 1.17 |
| C105um003G | um11374 | conserved hypothetical protein | 1.18 |
| W110um135G | um01647 | related to CDC20 - cell division control protein | 1.19 |
| C35um038G | um10892 | conserved hypothetical protein | 1.19 |
| W70um178G | um02014 | conserved hypothetical protein | 1.20 |
| C45um066G | um04189 | related to Cytochrome P450 | 1.20 |
| C85um178G | um02010 | related to family II 2-keto-3-deoxy-D-arabino-heptulosonate 7-phosphate synthase | 1.21 |
| C45um158G | um10874 | conserved hypothetical protein | 1.21 |
| W32um249G | um02978 | conserved hypothetical protein | 1.21 |
| W35um056G | um01883 | conserved hypothetical protein | 1.21 |
| W60um152G | um05272 | conserved hypothetical protein | 1.21 |
| C40um227G | um15040 | probable arginyl-tRNA synthetase, cytosolic | 1.23 |
| W20um195G | um01851 | conserved hypothetical protein | 1.23 |
| C75um027G | um04226 | probable RVB2 - RUVB-like protein | 1.23 |
| W32um195G | um10261 | conserved hypothetical protein | 1.24 |
| W70um122G | um01686 | conserved hypothetical protein | 1.24 |
| W125um040G | um00723 | related to stress response protein rds1p | 1.24 |
| W15um229G | um01894 | putative protein | 1.24 |
| C45um244G | um11225 | conserved hypothetical protein | 1.25 |
| W130um021G | um10636 | conserved hypothetical protein | 1.25 |
| W100um156G | um04259 | conserved hypothetical protein | 1.26 |
| C40um203G | um04984 | conserved hypothetical protein | 1.27 |
| C70um167G | um10414 | conserved hypothetical protein | 1.27 |
| C90um027G | um04223 | probable glutaredoxin | 1.28 |
| C135um049G | um00108 | related to D-arabinitol 2-dehydrogenase | 1.29 |
| C14um227G | um01467 | probable NOP2 - nucleolar protein | 1.29 |
| C175um119G | um01708 | probable HOM6 - homoserine dehydrogenase | 1.30 |
| C25um282G | um02683 | conserved hypothetical protein | 1.33 |
| C55um158G | um10872 | related to YSA1 - sugar-nucleotide hydrolase | 1.33 |
| C75um135G | um01654 | conserved hypothetical protein | 1.34 |
| W135um178G | um11385 | putative protein | 1.35 |
| C70um227G | um11818 | probable SDS22 - protein phosphatase 1, regulatory subunit 7 | 1.36 |
| W65um003G | um01968 | conserved hypothetical protein | 1.36 |
| W30um195G | um01849 | conserved hypothetical protein | 1.36 |
| C30um066G | um04192 | probable eukaryotic translational release factor 1 | 1.36 |
| UG14-32b6-121e6_RC | um01616 | related to MRPL24 - mitochondrial ribosomal protein, large subunit | 1.36 |
| C75um025G | um04128 | related to isopenicillin N epimerase | 1.37 |
| W15um135G | um11890 | probable DIC1 - Mitochondrial dicarboxylate carrier protein | 1.37 |

| | | | |
|---|---|---|---|
| C65um192G | um00196 | probable FUN34 - transmembrane protein involved in ammonia production | 1.37 |
| C70um087G | um11022 | related to SRY1 - 3-hydroxyaspartate dehydratase | 1.38 |
| CLUSTER60_RC | um01606 | related to NMD5 - Nam7p interacting protein (Importin-8) | 1.39 |
| C10um168G | um02060 | probable porphobilinogen synthase | 1.39 |
| W40um003G | um01974 | conserved hypothetical protein | 1.39 |
| C253um074G | um10879 | conserved hypothetical protein | 1.40 |
| W80um024G | um10806 | conserved hypothetical protein | 1.40 |
| C30um080G | um03246 | related to versicolorin b synthase | 1.40 |
| W55um098G | um00144 | putative protein | 1.40 |
| W100um191G | um11345 | conserved hypothetical protein | 1.41 |
| W10um227G | um01466 | related to acyl-coa dehydrogenase, long-chain specific precursor | 1.41 |
| W95um220G | um06298 | related to CCC1 - Proposed vacuolar iron transport protein | 1.42 |
| W35um193G | um00169 | related to AUT1 - essential for autophagocytosis | 1.42 |
| W120um024G | um01535 | conserved hypothetical protein | 1.44 |
| C45um177G | um11922 | related to Chitin deacetylase precursor | 1.45 |
| W50um156G | um04270 | probable DPS1 - aspartyl-tRNA synthetase, cytosolic | 1.46 |
| C60um254G | um04833 | probable isovaleryl-CoA dehydrogenase | 1.46 |
| C121um192G | um00210 | conserved hypothetical protein | 1.46 |
| W10um135G | um01666 | probable DIC1 - Mitochondrial dicarboxylate carrier protein | 1.47 |
| C35um027G | um10410 | probable HAS1 - helicase associated with Set1p | 1.47 |
| C40um167G | um04251 | conserved hypothetical protein | 1.48 |
| C60um013G | um03537 | probable ornithine carbamoyltransferase precursor | 1.48 |
| C25um122G | um01697 | probable LYS2 - L-aminoadipate-semialdehyde dehydrogenase, large subunit | 1.48 |
| W30um089G | um01550 | conserved hypothetical protein | 1.48 |
| C85um276G | um06010 | Leu1 alpha-isopropylmalate isomerase | 1.49 |
| C183um119G | um01706 | conserved hypothetical protein | 1.49 |
| W25um065G | um10887 | rad3 probable RAD3 - DNA helicase/ATPase | 1.49 |
| W20um056G | um01886 | related to carboxypeptidase | 1.50 |
| C50um119G | um01740 | conserved hypothetical protein | 1.50 |
| C130um074G | um11901 | related to Lactamase, beta 2 | 1.52 |
| UG23-1i5-133h4_RC | um05421 | related to Multidrug resistance protein | 1.52 |
| C160um019G | um11241 | related to aldehyde dehydrogenase [NAD(P)] | 1.53 |
| W75um156G | um10421 | related to DPP1 - diacylglycerol pyrophosphate phosphatase | 1.53 |
| C20um135G | um01665 | hypothetical protein | 1.53 |
| C120um003G | um01954 | conserved hypothetical protein | 1.54 |
| W140um027G | um04213 | putative protein | 1.56 |
| C95um156G | um04260 | conserved hypothetical protein | 1.56 |
| C115um024G | um01533 | related to n-acetyltransferase | 1.56 |
| C35um158G | um10875 | conserved hypothetical protein | 1.59 |
| W10um184G | um05521 | conserved hypothetical protein | 1.59 |
| W100um158G | um01753 | probable GCY1 - galactose-induced protein of aldo/keto reductase family | 1.63 |
| W65um024G | um01521 | Pyr3 dihydroorotase | 1.63 |
| W170um074G | um01799 | putative protein | 1.63 |
| W71um089G | um01559 | conserved hypothetical protein | 1.63 |
| C70um228G | um12176 | conserved hypothetical protein | 1.63 |
| W60um156G | um04268 | probable saccharopine dehydrogenase (NAD, L-lysine-forming) | 1.66 |
| W100um038G | um04156 | probable LEU4 - 2-isopropylmalalate synthase | 1.67 |
| C5um158G | um01775 | conserved hypothetical protein | 1.69 |
| W114um228G | um01905 | probable ubiquitin thiolesterase L3 | 1.71 |

| | | | |
|---|---|---|---|
| W116um074G | um01811 | related to complex I intermediate-associated protein CIA30 precursor, mitochondrial | 1.74 |
| W55um076G | um03349 | conserved hypothetical protein | 1.74 |
| W120um027G | um04217 | conserved hypothetical protein | 1.74 |
| C55um022G | um00123 | related to L-lactate dehydrogenase (cytochrome b2) | 1.75 |
| C80um195G | um01835 | related to carnitine acetyl transferase FacC | 1.76 |
| C130um025G | um04115 | probable LYS20 - homocitrate synthase | 1.77 |
| W140um049G | um00109 | probable DAK2 - dihydroxyacetone kinase | 1.77 |
| W210um003G | um11000 | conserved hypothetical protein | 1.79 |
| W95um122G | um11896 | probable NADH-ubiquinone oxidoreductase 30.4 kDa subunit, mitochondrial precursor | 1.81 |
| W30um200G | um03362 | conserved hypothetical protein | 1.86 |
| C115um021G | um03116 | conserved hypothetical protein | 1.86 |
| C125um003G | um01953 | conserved hypothetical protein | 1.86 |
| C127um119G | um01720 | probable phosphomannomutase | 1.87 |
| C60um186G | um10682 | probable CYB2 - L-lactate dehydrogenase (cytochrome b2) | 1.88 |
| C140um122G | um01669 | probable VPS4 - vacuolar sorting protein | 1.90 |
| C50um027G | um10408 | related to MRPL10 - mitochondrial ribosomal protein, large subunit | 1.92 |
| W35um185G | um05496 | related to cystathionine beta-lyase | 1.93 |
| C85um038G | um04159 | probable RKI1 - D-ribose-5-phosphate ketol-isomerase | 1.94 |
| C60um135G | um01656 | probable sugar transporter | 2.00 |
| W10um038G | um04176 | probable FRS1 - phenylalanyl-tRNA synthetase, beta subunit. cytosolic | 2.03 |
| C77um283G | um10095 | probable RNA helicase dbp2 (DEAD box protein) | 2.08 |
| C30um036G | um02774 | related to alternative oxidase precursor, mitochondrial | 2.12 |
| C105um027G | um04220 | probable ARO7 - chorismate mutase | 2.16 |
| W25um066G | um04194 | conserved hypothetical protein | 2.24 |
| C40um209G | um00005 | probable Benzoate 4-monooxygenase cytochrome P450 | 2.29 |
| W30um188G | um10689 | probable LYS4 - homoaconitase precursor | 2.32 |
| W190um074G | um01795 | conserved hypothetical protein | 2.35 |
| W15um028G | um00496 | mismatch base pair and cruciform DNA recognition protein Hmp1 | 2.42 |
| C45um074G | um01827 | related to acid phosphatase ACP2 precursor | 2.45 |
| W128um027G | um04216 | related to translation elongation factor HBS1 protein | 2.59 |
| W25um089G | um10815 | conserved hypothetical protein | 2.59 |
| W30um228G | um01926 | related to DAL2 - allantoinase | 2.60 |
| W15um195G | um01852 | related to Epoxide hydrolase 1 | 2.78 |
| UG21-14a22-110c6_RC | um05422 | conserved hypothetical protein | 4.68 |
| W42um026G | um02382 | a1-specific pheromone [mating factor a1] | -5.59 |
| W40um026G | um02383 | a2-pheromone receptor Pra1 | -2.14 |
| W25um216G | um12033 | Rop1 HMG-box transcription factor (C-terminal fragment) | -4.67 |
| C112um175G | um02713 | pheromone response factor Prf1 | -3.46 |
| C40um002G | um03908 | related to TPO1 - Vacuolar polyamine-H+ antiporter | -3.48 |
| W80um222G | um01429 | related to high-affinity nickel transport protein nic1 | -1.90 |
| W15um043G | um02803 | related to beta-1,3-glucan binding protein | -1.85 |
| C59um169G | um11701 | related to NUP57 - nuclear pore protein | -1.73 |
| W75um036G | um02763 | conserved hypothetical protein | -1.73 |
| W3um239G | um11544 | putative protein | -1.66 |
| C115um126G | um02191 | Yap1, yeast AP-1-like protein | -1.66 |
| C30um119G | um15043.2 | probable ENA2 - Plasma membrane P-type ATPase | -1.59 |
| C50um031G | um03568 | related to regulatory protein alcR | -1.48 |

| | | | |
|---|---|---|---|
| C50um227G | um11816 | related to gamma-tubulin complex component 2 | -1.47 |
| C100um172G_s | um02888 | related to ADH6 - NADPH-dependent alcohol dehydrogenase | -1.45 |
| C74um213G | um03649 | hypothetical protein | -1.43 |
| W40um042G | um05693 | probable rho GDP dissociation inhibitor | -1.40 |
| C15um138G | um02642 | conserved hypothetical protein | -1.37 |
| UG24-13m16-100g1_RC | um00249 | conserved hypothetical protein | -1.31 |
| UG24-1d14-47c8_RC | um00813 | conserved hypothetical protein | -1.28 |
| C45um047G | um03593 | probable sterol delta 5,6-desaturase | -1.27 |
| C75um151G | um05721 | putative protein | -1.26 |
| W10um134G | um05114 | related to multidrug resistance protein 4 | -1.21 |
| W7um037G | um11284 | related to glycogenin-2 beta | -1.20 |
| W206um132G | um10187 | putative protein | -1.19 |
| W105um049G | um00102 | conserved hypothetical protein | -1.18 |
| CLUSTER61_RC | um06287 | related to Phytoene synthase | -1.16 |
| C40um200G | um11010 | conserved hypothetical protein | -1.15 |
| C52um255G | um04851 | conserved hypothetical protein | -1.13 |
| W26um225G | um01507 | putative protein | -1.11 |
| C30um157G | um02182 | probable NADPH-dependent beta-ketoacyl reductase (rhlG) | -1.11 |
| W25um225G | um10062 | related to monooxygenase | -1.10 |
| W10um087G | um11030 | putative protein | -1.09 |
| C147um157G | um02159 | related to amino acid transport protein | -1.04 |
| W25um140G | um10665 | related to acyl-CoA dehydrogenase | -1.04 |
| UG20-1a2-51h1_RC | um00823 | conserved hypothetical protein | -1.03 |
| W125um157G | um02164 | probable NDE1 - mitochondrial cytosolically directed NADH dehydrogenase | -1.01 |

Data were filtered for log2 foldchange > 1 and an adjusted p-value of <0.01 for the comparison.
*MUMDB (http://mips.helmholtz-muenchen.de/genre/proj/ustilago/) (05/2007).
The non-secreted enzymes that might play a role in modification of the fungal cell wall are highlighted in grey.
The target genes of the pheromone responsive MAPK cascade are highlighted in green.

To connect the reduction in *rop1* expression with the failure to express *prf1* and *mfa1* in FB1Δrak1, FB1Δrak1rop1$^{con}$ was generated by introduction of *rop1* in the *ip* locus of FB1Δrak1 under the control of *otef* promoter. The expression of *mfa1* and the response to pheromone stimulation was examined. The overexpression of *rop1* in FB1 increased the expression of *mfa1*, and the overexpression of *rop1* in FB1Δrak1 induced the expression of *mfa1* to a level that was higher than the basal expression in FB1 (Fig. 25A). Upon pheromone stimulation, FB1Δrak1rop1$^{con}$ formed conjugation tubes as efficiently as FB1 (Fig. 25B). Furthermore, FB1Δrak1rop1$^{con}$ could fuse with FB2 and develop white fuzziness on charcoal-containing plates (Fig. 25C). Collectively, these results indicate that *rak1* is required for the efficient expression of *rop1*.

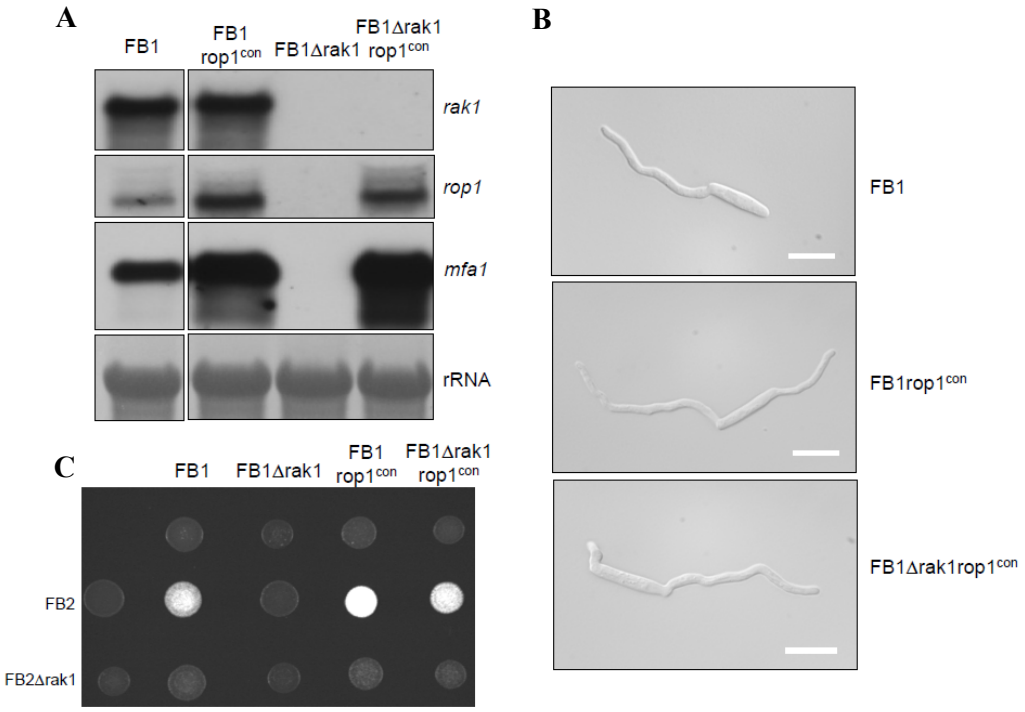


Figure 25 *rak1* is required for the expression of *rop1*. (A) Strains indicated on top were grown in CM medium with 1% glucose and RNA was prepared. 10 µg of total RNA was loaded in each lane and rRNA was stained with methylene blue as a loading control. The blot was hybridized successively with probes indicated on the right. (B) Strains indicated on the right were stimulated with synthetic a2 pheromone for 5 h. Bars, 10 µm. (C) Strains indicated on top were spotted alone and in combination with strains indicated on the left on charcoal-containing PD plates and incubated for 24 h at 28°C. Dikaryotic filaments display white fuzziness.

To test if the growth defect of FB1Δrak1 is also due to the abolishment of *rop1* expression, colony morphology of FB1Δrak1 and FB1Δrak1rop1$^{con}$ was compared. With respect to colony size and colony shape, both strains were similar, indicating that *rop1* is not responsible for the growth defect of FB1Δrak1 (Fig. 26).

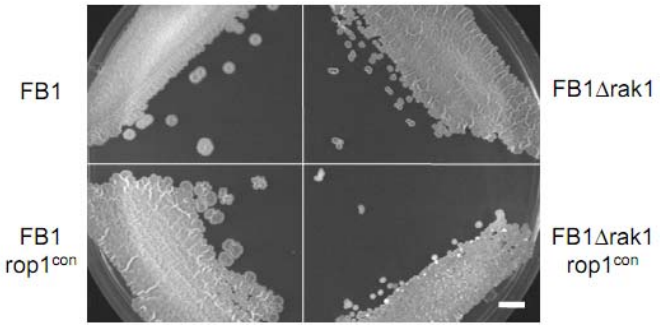


Figure 26 *rop1* does not suppress the growth defect of *rak1* deletion strain. Indicated strains were streaked on PD plates and incubated at 28°C for 2 d. Bar, 5 mm.

In addition, in the microarry data, *yap1*, one transcription factor, was found to be down-regulated more than threefold in FB1Δrak1 compared to FB1 (Table 2). To test whether *yap1* is involved in the regulation of *rop1* expression, the expression of *rop1* was analyzed in FB1Δyap1 by Northern blotting. In FB1Δrak1 the expression of *yap1* was reduced (Fig. 27A), which was consistent with the microarray result. However, in FB1Δyap1 the expression of *rop1* and *mfa1* was not dramatically affected compared to FB1 (Fig. 27B). This indicates that *yap1* is not the major regulator of *rop1* expression.

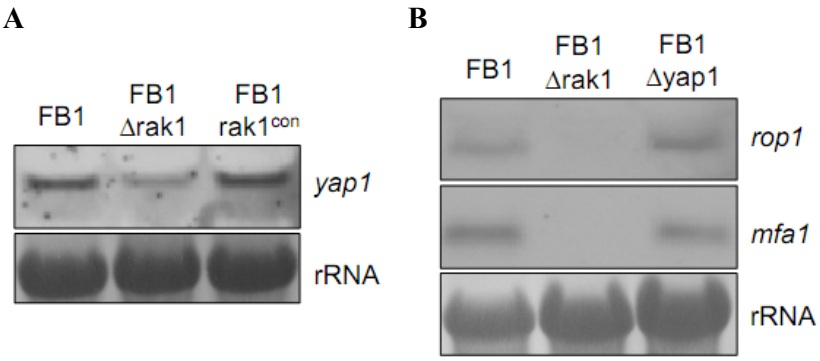


Figure 27 *yap1* is not the major regulator of *rop1* expression. (A) The deletion of *rak1* reduces the expression of *yap1*. The blot was hybridized with a *yap1* probe. (B) The deletion of *yap1* does not affect the expression of *mfa1* and *rop1*. The blot was hybridized successively with probes of *rop1* and *mfa1*. The indicated strains in (A) and (B) were grown in CM medium with 1% glucose. Total RNA was isolated and 10 µg of RNA was loaded in each lane. rRNA was stained with methylene blue as a loading control.

## 2.10 Which domains are essential for the function of Rak1?

To identify functional domains in Rak1, four truncated versions lacking different WD40 repeat domains were constructed under the control of the *otef* promoter (Fig. 28A) and integrated into the *ip* locus of SG200Δrak1. Filamentation and growth phenotypes were assayed. The introduction of full length *rak1* gene could complement the defect in filamentation and growth of SG200Δrak1 (Fig. 28B). None of these truncated versions could rescue the growth defect of SG200Δrak1, suggesting that the integrity of the β propeller structure might be crucial for this function. With respect to filamentation, WD37 version that lacks the N-terminal 92 aa of Rak1 could slightly rescue the filamentation defect; while all other versions could not.

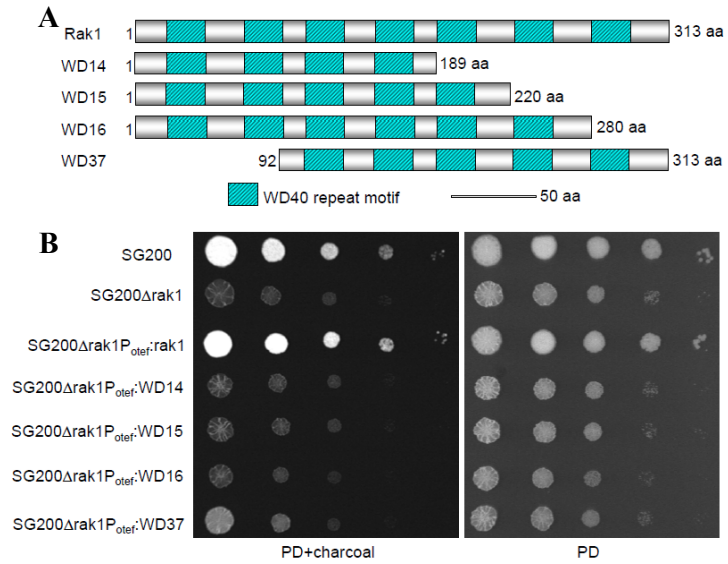


Figure 28 Mapping of functional domains of Rak1. (A) Schematic representation of truncated versions of Rak1. WD14: Rak1 lacking the C-terminal 190-313 aa; WD15: Rak1 lacking the C-terminal 221-313 aa; WD16: Rak1 lacking the C-terminal 281-313 aa; WD37: Rak1 lacking the N-terminal the 1-91 aa. (B) Complementation of filamentation and growth phenotypes by *rak1* truncated alleles. All truncated versions of Rak1 lacking different WD40 repeat domains were expessed under the control of the *otef* promoter and integrated in single copy into the *ip* locus of SG200Δrak1. Serial dilutions of the indicated strains on the left were spotted on charcoal-containing PD plates (left) and PD plates (right), and incubated at 28°C for 48 h.

## 2.11 Identification of Rak1 interactors by immunoprecipitation

To identify Rak1 interactors, a triple HA tag was fused to the 3'-end of *rak1* in the native locus. Upon synthetic a2 pheromone stimulation, the strain FB1rak1-HA could form conjugation tubes, indicating that Rak1-HA fusion protein is functional (data not shown). The synthesis of Rak1-HA was verified by Western blotting (data not shown). Subsequently, Rak1-HA immunoprecipitation was performed using an anti-HA affinity matrix. After elution with glycine-HCl (pH 2.5), the samples were precipitated with acetone, digested with trypsin and analyzed by LC-MS in collaboration with J. Kahnt. Fifty-four proteins were co-precipitated with Rak1-HA. Among of them, thirty-two are ribosomal proteins; four are involved in metabolism and energy production; five are related to cell division, DNA replication and rRNA processing protein, one is related to an UDP-galactose transporter and twelve of them are putative or conserved hypothetical proteins (Table 3).

**Table 3 Rak1 interactors identified by LC-MS from Rak1-HA immunoprecipitation experiment**

| Um number* | Peptides obtained from LC-MS | Function annotation* |
|---|---|---|
| | | Ribosomal proteins |
| Um10702 | AVYAHFPINIIIAGDKK | probable RPL9A - ribosomal protein L9.e |
| Um00862 | LTVPGLPR<br>WAQSGWAK<br>AIIDSPSTGVTR<br>SLSDFDRFNVMLLK | probable RPL14B - ribosomal protein |
| Um03533 | KVMPAVVVR<br>FVIAVHGIGAR<br>NLFVIAVHGIGAR<br>LNRLPAAAAGDMVVASVK | probable RPL23A - 60S large subunit ribosomal protein L23.e |
| Um02773 | AFLVEEAK<br>YLHVQKR<br>EYGTISKR | probable RPL34B - ribosomal protein L34.e |
| Um10701 | NGFQTGSAGK<br>NGFQTGSAGKK | probable RPL37A - ribosomal protein L37.e |
| Um11259 | SHVALKR<br>QKNAALVF<br>HFELGGDKK | probable RPL42B - ribosomal protein L36a.e |
| Um11412 | KIEISQHSK | probable RPL43B - 60S large subunit ribosomal protein |
| Um01060 | HYLGLR<br>QRDIVDGK<br>IPSWFLNR<br>AGELNSDELER<br>IKVQYALTQIK<br>SSQLLSNNIDSK<br>IVTILQNPAEFK<br>RAGELNSDELER | probable RPS18A - ribosomal protein S18.e.c4 |
| Um11551 | SGKIEVPTWVDIVK<br>EQAPYNPDWFYVR<br>GFRPSHHADASGSVQR<br>DVDASTFIDAYAQHLK<br>DVDASTFIDAYAQHLKR | probable RPS19B - ribosomal protein S19.e, cytosolic |
| Um00867 | ISVLNDALNSIVNAER | probable RPS22A - ribosomal protein S15a.e.c10, cytosolic |
| Um04488 | QTGQYVYPGQIIFR<br>YIAVSPNPETTFPLPAGTPR | related to MRP7 - mitochondrial ribosomal protein, large subunit |
| Um04632 | LASVPAGGAAPAAAAAGGAAP<br>AAAGAAK | probable ribosomal protein P2 |
| Um11619 | AGNLGDHVQITR<br>FFIDFSGPANDGILDAAAFEK | probable ribosomal protein L22 |
| Um04588 | YYKVDGDGNIK<br>LTFMFEEGTKPPTA | probable ubiquitin/ribosomal protein S27a fusion protein |
| Um04855 | WVINIER<br>DDEVLIVR<br>KWVINIER<br>AHFDAPAHIR<br>KAHFDAPAHIR<br>AHFDAPAHIRR<br>TNGATVPLGIHPSNVVITSLK<br>EKTNGATVPLGIHPSNVVITSL<br>K<br>TNGATVPLGIHPSNVVITSLKL<br>DEDR | probable 60S ribosomal protein L26 |
| Um10051 | LNQEVWK<br>SALNDVVTR<br>EYTVNLHKR<br>AIKEVVAFAQK<br>LYTYAVPVLGLGTAK | probable 60S ribosomal protein L31 |
| Um10147 | IGPLGLSPK<br>ATGGEVGASSALAPK | probable 60S ribosomal protein L12 |
| Um10182 | ADNKIQYNAK | probable 60S ribosomal protein L39 |
| Um10621 | GIDSAVR<br>HLMPNGYR<br>HLMPNGYRR | probable 60S ribosomal protein L32 |

| | | |
|---|---|---|
| | DVELLLMHNGVYAAEIAHNVS SK | |
| Um11716 | MIPGQSTNFPLSGFVR | probable 40S ribosomal protein S21 |
| Um11914 | KVHGSLAR<br>FVNVVAGPGGK<br>RFVNVVAGPGGK | probable 40S ribosomal protein S30 |
| Um11135 | LVQNPNSFFMDVK<br>TLAVDLLNPSAEQQAR | probable 40S ribosomal protein S27 |
| Um11202 | VEFMDETRR<br>ADDILALLESER<br>ADDILALLESEREAR<br>GPVKADDILALLESER | probable 40S ribosomal protein S28 |
| Um10334 | FKFPDNSLELYAEK | probable 40S ribosomal protein S3 |
| Um10360 | TPGPGAQAALR<br>IEDVTPVPTDSTR<br>IEDVTPVPTDSTRR<br>IGRIEDVTPVPTDSTR | probable 40S Ribosomal protein S14 |
| Um10469 | NAVYTPHTAGR | probable 40S ribosomal protein S5 |
| Um05040 | HVVFVGQR | probable 40S ribosomal protein S7 |
| Um01318 | ALIHDGLAR<br>GAMSIEDALQEVLK<br>GAMSIEDALQEVLKK | probable 40S ribosomal protein S12 |
| Um10114 | VFEPVLVVGEDKFSTVDIR | probable 40S ribosomal protein S16 |
| Um11535 | AEAPPNEKPATVK<br>AKAEAPPNEKPATVK | probable 40S ribosomal protein S15 |
| Um03237 | TWDHFEMR<br>LIDLHSPSEIVK | probable 40S ribosomal protein S20 |
| Um04965 | LASFQGAYLPLLR | related to Signal recognition particle 14 kDa protein |
| | | Metabolism and energy production |
| Um06158 | FAFEADKVR<br>QVLQDSRAAVGGGDVG | probable glutaminase A |
| Um06460 | IMLTNVIR<br>SQQVCDQIAK | probable fatty acid synthase, beta and alpha chains |
| Um03537 | RNAASPALR | probable ornithine carbamoyltransferase precursor |
| Um10180 | MESVVGFYK | related to ATP17 - ATP synthase complex, subunit f |
| | | Cell division, DNA replication and rRNA processing protein |
| Um02427 | GRGNGMK<br>AGVTSKQGDNDGR | related to negative regulator of mitosis |
| Um02989 | RAMELGR<br>RVLDADLQK | related to IME4 - positive transcription factor for IME2 |
| Um04368 | GVQSSVR | related to endo-1,3 (4)-beta-glucanase |
| Um02579 | QNDSPSGKK | related to RFA2 - DNA replication factor A, 36 kDa subunit |
| Um03354 | FSPDDKFSR<br>FGILPTQLPAKPL | probable NOP10 - nucleolar rRNA processing protein |
| | | Transporter |
| Um05783 | MIAILLK | related to UDP-galactose transporter |
| | | Function unknown |
| Um11475 | DRQVQASNVQR<br>QDDRQVQASNVQR | putative protein |
| Um10436 | GVAKLLLQR<br>DQLSYALLAK | putative protein |
| Um11830 | EVSFGQEDLDWMSVGGR | conserved hypothetical protein |
| Um01187 | EAGDKAFK | conserved hypothetical protein |
| Um05833 | SKLPIDLR | conserved hypothetical protein |
| Um02861 | NSGGNSLFDAHK | conserved hypothetical protein |
| Um04007 | LLPLPSASKPTLR<br>YEAQHEQEKEQYER | conserved hypothetical protein |
| Um10545 | SSSAGAPAQARL | conserved hypothetical protein |
| Um05270 | DMAAQLWLK | conserved hypothetical protein |
| Um05380 | GPLLPLADTWSSR | conserved hypothetical protein |
| Um05438 | AEYLTGFR<br>ANGASATAPSKVEVLPPSSR | conserved hypothetical protein |
| Um01012 | ERNAAVLGAQR<br>SSSSFLPSQIQR | conserved hypothetical protein |
| | | Control protein |
| Um10146 | SIVDELKPEFTGVGK<br>GWITAIATSQENPDLLLTA | Rak1 |

*MUMDB (http://mips.helmholtz-muenchen.de/genre/proj/ustilago/) (05/2007).

Um04007 is annotated as a conserved hypothetical protein and contains one high-mobility-group box domain, which may indicate a role in transcriptional regulation. The interaction between Rak1 and Um04007 was analyzed by yeast two hybrid assay. On SD medium without Leu/Trp/His, the yeast strain co-transformed with pGBKT7-Rak1 and pGADT7-Um04007 could not grow (Fig. 29A). Western blotting analysis indicated that both fusion proteins were expressed in AH109 (Fig. 29B), suggesting that there is no direct interaction between Rak1 and Um04007.

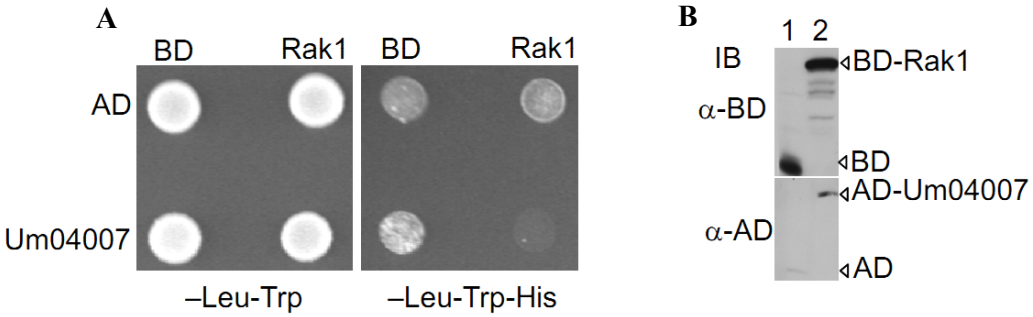


Figure 29 Yeast two hybrid assay for analyzing the interaction between Rak1 and Um04007. (A) After co-transforming pGBKT7 or pGBKT7-Rak1 (indicated on top) and pGADT7 or pGADT7-Um04007 (indicated on the left) in AH109. The indicated strains were grown in SD-Leu-Trp medium overnight. Cells were spotted on selective plates (-Leu-Trp) and on medium stringency plates (-Leu-Trp-His), and incubated for 3-5 d at 28°C. (B) Western blotting analysis for protein expression in yeast. Lane 1: AH109 co-transformed with control vectors; lane 2: AH109 co-transformed with pGBKT7-Rak1 and pGADT7-Um04007. Proteins were detected with antibodies against the Gal4 binding domain (top panel) and against the Gal4 activation domain (bottom panel). The fusion proteins are indicated by arrowheads on the right.

# 3 Discussion

In this study, Rak1, a conserved seven-WD40 repeat motif containing protein of *U. maydis*, was shown to regulate mating, filamentation as well as pathogenic development. Many of these defects could be attributed to defects in *rop1* gene expression in *rak1* deletion mutants. In addition, *rak1* was shown to regulate cell growth, colony morphology and response to cell wall stressors.

## 3.1 Rak1 is involved in cell growth and cell wall biosynthesis

An involvement of Rak1 orthologs in regulation of cell growth and stress response was found in other fungi like *T. brucei* (Rothberg *et al.*, 2006), *S. cerevisiae* (Coyle *et al.*, 2009) and *S. pombe* (Nunez *et al.*, 2009; Shor *et al.*, 2003). In *T. brucei track1* is essential for cell survival, the depletion of *track1* by RNAi leads to growth arrest and its overexpression causes a slow growth phenotype (Rothberg *et al.*, 2006). In *S. cerevisiae*, Asc1p was shown to exist in both a ribosome- and a non-ribosome-associated form during stationary growth (Baum *et al.*, 2004). Based on the analysis of mutated alleles with reduced ribosome binding affinity, it was concluded that ribosome-bound Ascp1p might play a role in the translational regulation of genes involved in cell wall integrity. For normal growth Asc1p localization at the ribosome appears to be less important (Coyle *et al.*, 2009). In *S. pombe* the ribosome-bound Cpc2 negatively regulates the cell wall integrity transduction pathway by favouring translation of the tyrosine-phosphatases Pyp1 and Pyp2 that deactivate the MAP kinase Pmk1 (Nunez *et al*., 2009). In *U. maydis*, the *rak1* gene was constitutively expressed and Rak1 protein localized in the cytoplasm as well as membrane fraction. Expression of *rak1* in an asc1Δ mutant of *S. cerevisiae* could partially complement the growth defect of at elevated temperature, indicating that Rak1 could to some extent replace some function of Asc1p. The *rak1* deletion strain is viable, shows a doubling time increase of 27% and increased sensitivity to cell wall stressors. Some of these phenotypes could be attributed to a potential role of Rak1 as a ribosomal protein as described for Asc1p in *S. cerevisiae* (Coyle *et al*., 2009) and Cpc2 in *S. pombe* (Nunez *et al*., 2009). Cell growth and division are coupled by multiple conserved mechanisms, such as protein synthesis and cell cycle control (Jorgensen *et al.*, 2002). In *U. maydis* thirty-one ribosomal proteins that locate at 40S and 60S subunits were precipitated by Rak1 immunoprecipitation, suggesting that Rak1 is likely to be a ribosomal protein or at least binds to ribosomal

proteins in *U. maydis*. In addition, a signal recognition particle protein, Um04965 was also precipitated. This protein might be involved in the targeting of the translating peptide to ER membrane (Halic *et al.*, 2004). The co-precipitation of Rak1 with Um04965 and components of translating eukaryotic 80S ribosome which is assembled by the 40S and 60S subunits (Armache *et al.*, 2010) suggests that during log-phase growth Rak1 is localized in the translating ribosome and the deletion of *rak1* may therefore affect the protein synthesis in *U. maydis*. Among the precipitated ribosomal proteins, Um10621, its ortholog Rpl32-2 has been shown to interact with Cpc2 in *S. pombe*. Cpc2 forms a complex with MOC1/2/3 and Rpl32-2, which may act as a translational regulator involved in the control of sexual differentiation (Paul *et al.*, 2009). An additional binding partner of Rak1 is Um02427, a protein related to a negative regulator of mitosis that localizes in the nucleus of budding cells (data not shown). In *S. cerevisiae* its homolog Acp1 acts as one subunit of the APC/C complex which is a ubiquitin ligase essential for the completion of mitosis in all eukaryotic cells (Herzog *et al.*, 2009; Matyskiela and Morgan, 2009). The identification of Acp1 homolog by Rak1 immunoprecipitation points out that Rak1 may regulate the cell cycle of *U. maydis*.

In *S. cerevisiae*, calcofluor white binds primarily to chitin and the change of cell wall chitin content affects the response to calcofluor white. The deletion of *asc1* exhibits elevated levels of chitin and increased sensitivity to calcofluor white (Coyle *et al.*, 2009; Lesage *et al.*, 2005). In *U. maydis*, the sensitivity towards cell wall stressors might result from the change in the cell wall composition. In line with this assumption, the microarray analysis revealed that in the *rak1* deletion mutant three cell wall modifying enzymes were induced, two chitin deacetylases and one chitinase. The deregulation of these genes might affect the chitin content of cell wall and hence lead to increased susceptibility towards cell wall stressing agents. Collectively, these outcomes indicate that the role of Rak1 in the regulation of cell growth and cell wall biosynthesis (Fig. 30A) is conserved not only in ascomycete, but also in basidiomycete fungi.

### 3.2 Rak1 does not act as a Gβ subunit in cAMP signaling pathway

In *S. cerevisiae* Asc1p acts as a negative regulator of cAMP signaling by directly binding to GDP-Gpa2 and inhibiting Gpa2 guanine nucleotide exchange (Zeller *et al.*, 2007). In *C. neoformans* Gib2 has been shown to interact with Gα subunit Gpa2 and

two Gγ subunits Gpg1 and Gpg2. This allows Gib2 to act as an atypical Gβ subunit in cAMP signaling, positively regulating melanization and capsule formation (Palmer *et al.*, 2006). In mammalian cells, RACK1 was also shown to bind retinal Gβ1γ1 *in vitro*. The association with Gβγ promotes the translocation of RACK1 from the cytosol to the membrane and specifically inhibits Gβγ-mediated activation of phospholipase C β2 and adenylyl cyclase II (Chen *et al.*, 2004; Dell *et al.*, 2002). The predicted β-propeller structure of Rak1 is similar to the structure determined for Asc1p and Gib2, which led me to test the hypothesis that Rak1 acts as a Gβ subunit in *U. maydis*. Three lines of evidence suggest that Rak1 is unlikely to function as a Gβ subunit in the cAMP signaling pathway. First, at the genetical level, the *rak1* deletion strain shows yeast-like growth, colonies are non-filamentous and donut-shaped. This situation is different from the phenotypes of disruption or hyperactivation in the cAMP signaling pathway: the deletion of adenylyl cyclase *uac1*, protein kinase A catalytic subunit *adr1* or Gα subunit *gpa3* leads to the constitutively filamentous growth (Durrenberger *et al.*, 1998; Gold *et al.*, 1994; Regenfelder *et al.*, 1997), while the deletion of the PKA regulatory subunit *ubc1* or expression of a constitutively active form of *gpa3* results in a multiple-budding phenotype and glossy colony phenotype, respectively (Gold *et al.*, 1994; Regenfelder *et al.*, 1997). Second, at the transcriptional level, the induction of the cAMP signaling pathway negatively regulates *crk1* expression, i.e. the deletion of *gpa3* or *uac1* enhances the expression of *crk1* (Garrido and Perez-Martin, 2003). Here I have shown that the deletion of *rak1* does not affect the expression of *crk1*. In addition, the disruption of the cAMP signaling pathway abolishes the expression of *frb34* and *fer2* (Brachmann *et al*., 2001; Eichhorn *et al*., 2006), while in Δrak1 strain an up-regulation of *frb34* expression was observed and *fer2* expression was unaffected with respect to wild type strain. Furthermore, the constitutive expression of *adr1* in the *rak1* deletion strain could not induce *mfa1* expression, suggesting that the regulation of *mfa1* expression by Adr1 is dependent on the presence of *rak1*. Adr1 regulates *mfa1* expression by the phosphorylation of Prf1 (Kaffarnik *et al.*, 2003). The deletion of *rak1* abolishes the expression of *prf1*, which explains the inability of Adr1 to induce *mfa1* expression in the *rak1* deletion mutant. The transcriptome comparison of FB1Δrak1 and FB1Δgpa3 showed that only 18 genes are differentially regulated by both *rak1* and *gpa3*. Ten of these differentially regulated genes have unknown functions and for five genes the expression changes in the respective deletion mutants have opposite consequences

(Table 4). If Rak1 would function as a Gβ subunit in the cAMP signaling pathway, one would expect that more differentially regulated genes are overlapped in *rak1* and *gpa3* deletion mutants. Third, at the biochemical level, conventional or non-conventional Gβ subunits physically and directly associate with Gα subunits (Hoffman, 2007; Palmer *et al.*, 2006; Zeller *et al.*, 2007). In *U. maydis* an interaction between Rak1 and Gα subunit Gpa3 or between Rak1 and Gγ subunit Gpg1 (Um11029) by yeast two hybrid assay or co-immunoprecipitation could not be demonstrated. In *Arabidopsis thaliana*, it was also not possible to demonstrate a direct interaction between RACK1 and G proteins by genetic or biochemical approaches (Guo *et al.*, 2009). In *S. pombe* Cpc2 was found to function independently of PKA pathway (McLeod *et al.*, 2000). Nevertheless, in *U. maydis* the application of exogenous cAMP to the *rak1* deletion strain could partially rescue the expression of *mfa1* and mating. Most likely this reflects that except for PKA, cAMP has additional as yet indentified targets which affect *mfa1* or *prf1* expression (Hartmann *et al.*, 1999; Kruger *et al.*, 1998).

**Table 4 List of differential expressed genes which are differentially regulated in both FB1Δgpa3 and FB1Δrak1 strains**

| um number[a] | Annotation[a] | Fold change in FB1Δgpa3[b] | Fold change in FB1Δrak1 |
|---|---|---|---|
| **Um05272** | **conserved hypothetical protein** | **-3.2** | **2.31** |
| **Um01812** | **conserved hypothetical protein** | **-2.4** | **2.17** |
| **Um10815** | **conserved hypothetical protein** | **-2.2** | **8.8** |
| **Um01775** | **conserved hypothetical protein** | **-2.2** | **3.23** |
| **Um02763** | **conserved hypothetical protein** | **2.2** | **-4.45** |
| Um00102 | conserved hypothetical protein | -7.2 | -2.27 |
| Um11544 | putative protein | -5.2 | -3.16 |
| Um03568 | related to regulatory protein alcR | -2.2 | -2.79 |
| Um01926 | related to DAL2 - allantoinase | 2.1 | 5.57 |
| Um04145 | conserved hypothetical Ustilago-specific protein | 2.5 | 2.71 |
| Um03116 | conserved hypothetical protein | 2.5 | 3.6 |
| Um11922 | related to Chitin deacetylase precursor | 3.6 | 3.45 |
| Um01656 | probable sugar transporter | 4.1 | 4.00 |
| Um00196 | probable FUN34 - transmembrane protein involved in ammonia production | 5.1 | 2.68 |
| Um10636 | conserved hypothetical protein | 5.4 | 2.38 |

Data were filtered for more than two fold change and an adjusted p-value of <0.05 for the comparison.
a. MUMDB (http://mips.helmholtz-muenchen.de/genre/proj/ustilago/) (05/2007).
b. Data from Greilinger (2007).
Genes with opposite expression levels in FB1Δgpa3 and FB1Δrak1 are labeled in bold.

## 3.3 *rak1* is involved in the regulation of gene expression

### 3.3.1 *rak1* regulates the expression of *rop1*

The deletion of *rak1* in *U. maydis* abolishes the expression of *a* and *b* genes, impairs conjugation tube formation and causes a strong mating defect. Three lines of evidence indicate that these defects are caused by severely reduced basal expression of *prf1*. First, in the absence of *rak1*, *prf1* transcripts were undetectable. Second, a *rak1* deletion strain harboring a constitutively expressed pheromone receptor gene *pra1* could form conjugation tubes, express *mfa1* upon pheromone stimulation and mate. The expression of *pra1* leads to the restoration of pheromone perception, which also indicates that Rak1 does not play a role in transduction of the pheromone stimulation in the MAPK signaling pathway. Perception of pheromone by the presence of pheromone receptor leads to activation of the pheromone responsive MAPK cascade, which in turn induces the expression of *prf1*, thus restoring *prf1*-dependent downstream signaling in the *rak1* deletion mutant. In addition, I could not observe the interaction between Rak1 and Fuz7 or Rak1 and Kpp2 by co-immunoprecipitation or yeast two hybrid (data not shown). Third, the constitutive expression of *prf1* rescued the defect in conjugation tube formation in the *rak1* deletion strain upon pheromone stimulation. Since *crk1* expression was not affected by the absence of *rak1*, it was unlikely that *rak1* acts as a regulator of *crk1* expression. Interestingly, DNA microarray analysis revealed that the expression of *rop1*, besides *mfa1*, was the most down-regulated gene in the *rak1* deletion mutant. Rop1 is a transcriptional regulator of *prf1*, its deletion leads to the abolishment of *prf1* expression in axenic culture in *U. maydis* (Brefort *et al.*, 2005). I could show that the constitutive expression of *rop1* in the *rak1* deletion mutant rescues the expression of *mfa1*, leads to conjugation tube formation upon pheromone stimulation and restores the mating ability, while it could not restore the growth defect. The finding that *rak1* regulates the expression of *rop1* in axenic culture could explain the phenotypes of the *rak1* deletion mutant related to conjugation tube formation, mating and filamentation (Fig. 30A). Rak1 homologous proteins of other fungi are also involved in regulation of cellular differentiation as in *N. crassa* the deletion of *cpc-2* leads to female infertility (Müller *et al.*, 1995) and in *A. nidulans cpcB* regulates a control point for sexual development (Hoffmann *et al.*, 2000).

Tup1 (Um03280), is a general transcription repressor in *U. maydis*. Its deletion leads to similar phenotypes to the deletion of *rak1* like loss of *mfa1* expression and mating,

abolishment of *rop1* expression and reduction in tumor formation (Elias-Villalobos, personal communication). In FB1Δrak1 the expression of *tup1* was not affected compared to FB1 and overexpression conditions of *rak1* (data not shown), suggesting that the defect of *rop1* expression in *rak1* deletion mutant is not affected by *tup1*. In addition, *yap1*, one of the the down-regulated transcription factors in the *rak1* deletion mutant was not associated with the regulation of *rop1* expression. The expression of *rop1* is repressed by cAMP signaling and enhanced by MAPK signaling, and the phosphorylation of Kpp2 is required for the basal expression of *rop1* (Brefort *et al.*, 2005). In the microarray analysis the expression of *um02103*, annotated as a probable activator of the phosphotyrosyl phosphatase activity of PP2A, was twofold increased in the *rak1* deletion mutant. In animal cells, PP2A has been shown to dephosphorylate the MAP kinases (Letourneux *et al.*, 2006; Liu and Hofmann, 2003; Silverstein *et al.*, 2002). I speculate that the activation of PP2A in the *rak1* deletion mutant is likely to affect the status of Kpp2 phosphorylation and leads to reduced expression of *rop1*.

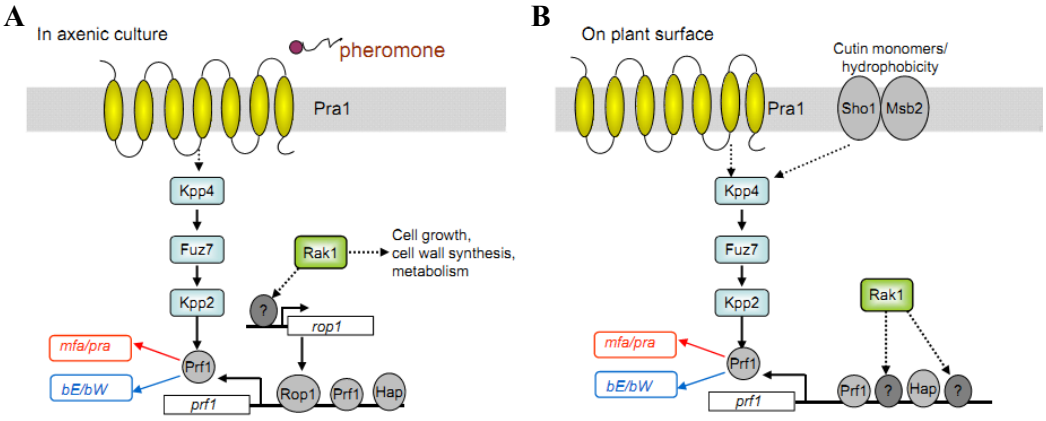


Figure 30 Model of Rak1 regulating *prf1* expression in *U. maydis*. (A) In axenic culture, Rak1 regulates the expression of *rop1* via an unknown component (labeled with question mark) and indirectly regulates the expression of *prf1*. In parallel, Rak1 also plays additional roles, for example, involvement in the regulation of cell growth, cell wall synthesis. (B) On plant surface, Rak1 regulates the expression of *prf1* by an unidentified transcription factor (labeled with question mark). Rak1 may either regulate the expression of unidentified transcription factor or post-transcriptionally regulate its function.

### 3.3.2 *rak1* regulates the expression of genes involved in metabolism and energy

In addition to specifically regulating the expression of genes downstream of the MAPK pathway, the deletion of *rak1* also up-regulates the expression of genes involved in metabolism, energy, virulence and resistance, and alcohol fermentation. The up-regulation of genes involved in energy may lead to increase in ATP production and oxidative stress by reactive oxygen species, affecting cell growth (Ikner and Shiozaki,

2005). In *S. pombe* Rds1 represents a general stress protein and its expression was up-regulated under stress conditions (Chen *et al.*, 2003; Ludin *et al.*, 1995). In the *rak1* deletion mutant, *um00723*, a homolog of *rds1* was found to be up-regulated. This could indicate that the *rak1* mutant is showing signs of a stress response even during exponential growth under non-stressing conditions. The involvement of Rak1 homologs in the transcriptional regulation of genes related to metabolism was also demonstrated in *S. pombe* (Shor *et al.*, 2003) and *S. cerevisiae* (Hoffmann *et al*., 1999). In *S. pombe* the deficiency of *cpc2* decreases the gene expression of *sam1* and *thi2* which are involved in methionine biosynthesis (Shor *et al.*, 2003). In *S. cerevisiae asc1* negatively affects the expression of Gcn4-regulated genes, e.g. *his3, his7* and *aro4* genes. Asc1p regulates the expression of amino acid biosynthesis genes by repressing the Gcn4 protein activity (Hoffmann *et al*., 1999). An ortholog of Gcn4 protein could not be identified by bioinformatic analysis in *U. maydis* (data not shown).

In the microarray analysis of the *rak1* mutant, three genes involved in protein synthesis, translation elongation factor HBS1 (*um04216*), eukaryotic translational release factor 1 (*um04192*) and signal recognition particle receptor SRP101 (*um01242*) were also found to be up-regulated in the *rak1* deletion mutant, which may affect the process of protein synthesis. Changes in the translation of mRNA transcripts for transcription factors might result in overall changes in gene expression of a variety of genes e.g. involved in metabolism and energy. So far, the mechanism how Rak1 influences the expression of genes involved in metabolism (Fig. 30A) remains unclear.

### 3.4 Integrity of β-propeller structure is required for the function of Rak1

Rak1 has 7 WD40 repeat domains and is predicted to fold into a seven-bladed β-propeller structure. Each propeller blade consists of a four-stranded anti-parallel β-sheet (Ullah *et al.*, 2008). Rak1 does not have a coiled-coil domain normally found at the N-terminus of Gβ subunits (Ullah *et al.*, 2008; Zeller *et al.*, 2007). In *S. cerevisiae* Rak1 and different truncated alleles fused to Gal4 DNA-binding domain could be expressed (data not shown). The integration of *rak1* gene into the *ip* locus in SG200Δrak1 complements the filamentation and growth phenotypes, while different truncated alleles of Rak1 lacking the N-terminal or C-terminal WD40 domains could not restore the defect in filamentation and growth phenotype. This suggests that the integrity of β-propeller structure is crucial for its function. Currently, the information about the three-

dimensional structure of Rak1 homologs are based on the whole proteins (Sengupta *et al.*, 2004; Ullah *et al.*, 2008). However, how the truncations of different WD40 repeat domains affect the three-dimensional structure of Rak1 homologs is not known. The generation of different point mutations of Rak1 will contribute to study the functional domains of Rak1 and distinguish the different roles of Rak1 in regulating cell growth and filamentation. Mutational studies imply that blades 5 and 6 act as major docking stations for interaction with RACK1 (Chang *et al.*, 2001; Sengupta *et al.*, 2004; Steele *et al.*, 2001). The mutations of *S. cerevisiae* Asc1p at Arg38 and Lys40 (Arg36 and Lys38 in mammalian RACK1) disrupt the Asc1p interaction with the 40S subunit (Sengupta *et al.*, 2004) and leads to increased sensitivity towards calcofluor white (Coyle *et al.*, 2009). In *U. maydis*, the positions 36 and 38 are both Arginine and not as in the previously studied models (Sengupta *et al.*, 2004). Lysine and Arginine are basic and electrically charged amino acids, which may play the same role in the binding with the ribosome. This hints towards a role of these conserved residues for the function of Rak1 in *U. maydis*. Mammalian RACK1 is phosphorylated at Tyr228 and/or Tyr246 by tyrosine kinase Src (Chang *et al.*, 2001). In *T. brucei* tyrosine residue phosphorylation on TRACK1 was undetectable (Rothberg *et al.*, 2006). Both amino acids are also conserved in Rak1, in axenic culture I did not observe migration shift of Rak1 on SDS gel (Fig. 12D) and no Src kinase homolog could be identified by bioinformatic analysis (data not shown). The possible presence of some kinase which plays a similar role to Src kinase could not be ruled out. Determining the role of these phosphorylation sites for the function of Rak1 would require additional experiments with strains carrying point mutations in the respective phosphorylation sites rendering them non-phsophorylatable.

### 3.5 Rak1 is involved in pathogenic development

Rak1 homologs play an important role in virulence in the pathogens *C. neoformans, T. brucei* and *Candida albicans* (Kim *et al.*, 2010; Liu *et al.*, 2010; Palmer *et al.*, 2006; Rothberg *et al.*, 2006). In *C. neoformans,* Gib2 is essential for cell survival, acts as a Gβ subunit and positively regulates virulence by cAMP signaling pathway (Palmer *et al.*, 2006). In *C. albicans,* the deletion of *asc1* leads to a severe defect in hyphal development under hypha-inducing conditions and attenuates virulence (Kim *et al.*, 2010; Liu *et al.*, 2010). In *U. maydis* the deletion of *rak1* significantly reduces filamentation and virulence and these defects could be partially rescued by

constitutively expressing the bE1/bW2 heterodimer. This indicates that the primary virulence defect is due to the insufficient expression of *b* genes. The pheromone responsive MAP kinase module is essential for the response to both hydrophobic surface and fatty acids (Mendoza-Mendoza *et al.*, 2009a). In HA103Δkpp4 or HA103Δfuz7, the constitutive expression of *b* heterodimer rescues the filamentation defect, while tumor formation on planta cannot be observed (Muller *et al.*, 2003b). In contrast to HA103Δkpp4 and HA103Δfuz7, HA103Δrak1 could induce tumor formation even though it was slightly weaker than in the progenitor strain. This suggests that in *rak1* deletion mutant, the stimuli of hydrophobic surface and fatty acids still can be perceived and transmitted through the MAP kinase module. Therefore Rak1 does probably not play a direct role in the integration of the plant stimuli into the MAPK module. However the response to these stimuli and the disease symptoms accordingly are weaker in the *rak1* mutant, probably due to the lowered expression of *prf1*.

Since the *rop1* deletion strain could express *prf1* after perception of the plant stimuli and subsequently induce tumor formation after infection (Brefort *et al*., 2005), it is unlikely that the virulence defect of the *rak1* deletion mutant results from insufficient *prf1* expression only via *rop1*. It has been speculated that the role of *rop1* during biotrophic development is taken over by an as yet unidentified transcription factor (Brefort *et al*., 2005). Eleven transcription factors were found to be up-regulated in SG200 in response to the hydrophobic stimulus alone, while under appressorium inducing conditions, i.e. in the presence of fatty acids, 26 transcritption factors are significantly induced (P. Berndt, personal communication). The crucial role of *rak1* during pathogenic development implies that this unknown transcription factor is either not expressed in the *rak1* deletion mutant or needs Rak1 post-transcriptionally for its function (Fig. 30B). Further, Rak1 could also regulate translation or somehow affect the signal transduction in the conserved MAPK module leading to severely reduced *prf1* expression. The transcriptional pattern of the down-regulated genes in the *rak1* mutant revealed by microarray analysis argues for a very specific role of *rak1* in the regulation of the genes involved in the regulation of mating and pathogenic development. The identification of a possible transcription factor and whether Rak1 contributes in any way to the signal transduction of the pheromone responsive MAPK cascade will constitute an important task for future studies.

# 4 Materials and Methods

## 4.1 Chemicals, Enzymes, Buffers and Solutions

### 4.1.1 Chemicals and enzymes

All chemicals used in this study were purchased from Sigma, Fluka, Merck, Roche and Invitrogen.

Restriction enzymes and Phusion™ High-Fidelity DNA Polymerase were purchased from New England Biolabs (NEB) and were used as specified by the manufacturer. T4 ligase was obtained from Roche. *Taq* DNA Polymerase was purchased from Fermentas.

### 4.1.2 Buffers and solutions

Standard buffers and solutions were prepared according to Ausubel *et al*. (1987) and Sambrook *et al*. (1989). Specific buffers and solutions are listed with the corresponding methods.

### 4.1.3 Kits

The following kits were used following protocols recommended by the suppliers:

TA Cloning Kit (Invitrogen) for direct cloning of PCR products, Wizard SV Gel and PCR clean-up system (Promega) for DNA extraction from gels, QIAquick plasmid Purification Kit (QIAGEN) for plasmid isolation and purification, Western Blotting Detection Kit (GE Healthcare) for chemiluminescene detection. Genechip 3' IVT express kit (Affymetrix) for DNA microarray analysis.

## 4.2 Media

### 4.2.1 Media for *E. coli* growth

*E. coli* was grown in liquid dYT medium and on YT agar or LB agar plates (Ausubel *et al.*, 1987; Sambrook *et al.*, 1989).

**dYT:** 20 g Trypton, 10 g Yeast-Extract, 5 g NaCl, dd$H_2O$ was added to 1 liter following autoclaving at 121°C for 5 min.

**YT agar:** 10 g Trypton, 5 g Yeast-Extract, 5 g NaCl, 20 g Bacto Agar (Difco), dd$H_2O$ was added to 1 liter following autoclaving at 121°C for 5 min.

### 4.2.2 Media for yeast growth

**YPD:** 10 g Yeast extract, 20 g Peptone, dd$H_2O$ was added to 960 ml following autoclaving at 121°C for 5 min. 40 ml of 50% (w/v) glucose was added for yeast growth. For solid media, agar was added to a final concentration of 2%.

**Synthetic complete medium without uracil (SC-Ura):** 6.7 g Difco Yeast Nitrogen Base (w/o amino acids), 20 g galactose, 100 ml of 10X Drop-out Mix without Ura, 20 g Difco Bacto Agar. dd$H_2O$ was added to 1 liter and adjust the pH to 5.8 with 5 M NaOH following autoclaving at 121°C for 5 min.

**10X Drop-out Mix without Uracil**: Adenine hemisulfate 200 mg/L, Arginine HCl 200 mg/L, Histidine HCl 200 mg/L, Isoleucine 200 mg/L, Leucine 200 mg/L, Lysine HCl 200 mg/L, Methionine 200 mg/L, Phenylalanine 300 mg/L, Serine 200 mg/L, Tryptophan 300 mg/L, Tyrosine 200 mg/L, Valine 900 mg/L. Autoclaved at 121°C for 5 min.

### 4.2.3 Media for *U. maydis* growth

**YEPS light medium** modified from Tsukuda *et al.* (1988): 10 g Yeast extract, 10 g Peptone, 10 g Saccharose, and dd$H_2O$ was added to 960 ml following autoclaving at 121°C for 5 min.

**CM Complete Medium** (Holliday, 1974): 1.5 g $NH_4NO_3$, 2.5 g casamino Acids, 0.5 g DNA, 1.0 g yeast extract, 10 ml vitamin solution (see below), 62.5 ml salt solution (see below), dd$H_2O$ was added to 980 ml and adjust pH to 7.0 with 5 M NaOH following autoclaving at 121°C for 5 min. 20 ml of 50% (w/v) glucose was added for *U. maydis* growth. For media with arabinose as sole carbon source, 40 ml of 25% arabinose solution was added to 960 ml medium after autoclaving (f. c. 1%). For solid media, agar was added to a final concentration of 2%.

**Vitamin solution** (Holliday, 1974): 100 mg Thiamine, 50 mg Riboflavin, 50 mg Pyridoxine, 200 mg Calcium pantothenate, 500 mg p-Amino benzo acid, 200 mg Nicotinic acid, 200 mg Choline chloride, 1000 mg myo-inositol, dd$H_2O$ was added to 1 liter following filter sterilization.

**Salt solution** (Holliday, 1974): 16 g $KH_2PO_4$, 4 g $Na_2SO_4$, 8 g KCl, 4 g $MgSO_4$X 7 $H_2O$, 1.32 g $CaCl_2$X 2 $H_2O$, 8 ml trace elements solution (see below), dd$H_2O$ was added to 1 liter following filter sterilization.

**Trace elements solution** (Holliday, 1974): 60 mg $H_3BO_3$, 140 mg $MnCl_2X\ 4H_2O$, 400 mg $ZnCl_2$, 40 mg $NaMoO_4X\ 2H_2O$, 100 mg $FeCl_3X\ 6H_2O$, 40 mg $CuSO_4X\ 5H_2O$, $ddH_2O$ was added to 1 liter following filter sterilization.

**Potato dextrose agar with activated charcoal:** 24 g Potato dextrose broth, 10 g charcoal, 20 g Bacto Agar, $ddH_2O$ was added to 1 liter following autoclaving at 121°C for 5 min.

**Regeneration agar** (Schulz *et al*., 1990): 10 g yeast extract (Difco), 20 Bacto Pepton (Difco), 20 g sucrose, 182.2 g sorbitol, 15 g Bacto Agar, $ddH_2O$ was added to 1 liter following autoclaving at 121°C for 5 min. For the bottom layer, 10 ml Regeneration agar was poured in a petri dish containing double concentrated antibiotics. After solidification, 10 ml of Regeneration agar medium without antibiotics was added. Antibiotics in the bottom layer were used in the following concentrations: carboxine (4 µg/ml), ClonNAT (300 µg/ml), hygromycin (400 µg/ml).

**NSY-Glycerol:** 8 g Bacto nutrient broth, 1 g Yeast extract, 5 g Sucrose, 800 ml of 87% glycerol, $ddH_2O$ was added to 1 liter following autoclaving at 121°C for 5 min.

## 4.3 Strains

### 4.3.1 *Escherichia coli* strains

*E. coli* strains TOP10 (Invitrogen) and DH5α were used as host strains for plasmid constructions and amplifications.

### 4.3.2 Yeast strains

BY4741 (*MATa his3Δ1 leu2Δ0 met15Δ0 ura3Δ0*) (Zeller *et al.*, 2007),

BY4741asc1Δ (*MATa his3Δ1 leu2Δ0 met15Δ0 ura3Δ0 asc1Δ*) (Zeller *et al.*, 2007),

AH109 (*MATa, trp1-901, leu2-3, 112, ura3-52, his3-200, gal4Δ, gal80Δ, LYS2::GAL1$_{UAS}$-GAL1$_{TATA}$-HIS3, GAL2$_{UAS}$-GAL2$_{TATA}$-ADE2, URA3::MEL1$_{UAS}$-MEL1$_{TATA}$-lacZ, MEL1*) (Clontech).

The following strains were generated by transformation.

BY4741pYES2, BY4741asc1ΔpYES2, BY4741pYES2-rak1HA, BY4741asc1ΔpYES2-rak1HA

### 4.3.3 *U. maydis* strains

**Table 5 Used and generated *U. maydis* strains in this study**

| Strain | Genotype | Resistance | Reference |
|---|---|---|---|
| FB1 | *a1b1* | | (Banuett and Herskowitz, 1989) |
| FB2 | *a2b2* | | (Banuett and Herskowitz, 1989) |
| SG200 | *a1mfa2bE1bW2* | Phleo | (Bolker *et al.*, 1995) |
| FBD12-17 | *a2a2b1b2* | | (Banuett and Herskowitz, 1989) |
| FB1Δrak1 | *a1b1Δrak1* | Hyg | This study |
| FB2Δrak1 | *a2b2Δrak1* | Hyg | This study |
| SG200Δrak1 | *a1mfa2bE1bW2Δrak1* | Phleo/Hyg | This study |
| FB1$P_{crg1}$:fuz7DD | *a1b1 ip$^r$[$P_{crg1}$:fuz7DD]ip$^s$* | Cbx | (Muller *et al.*, 2003b) |
| FB1$P_{crg1}$:fuz7DDΔrak1 | *a1b1 ip$^r$[$P_{crg1}$:fuz7DD]ip$^s$ Δrak1* | Cbx/Hyg | This study |
| FB1Δrak1prf1$^{con}$ | *a1b1Δrak1 ip$^r$[$P_{otef}$:prf1]ip$^s$* | Hyg/Cbx | This study |
| FB1Δrak1pra1$^{con}$ | *a1b1Δrak1 ip$^r$[$P_{otef}$:pra1-eGFP]ip$^s$* | Hyg/Cbx | This study |
| FB1rak1-eGFP | *a1b1rak1-eGFP* | Hyg | This study |
| FB1Δuac1 | *a1b1Δuac1* | Hyg | (Kruger *et al.*, 1998) |
| FB1Δrak1-rak1 | *a1b1Δrak1 ip$^r$[$P_{otef}$:rak1]ip$^s$* | Hyg/Cbx | This study |
| FB1Δgpa3 | *a1b1Δgpa3* | Hyg | (Kruger *et al.*, 1998) |
| FB1Δubc1 | *a1b1Δubc1* | Nat | (Hartmann *et al.*, 1999) |
| FB1rak1$^{con}$ | *a1b1 ip$^r$[$P_{otef}$:rak1]ip$^s$* | Phleo/Cbx | This study |
| SG200rak1$^{con}$ | *a1mfa2bE1bW2 ip$^r$[$P_{otef}$:rak1]ip$^s$* | Phleo/Cbx | This study |
| SG200Δrak1-rak1 | *a1mfa2bE1bW2 Δrak1 ip$^r$[$P_{otef}$:rak1]ip$^s$* | Phleo/Hyg/Cbx | This study |
| SG200Δrak1/WD14$^{con}$ | *a1mfa2bE1bW2 Δrak1/ip$^r$[$P_{otef}$:WD14]ip$^s$* | Phleo/Hyg/Cbx | This study |
| SG200Δrak1/WD15$^{con}$ | *a1mfa2bE1bW2 Δrak1/ip$^r$[$P_{otef}$:WD15]ip$^s$* | Phleo/Hyg/Cbx | This study |
| SG200Δrak1/WD16$^{con}$ | *a1mfa2bE1bW2 Δrak1/ip$^r$[$P_{otef}$:WD16]ip$^s$* | Phleo/Hyg/Cbx | This study |
| SG200Δrak1/WD37$^{con}$ | *a1mfa2bE1bW2 Δrak1/ip$^r$[$P_{otef}$:WD37]ip$^s$* | Phleo/Hyg/Cbx | This study |
| FB1rak1-HA | *a1b1rak1-HA* | Nat | This study |
| SG200Δsho1Δmsb2/sho1-Flag | *a1mfa2bE1bW2Δsho1Δmsb2/sho1-Flag* | | (Lanver *et al.*, 2010) |
| SG200AM1 | *a1mfa2bE1bW2 ip$^r$[$P_{um01779}$:eGFP]ip$^s$* | Phleo/Cbx | (Mendoza-Mendoza *et al.*, 2009a) |
| SG200AM1Δrak1 | *a1mfa2bE1bW2 ip$^r$[$P_{um01779}$:eGFP]ip$^s$Δrak1* | Phleo/Cbx/Hyg | This study |
| HA103 | *a1bE1bW2$^{con}$* | Cbx | (Hartmann *et al.*, 1996) |
| HA103Δrak1 | *a1bE1bW2$^{con}$Δrak1* | Cbx/Hyg | This study |
| FB1$P_{crg1}$:adr1 | *a1b1 ip$^r$[$P_{crg1}$:adr1]ip$^s$* | Cbx | (Eichhorn *et al.*, 2006) |
| FB1Δrak1$P_{crg1}$:adr1 | *a1b1Δrak1 ip$^r$[$P_{crg1}$:adr1]ip$^s$* | Hyg/Cbx | This study |
| FB1rop1$^{con}$ | *a1b1 ip$^r$[$P_{otef}$:rop1]ip$^s$* | Cbx | This study |
| FB1Δrak1rop1$^{con}$ | *a1b1Δrak1 ip$^r$[$P_{otef}$:rop1]ip$^s$* | Hyg/Cbx | This study |
| FB1Δyap1 | *a1b1Δyap1* | Hyg | (Molina and Kahmann, 2007) |

## 4.4 Oligonucleotides and plasmids

### 4.4.1 Oligonucleotides

All Oligonucleotides (Table 5) used in this study were purchased from Eurofins MWG Operon.

**Table 6 Oligonucleotides used in this study**

| Primers No.# | Primer Names | Primer Sequences |
|---|---|---|
| LW1 | LW1 10146kolb1 | AATGGCGGAGTGTCTGTGAATGC |
| LW2 | LW210146kolb2SfiI | CACGGCCTGAGTGGCCTGTGTGGCGGTAGTTGCTATTGC |
| LW3 | LW3 10146korb1Sfi | GTGGGCCATCTAGGCCACCTCCTCTACTGCACTGTATCG |
| LW4 | LW4 10146korb2 | GACCCGTCTATGGTTTCCAATGG |
| LW5 | LW10146L-BamHI | CGGGATCCATGTCTGAGTCTCTCGTCTACAAGG |
| LW6 | 10146R-NotI | TTCGGGAATTGCGGCCGCTTACAAAACAGTGAAGACACGGACAATG |
| LW7 | WD14RNotIc | TTCGGGAATTGCGGCCGCGTAGTGGTTGGTCTTCAACTTGCA |
| LW8 | WD15RNotIc | TTCGGGAATTGCGGCCGCCTCCCAAAGCATGGTGATACCGTCC |
| LW9 | WD37L-BamHI | CAGGATCCATGTTGAACACCGGCACCACCACCCGTCG |
| LW10 | WD47L-BamHI | CAGGATCCATGACCCTCGGCGAGTGCAAGTTCAACATCACC |
| LW11 | 2048-for | CGCAGTTGCATATGTCTGAGTCTCTCGTCTAC |
| LW12 | 2048-rev | CACGTACCGCGGATCCTTACAAAACAGTGAAGACACGGACAATG |
| LW13 | LW-WD16rNotI | TTCGGGAATTGCGGCCGCGTTCTTGCCAACACCGGTGAACTCG |
| LW14 | LW10146comp-L | TCGACCTGCAGGTCTTGGGCGCCATTGTGAATAGG |
| LW15 | LW-WD27LBamHI | CAGGATCCATGCTTTCGCGCGACGACTCCAACTACG |
| LW16 | LW10146comp-L-NdeI | TTGCCAAGCATATGTCTTGGGCGCCATTGTGAATAGG |
| LW17 | LW10146L2-SfiI | CACGGCCGCGTTGGCCCCGGTGGCGATCGAGCGCAAAACAGTG AAGACACGGACAATG |
| LW18 | LW10146R3SfiI | CACGGCCTGAGTGGCCACCTCCTCTACTGCACTGTATCG |
| LW27 | LW10146Com-R | TTTACCCGGGCAAAACAGTGAAGACACGGACAATGTTGTCC |
| LW28 | LW10146R-XhoI | CCGCTCGAGTTACAAAACAGTGAAGACACGGAC |
| LW29 | LW10146R-PstI | AACTGCAGTTACAAAACAGTGAAGACACGGAC |
| LW30 | LW10146HAL2SfiI | CACGGCCGCGTTGGCCAACAAAACAGTGAAGACACGGAC |
| LW31 | LW10146HAR1SfiI | CACGGCCTGAGTGGCCACCTCCTCTACTGCACTGTATCG |
| LW60 | LW10146OverNcoI-R | CATGCCATGGACAAAACAGTGAAGACACGGACAATGTTGTCC |
| LW65 | LW-gpa3-NdeI | CGCAGTTGCATATGGGAAACTGTCTTTCTTCCTCTGATCAAAAGG |
| LW66 | LW-gpa3-XmaI | TCCCCCCGGGCTACAAGATGCCGCTGTCCTTGAGC |
| LW67 | LW-gamma-BamHIR | AAGGATCCCTACATGGCAACACAGTTGCATCCTCC |
| LW68 | LW-gamma-NdeIL | CGCAGTTGCATATGAACGTCAAGCCGCACAAACAGTCC |
| LW69 | Gpa3LsfiI | CACGGCCTGAGTGGCCATGGGAAACTGTCTTTCTTCCTCTG |
| LW70 | Gpa3RSfiI | GTGGGCCGCGTTGGCCCTCAAGATGCCGCTGTCCTTGAGCGCGTTGG |
| LW84 | frb34L | ATGACTAGCGGCAGCAATCAACTTCG |
| LW85 | frb34r | TCTTCCAAGCATGATACTTGTTCC |
| LW86 | mfa1L | ATGCTTTCGATCTTCGCTCAGACC |
| LW87 | mfa1R | CTAGGCAACAACACAGCTGGAGTAGC |
| LW88 | Gpa3LXmaI | TCAGCCCGGGATGGGAAACTGTCTTTCTTCCTCTG |
| LW89 | Gpa3RmycNotI | TTCGGGAATTGCGGCCGCCAGGTCCTCCTCTGAGATCAGCTTCTGCTC CTCCAAGATGCCGCTGTCCTTGAG |
| LW90 | Gpa3RHindIII | CCCCAAGCTTCTACAAGATGCCGCTGTCCTTGAGC |
| LW93 | Gpa3LPstI | AACTGCAGCATGGGAAACTGTCTTTCTTCCTCTG |
| LW97 | LW-bW1L | CAGTCGCGACTTTACCCTTTCC |
| LW98 | LW-bW1R | ATGGGCTTGGTATGACAAGCTGC |
| LW105 | bfor | ATCGATCATATGTCAGCACCAGCAGCCGATTTGCAGGAG |
| LW106 | brev | ACTAACGGATCCTTAAGCCCAGATGAGGAGGCGCGAGTC |
| LW108 | LW-gpa1-XmaI | TCCCCCCGGGCTAGAGCAAACCGCAATCGCGCAGG |
| LW109 | LW-gpa1-NdeI | CGCAGTTGCATATGGGTTGCGGTGCTTCCAAGG |
| LW110 | LW-gpa2-XmaI | TCCCCCCGGGTCATAGTACGATATCCCTCAAGTTGTTGG |
| LW111 | LW-gpa2-NdeI | CGCAGTTGCATATGGGCGCTTGTCTGTCTGCTGAGC |
| LW112 | LW-gpa4-NdeI | CGCAGTTGCATATGTCGCCCTCAGTCTCAAGCCCACAGC |

| | | |
|---|---|---|
| LW113 | LW-gpa4-XmaI | TCCCCCCGGGCTACCCTACTAGACCAGTCAGTTTGAGG |
| LW139 | fuz7-for1 | GATACTCATATGCTTTCGTCCGGTGCGGGATCTTC |
| LW140 | fuz7-rev1 | CGCATATGGATCCTTACTTCATCCCATCGGCCCATGCTTG |
| LW141 | Rak1RHA-NotI | ATTGCGGCCGCTTAAGCGTAATCTGGAACATCGTATGGGTACAAAACA GTGAAGACACGGACAATG |
| LW145 | um04007LNdeI | CGCAGTTGCATATGAGGACAGCCGTCCGTAACCAGCAG |
| LW146 | um04007RBamHI | CACGTACCGCGGATCCCTAGAGCTCGGGACCGCGCGTGCTG |
| LW148 | GammaBamHIwo/c | GCCGGATCCCTAGTTGCATCCTCCACCGGCGGGTGC |
| LW174 | Pra1L-BamHI | AAGGATCCATGCTCGACCATATCACGCCTTTCTTTGC |
| LW175 | Pra1R-NcoI | CATGCCATGGCCGCTTCAGATCCCCGCATGTCG |
| LW194 | fer2For | GATTCCGCTTCTGCTTCATCCTC |
| LW195 | fer2rev | GTTGGACTCCCAGTAGGTCTTTC |
| LW198 | Prf1NdeI | CGCAGTTGCATATGCGAGATCCAGGCTGCGCCGACG |
| LW199 | Prf1XmaI | TCCCCCCGGGTCAGATGCAGTGCTGAGGAGATGAAT |
| LW200 | Prf1NcoI | TACTCCATGGATGCGAGATCCAGGCTGCGCCGACG |
| LW202 | um02191NcoI | TACTCCATGGATGTCATCTCCAGCTATGGCACAGA |
| LW204 | um02191rev1 | CATCCTGGGCCAGATCTGTTGC |
| LW205 | gammaNotI | AATTGCGGCCGCCTACATGGCAACACAGTTGCATCC |

### 4.4.2 Plasmids for cloning in *E. coli*

TA vectors: pCR®2.1-TOPO® and pCR®4-TOPO® (Invitrogen) were used for TA TOPO cloning of PCR products or restriction fragments.

### 4.4.3 Plasmids for yeast complementation

The pYES2 vector is a free replication plasmid harboring a 2μ origin for high-copy maintenance. The vector carries the Amp resistance marker for selection in *E. coli* and the *URA3* marker for selection in yeast. It can be used for inducible expression of recombinant proteins under the control of *Gal1* promoter which is induced by galactose and repressed by glucose in *S.cerevisiae*.

To generate pYES2-rak1HA, the *rak1* open reading frame was amplified by primer pairs LW10146L-BamHI (5'-CAGGATCCATGTCTGAGTCTCTCGTCTACAAGG-3') and Rak1HA-NotI (5'-ATTGCGGCCGCTTAAGCGTAATCTGGAACATCGTATGGGTACAAAACAGTG AAGACACGGACAATG-3') using FB1 cDNA as template and cloned into BamHI/NotI double digested pYES2.

### 4.4.4 Plasmids for yeast two hybrid assay

pGBKT7 (Clontech) is a yeast expression vector, in which target bait proteins are fused to amino acids 1-147 of the GAL4 DNA binding domain (DNA-BD). This vector also contains a c-myc epitope following the DNA binding domain. In yeast, fusion proteins are expressed at high levels under the control of the constitutive *ADH1* promoter and the *T7* and *ADH1* transcription terminators. The vector carries a Kan resistance marker for selection in *E. coli* and the *TRP1* marker for selection in yeast.

pGADT7 (Clontech) is a yeast expression vector, in which target prey proteins are fused to amino acids 768-881 of the GAL4 activation domain (AD), and this vector also contains an HA epitope following the DNA activation domain. In yeast, fusion proteins are expressed at high levels under the control of the constitutive *ADH1* promoter and the *T7* and *ADH1* transcription terminators. The vector carries the Amp resistance marker for selection in *E. coli* and the *LEU2* marker for selection in yeast.

To generate pGBKT7-Rak1, the *rak1* open reading frame was amplified by primer pairs 2048-for (5'-CGCAGTTGCATATGTCTGAGTCTCTCGTCTAC-3') and 2048-rev (5'-CACGTACCGCGGATCCTTACAAAACAGTGAAGACACGGACAATG-3') using FB1 cDNA as template, digested with NdeI and BamHI and ligated to NdeI/BamHI double digested pGBKT7. This plasmid was used to express BD-Rak1 fusion protein in yeast.

To generate pGADT7-Gpa1, the *gpa1* open reading frame was amplified by primer pairs LW-gpa1-NdeI (5'-CGCAGTTGCATATGGGTTGCGGTGCTTCCAAGG-3') and LW-gpa1-XmaI (5'-TCCCCCCGGGCTAGAGCAAACCGCAATCGCGCAGG-3') using FB1 genomic DNA as template, digested with NdeI and XmaI and ligated to NdeI/XmaI double digested pGADT7. This plasmid was used to express AD-Gpa1 fusion protein in yeast.

To generate pGADT7-Gpa2, the *gpa2* open reading frame was amplified by primer pairs LW-gpa2-XmaI (5'-TCCCCCCGGGTCATAGTACGATATCCCTCAAGTTGTTGG-3') and LW-gpa2-NdeI (5'-CGCAGTTGCATATGGGCGCTTGTCTGTCTGCTGAGC-3') using FB1 genomic DNA as template, digested with NdeI and XmaI and ligated to NdeI/XmaI double digested pGADT7. This plasmid was used to express AD-Gpa2 fusion protein in yeast.

To generate pGADT7-Gpa3, the *gpa3* open reading frame was amplified by primer pairs LW-gpa3-NdeI (5'-CGCAGTTGCATATGGGAAACTGTCTTTCTTCCTCTGATCAAAAGG-3') and LW-gpa3-XmaI (5'-TCCCCCCGGGCTACAAGATGCCGCTGTCCTTGAGC-3') using FB1 genomic DNA as template, digested with NdeI and XmaI and ligated to NdeI/XmaI double digested pGADT7. This plasmid was used to express AD-Gpa3 fusion protein in yeast.

To generate pGADT7-Gpa4, the *gpa4* open reading frame was amplified by primer pairs LW-gpa4-NdeI (5'-

CGCAGTTGCATATGTCGCCCTCAGTCTCAAGCCCACAGC-3') and LW-gpa4-XmaI (5'- TCCCCCCGGGCTACCCTACTAGACCAGTCAGTTTGAGG-3') using FB1 genomic DNA as template, digested with NdeI and XmaI and ligated to NdeI/XmaI double digested pGADT7. This plasmid was used to express AD-Gpa4 fusion protein in yeast.

To generate pGADT7-Gpg1, the *gpg1* open reading frame was amplified by primer pairs LW-gamma-NdeIL (5'-CGCAGTTGCATATGAACGTCAAGCCGCACAAACAGTCC-3') and LW-gamma-BamHIR (5'-AAGGATCCCTACATGGCAACACAGTTGCATCCTCC-3') using cDNA as template, digested with NdeI and BamHI and ligated to NdeI/BamHI double digested pGADT7. This plasmid was used to express AD-Gpg1 fusion protein in yeast.

To generate pGADT7-Gpg1woC, the *gpg1* open reading frame lacking of the CAAX motif was amplified by primer pairs LW-gamma-NdeIL (5'-CGCAGTTGCATATGAACGTCAAGCCGCACAAACAGTCC-3') and GammaBamHIwo/c (5'-GCCGGATCCCTAGTTGCATCCTCCACCGGCGGGTGC-3') using pGADT7-Gpg1 as template, digested with NdeI and BamHI and ligated to NdeI/BamHI double digested pGADT7. This plasmid was used to express fusion protein of AD-Gpg1 lacking of the CAAX motif in yeast.

To generate pGADT7-Um04007, the *um04007* open reading frame was amplified by primer pairs um04007LNdeI (5'-CGCAGTTGCATATGAGGACAGCCGTCCGTAACCAGCAG-3') and um04007RBamHI (5'-CACGTACCGCGGATCCCTAGAGCTCGGGACCGCGCGTGCTG-3') using FB1 genomic DNA as template, digested with NdeI and BamHI and ligated to NdeI/BamHI double digested pGADT7. This plasmid was used to express AD-Um04007 fusion protein in yeast.

### 4.4.5 Plasmids for *U. maydis*

pBS-hhn (Kamper, 2004) contains the hygromycin phosphotransferase gene (*hph*) fused to the *hsp70* promoter and the *nos* terminator. The cassette is flanked by two incompatible SfiI sites upstream of the *hsp70* promoter and downstream of of the *nos* terminator.

p123 (Spellig *et al*., 1996) is a plasmid containing the carboxin resistance gene and an *eGFP* gene which is fused to the *otef* promoter and *nos* terminator.

pMF3-h (Brachmann *et al*., 2004) contains the hygromycin resistance cassette and the C-terminal fusion eGFP. This plasmid was used to construct the C-terminal fusion eGFP plasmid.

The pRU11 plasmid (Brachmann *et al*., 2001) is an integrative *U. maydis* vector that contains the *crg1* promoter as a 3.5 kb NotI/NdeI fragment and the carboxin resistance gene.

pONG (Lanver *et al.*, 2010) is derived from p123 by replacing the *eGFP* gene with the mcherryHA fragment and the sho1 part flanked by SfiI sites as stuffer locates between the *otef* promoter and the mcherryHA fragment, which is easily to integrate interesting genes to be fused to mcherry-HA.

pCR4.0-KOrak1 is a plasmid used to generate *rak1* deletion. Two 1.0 kb fragments containing the 5'- and the 3'-flanking regions of the *rak1* gene respectively, were amplified by PCR using FB1 genomic DNA as template with the primer pairs LW1 10146kolb1 (5'-AATGGCGGAGTGTCTGTGAATGC-3') and LW2 10146lb2SfiI (5'-CACGGCCTGAGTGGCCTGTGTGGCGGTAGTTGCTATTGC-3') for the left border and LW3 10146korb1SfiI (5'-GTGGGCCATCTAGGCCACCTCCTCTACTGCACTGTATCG-3') and LW4 10146korb2 (5'-GACCCGTCTATGGTTTCCAATGG-3') for the right border, respectively. The PCR fragments were digested with SfiI and ligated to the hygromycin resistance cassette isolated as a 1.9 kb SfiI fragment from plasmid pBS-hhn (Kamper, 2004). The ligation product was cloned into pCR4.0 (Invitrogen) by TA cloning. From this plasmid, a fragment was amplified by primer pairs LW1 10146kolb1 and LW4 10146korb2.

p123$P_{otef}$:rak1 is a plasmid in which *rak1* is under the control of *otef* promoter. The *rak1* open reading frame was amplified by primer pairs LW10146L-BamHI (5'-CAGGATCCATGTCTGAGTCTCTCGTCTACAAGG-3') and LW10146comp-R-NotI (5'-TTCGGGAATTGCGGCCGCTTACAAAACAGTGAAGACACGGACAATG-3') using cDNA as template, digested with BamHI and NotI and ligated to BamHI/NotI double digested p123. This plasmid was used to complement *rak1* mutants or overexpress *rak1* in *U. maydis*.

p123$P_{otef}$:rak1Δ190-313 is a plasmid used to express the C-terminal 190-313 aa truncated version of Rak1 in SG200Δrak1. The 567 bp fragment was amplified by primer pairs LW10146L-BamHI (5'-CAGGATCCATGTCTGAGTCTCTCGTCTACAAGG-3') and WD14RNotIc (5'-

TTCGGGAATTGCGGCCGCGTAGTGGTTGGTCTTCAACTTGCA-3') using p123P$_{otef}$:rak1 as template, digested with BamHI and NotI and ligated to BamHI/NotI double digested p123.

p123P$_{otef}$:rak1Δ221-313 is a plasmid used to express the C-terminal 221-313 aa truncated version of Rak1 in SG200Δrak1. The 660 bp fragment was amplified by primer pairs LW10146L-BamHI (5'-CAGGATCCATGTCTGAGTCTCTCGTCTACAAGG-3') and WD15RNotIc (5'-TTCGGGAATTGCGGCCGCCTCCCAAAGCATGGTGATACCGTCC-3') using p123P$_{otef}$:rak1 as template, digested with BamHI and NotI and ligated to BamHI/NotI double digested p123.

p123P$_{otef}$:rak1Δ281-313 is a plasmid used to express express the C-terminal 281-313 aa truncated version of Rak1 in SG200Δrak1. The 840 bp fragment was amplified by primer pairs LW10146L-BamHI (5'-CAGGATCCATGTCTGAGTCTCTCGTCTACAAGG-3') and LW-WD16rNotI (5'-TTCGGGAATTGCGGCCGCGTTCTTGCCAACACCGGTGAACTCG-3') using p123P$_{otef}$:rak1 as template, digested with BamHI and NotI and ligated to BamHI/NotI double digested p123.

p123P$_{otef}$:rak1Δ1-91 is a plasmid used to express express the N-terminal 1-91 aa truncated version of Rak1 in SG200Δrak1. The 666 bp fragment was amplified by primer pairs WD37L-BamHI (5'-CAGGATCCATGTTGAACACCGGCACCACCACCCGTCG-3') and LW10146comp-R-NotI (5'-TTCGGGAATTGCGGCCGCTTACAAAACAGTGAAGACACGGACAATG-3') using p123P$_{otef}$:rak1 as template, digested with BamHI and NotI and ligated to BamHI/NotI double digested p123.

pCR2.1-rak1-eGFP is a plasmid in which *rak1* is fused C-terminally to eGFP. Two 1.0 kb fragments containing the 3'-ORF and the 3'-flanking regions of the *rak1* gene respectively were amplified by PCR using FB1 genomic DNA as template with the primer pairs LW-WD47L-NdeI (5'CGCAGTTGCATATGACCCTCGGCGAGTGCAAGTTCAACATCACC-3') and LW10146L2-SfiI (5'-CACGGCCGCGTTGGCC**CCGGTGGCGATCGAGCG**CAAAACAGTGAAGACA CGGACAATG-3') for the left border and LW10146R3SfiI (5'-

CACGGCCTGAGTGGCCACCTCCTCTACTGCACTGTATCG-3') and LW4 10146korb2 (5'-GACCCGTCTATGGTTTCCAATGG-3') for the right border. The PCR fragments were digested with SfiI and ligated to a SfiI fragment of pMF3-h (Brachmann *et al*., 2004). A short linker RSIAT was introduced between *rak1* and *eGFP*, the region coding for the linker is shown in bold type. Afterwards, the ligation product was cloned into PCRII-TOPO (Invitrogen) to get the plasmid pCR2.1-rak1-eGFP. From this plasmid *rak1-eGFP* was amplified using primers LW-WD47L-NdeI and LW4 10146korb2 and transformed in FB1. In the resulting strain FB1rak1-eGFP, *rak1-eGFP* has placed the *rak1* gene. This plasmid was used to analyze the subcellular localization of Rak1.

p123P$_{otef:}$pra1-eGFP is a plasmid containing a *pra1-eGFP* fusion gene. The *pra1* genomic DNA was amplified by primer pairs Pra1L-BamHI (5'-AAGGATCCATGCTCGACCATATCACGCCTTTCTTTGC-3') and Pra1R-NcoI (5'-CATGCCATGGCCGCTTCAGATCCCCGCATGTCG-3') using FB1 genonic DNA as template, digested with BamHI and NcoI and ligated to BamHI/NcoI double digested p123. This plasmid was used to overexpress *pra1* in *U. maydis*.

pRF$^{con}$ (Hartmann *et al.*, 1999) is a plasmid containing carboxin resistance cassette, 1.0 kb 5'-flanking region of *prf1* and the open reading frame of *prf1* which is under the control of *otef* promoter. This plasmid can be used to overexpress *prf1* by integration in the *ip* locus digested by AgeI or in the *prf1* locus digested by HindIII.

pHEcrg:adr1 (Eichhorn *et al*., 2006) is an integrative plasmid expressing *adr1* under the *crg1* promoter.

p123P$_{otef}$:rop1 (Brefort *et al*., 2005) is a plasmid which is used to overexpress *rop1* in *U. maydis*.

## 4.5 Microbiological methods

### 4.5.1 *E. coli* methods

*E. coli* was grown in liquid dYT medium or on YT agar plates (Ausubel *et al*., 1987). Antibiotics were added to media with the following final concentrations: Ampicillin (100 μg/ml), Kanamycin (40 μg/ml). *E. coli* strains were prepared in liquid medium at 37°C with shaking (200 rpm) or incubated on plates at 37°C.

#### 4.5.1.1 Preparation of chemical compentent *E. coli* cells and transformation

The preparation of chemical compentent *E. coli* cells followed the protocol of Hanahan (1985).

For the transformation, an aliquot of compentent cell was thawn on ice, 1-5 µl DNA or ligation mix was added and incubated on ice for 30 min. After a heat shock at 42°C for 60 sec, the aliquote was immediately placed on ice for 30 sec and followed by the addition of 500 µl dYT medium and incubated at 37°C for 30 min to 1 h with shaking, spread and incubated at 37°C overnight.

4.5.1.2 TOPO TA cloning

The TOPO TA cloning followed the TOPO TA Manual (Invitrogen).

### 4.5.2 Yeast methods and Yeast two hybrid assay

*Sacchromycere cerevisiae* wild type strains were grown in liquid YPD medium or on YPD plates at 28°C.

For yeast transformation, the protocol of Burke *et al.* (2000) was followed.

The yeast two hybrid analysis was performed using the MATCHMARKER GAL4 two-hybrid system 3 (Clontech) following the manufacturer's instructions. Plasmid pGBKT7 or pGBKT7-Rak1 was transformed into strain AH109 in combination with pGADT7, pGADT7-Gpa1, pGADT7-Gpa2, pGADT7-Gpa3, pGADT7-Gpa4, pGADT7-Gpg1 or pGADT7-Gpg1wo/C, pGADT7-Um04007. Transformants were spread on synthetic dropout medium plates without leucine and tryptophan. Growth assays were tesed on synthetic dropout medium plates either without leucine, tryptophan or without leucine, tryptophan and histidine containing 3 mM of 3-AT, and incubated for 3-6 d at 28$^{o}$C respectively.

### 4.5.3 *U. maydis* methods

*U. maydis* strains were grown at 28°C in liquid medium with shaking at 200 rpm to a density of $OD_{600}$ =0.5-0.6. The cell density of culture was determined using a Novosec II Photometer (Pharmacia Biotech) at an optical density of 600 nm ($OD_{600}$). The corresponding culture medium was used as a reference. A culture density of $OD_{600}$ ~1.0 corresponds to about 1-5 $X10^{7}$ cells $ml^{-1}$. Glycerol stocks were prepared from exponentially growing cultures, mixed with NSY-Glycerol at a 1:1 ratio and stored at -80°C. To grow strains from glycerol stocks, cells were streaked onto agar plates and incubated at 28°C.

4.5.3.1 Transformation of *U. maydis*

Transformation of *U. maydis* was performed as described previously (Schulz *et al*., 1990). In brief, *U. maydis* cells were grown in YEPS light medium at 28°C to an $OD_{600}$

=0.5-0.8. 50 ml cultures were harvested by centrifugation for 5 min at 3,500 rpm, washed with 25 ml of SCS (20 mM sodium citrate, 1 M sorbitol, pH 5.8) and centrifuged again for 5 min at 3,500 rpm. The cells were resuspended in 2 ml filter stelized SCS containing 2.5 mg $ml^{-1}$ Novozyme. Cells were incubated for 5-10 min at room temperature for the digestion of cell wall. This process was checked under the microscope until about 50% of the cells started to protoplast. 20 ml of SCS was added following centrifugation at 2,300 rpm for 10 min. Cells were carefully resuspended in 20 ml of SCS, centrifuged at 2,300 rpm for 10 min. Cells were carefully resuspended in 10 ml of SCS, centrifuged at 2,300 rpm for 10 min. Afterwards, cells were carefully resuspended in 20 ml of STC (10 mM Tris-HCl, 100 mM $CaCl_2$, 1 M sorbitol), centrifuged at 2,400 rpm for 10 min. Finally, the protoplast pellet was resuspended in 0.5 ml ice cold STC and aliquots of 70 µl were used immediately or stored at -80°C. For transformation of protoplasts, 5 µg linerized DNA (in a volume of 1-10 µl) and 1 µl heparin (15 mg $ml^{-1}$) were added to the protoplasts and incubated on ice for 10 min. Subsequently, 500 µl of STC/40% PEG was added and incubated for 15 min on ice. In the end, the transformation mixture was plated on Regeneration agar and incubated at 28°C for 4-7 d.

4.5.3.2 Mating, pheromone stimulation and pathogenicity assays

For mating assays, compatible strains were grown in YEPS light medium to an $OD_{600}$ of 0.8 and adjusted to an $OD_{600}$ of 1.0. After mixing in 1:1 (v/v) and 6 µl of culture was spotted on charcoal-containing PD plate (Holliday, 1974). The plate was sealed with Parafilm and incubated at 28°C for 48 h.

For pheromone stimulation, strains were grown in CM medium with 1% glucose to an $OD_{600}$ of 0.6. Synthetic a2 pheromone (Bachem AG Weil am Rhein, Germany) was dissolved in dimethyl sulfoxide (DMSO) and added to a final concentration of 2.5 µg $ml^{-1}$. Cells were incubated at 28°C with shaking. After 5 h incubation, quantification of conjugation tubes was performed with photomicrographs by manual counting. After harvesting, RNA was prepared for Northern blotting analysis.

Plant infections of the corn variety Early Golden Bantam (Olds Seeds, Madison, Wis.) were performed as described previously (Muller *et al*., 1999). Strains were grown in YEPS light medium to an $OD_{600}$ of 0.8, washed twice with $ddH_2O$ and resuspended in $ddH_2O$ to a final $OD_{600}$ of 1.0. This suspension was used to inoculate seven-day-old maize seedlings. Compatible haploid strains were mixed (1:1) prior to infection. Twelve

days after infection, disease symptoms were scored according to the disease rating criteria reported by Kämper *et al.* (2006). All experiments were repeated three times and each replicate invovled at least 35 infected plants.

4.5.3.3 Analysis of filaments and appressoria differentiation in *vitro*

The *in vitro* induction of filaments and appressoria of *U. maydis* was performed as described previously (Berndt *et al.*, 2010; Mendoza-Mendoza *et al.*, 2009a). Briefly, SG200AM1 and its derivative SG200AM1Δrak1 were grown at 28°C to an $OD_{600}$ of 0.3-0.5 in YEPS light medium, washed with $ddH_2O$, resuspended to an $OD_{600}$ of 0.1 in 2% YEPSL and supplemented with either 100 µM (f.c.) 16-hydroxy-hexadecanoic acid dissolved in ethanol (Sigma-Aldrich) or 1% ethanol. To quantify appressoria formation on a hydrophobic surface, SG200AM1 and SG200AM1Δrak1 were sprayed with an aerosol sprayer (EcoSpray, Roth) on Parafilm M and incubated in 100% humidity at 28°C for 18 h. Samples were stained with calcofluor white to visualize fungal cells. To determine the percentage of filaments that had developed appressoria, fluorescence microscopy was used, which relied on the expression of the AM1 marker in cells that have developed appressoria (Mendoza-Mendoza *et al.*, 2009a). All experiments were performed in three biological replicates.

4.5.3.4 Induction of the *crg1* promoter

The *crg1* promoter is a carbon-regulated promoter, which can be repressed by glucose and induced by arabinose (Bottin *et al.*, 1996). Cells were incubated in CM medium with 1% glucose to an $OD_{600}$ of 0.5 at 28°C and collected by centrifugation at 3,500 rpm for 5 min at room temperature. The supernant was discarded, the cells were washed twice with $ddH_2O$ and resuspended in CM medium with 1% glucose or with 1% arabinose. Cultures were incubated at 28°C with shaking at 200 rpm for 5 h. Cells were subjected to microscopy or collected for RNA preparation.

## 4.6 Molecular biological methods

### 4.6.1 DNA isolation and Southern blotting

4.6.1.1 Plasmid preparation from *E.coli*

The boiling preparation of *E. coli* plasmid was based on the protocol of Sambrook *et al*. (1989).

The plasmid DNA purification was followed by the QIAprep spin miniprep kit (QIAGEN).

4.6.1.2 Genomic DNA isolation from *U. maydis*

The preparation of genomic DNA from *U. maydis* was followed by the protocol of (Hoffman and Winston, 1987).

4.6.1.3 Southern blotting

10 µl of genomic DNA was digested with respective restriction enzyme in 20 µl reaction volume overnight. Samples were loaded onto 0.8% TAE agarose gel and run at 80 V for 4 h. Gels were soaked in 0.25 M HCl solution with shaking for 20-30 min until bromothymol blue turns yellow. HCl solution was replaced with 0.4 M NaOH and incubated for 20-30 min with shaking until the color turns blue. DNA was transferred from the gel to nylon membrane with 0.4 M NaOH overnight. Next day, membrane UV crosslinking was performed at the energy of 1500. Dig-labeling probe was generated as described in the PCR DIG Labeling Mix protocol (Roche, Mannhein, Germany). The hybridization, wash and exposure steps were followed by the protocol of Sambrook *et al*. (1989).

### 4.6.2 RNA isolation and Northern blotting

4.6.2.1 RNA preparation from *U. maydis*

RNA preparation with Trizol reagent

This procedure was performed as described by the manufacturer (Invitrogen). In brief, 50 ml of *U. maydis* culture with an $OD_{600}$ ~0.5-1.0 was harvested by centrifugation at 3,500 rpm for 5 min. The pellet was resuspended in 1 ml Trizol reagent and transferred to a 2 ml centrifuge tube containing 100 mg of glass beads followed by homogenization on a Vibrax-VXR shaker (IKA) with shaking at 1,200 rpm. Afterwards, samples were incubated for 5 min at room temperature, 200 µl of chloroform was added, mixed for 15 sec and incubated for an additional 2-3 min. Samples were centrifuged at 4°C for 15 min at 11,500 rpm. The upper aqueous phase (500 µl) was transferred to a 1.5 ml RNase free centrifuge tube. RNA was precipitated by the addition of 500 µl isopropanol and incubated for 10 min at room temperature. After centrifugation at 4°C for 10 min at 11,500 rpm, the pellet was washed once with 1 ml of 70% ethanol and air dried. The RNA pellet was dissolved in 50 µl RNase-free water.

RNA preparation with water-phenol

50 ml of *U. maydis* culture with $OD_{600}$ ~0.5-1.0 was centrifuged for 5 min at 3,500 rpm. The pellet was resuspended in 500 µl AE buffer (50 mM sodium acetate, 10 mM $Na_2$-EDTA∗$2H_2O$, pH 5.3) with 1% SDS, transferred to a 2 ml eppendorf tube and 500 µl

water-phenol as well as 100 mg of glass beads were added. The mixture was placed on a Vibrax-VXR shaker (IKA) set to 1,200 rpm for 5 min. Following incubatation for 10 min at 60°C, a freezing step at -80°C for 10 min and centrifugation at 13,000 rpm for 15 min at room temperature. The supernatant was transferred to a 1.5 ml eppendorf tube. 500 µl of water-phenol/chloroform (v/v 1:1) were added followed by vortexing and centrifugation for 15 min at 13,000 rpm at room temperature. 400 µl of the supernant were transferred to a 1.5 ml eppendorf tube, 1 ml of cold 100% ethanol and 40 µl of 3 M NaAc were added followed by vortexing and centrifugation at 22,000 rpm for 30 min at 4°C. The pellet was dissolved in 30 µl RNase-free $H_2O$ at 55°C for 10 min with shaking. An aliquot of 1 µl was used for RNA quality analysis (1% TBE agarose gel).

4.6.2.2 Northern blotting

5-15 µg of RNA sample was transferred to a 1.5 ml eppendorf tube and the volume of RNA was adjusted to 4.8 µl with DEPC-$H_2O$. 1.6 µl of 10X MOPS, 1.6 µl of 8 M glyoxal and 8 µl DMSO were individually added followed by incubatation at 55°C for 15 min. 4 µl of 5X RNA loading buffer was added to the mixture of RNA sample followed by loading onto 1X MOPS gel. The gel was run at 80 V for 2 h in 1X MOPS buffer. The orientation of the gel in the chamber and the polarity of the chamber were inverted every 30 min. The gel was soaked in 20X SSC buffer for 15 min with gentle shaking. Afterwards, RNA was transfered from the gel to a nitrocellulose membrane with 20X SSC buffer overnight. The hybridization, wash and exposure steps were followed by the protocol of Sambrook *et al*. (1989).

4.6.2.3 Probes for Northern blotting

Probes of Northern hybridization were prepared using a PCR DIG-labeling kit (Roche) following the specification of the manufacturer.

A 0.67 kb EcoRV fragment and a 1.3 kb EcoRI/EcoRV fragment from pSP4.2EcoRV (Brachmann *et al*., 2004) were used for detecting *mfa1* and *pra1* respectively.

A 1.6 kb EcoRV fragment from pRF-6.0B (Hartmann *et al.*, 1999) was used for *prf1* detection.

A 2.6 kb PvuII fragment from pbW2-Nde-bE1 (Brachmann *et al*., 2001) was used to detect *bE* and *bW* transcripts.

For *frb34*, a 1.2 kb fragment was amplified with primer pairs frb34L (5'-ATGACTAGCGGCAGCAATCAACTTCG-3') and frb34R (5'-

TCTTCCAAGCATGATACTTGTTCC-3') by PCR using FB1 genomic DNA as template.

For *gpa3*, a 1.1 kb fragment was amplified with primer pairs Gpa3LSfiI (5'-CACGGCCTGAGTGGCCATGGGAAACTGTCTTTCTTCCTCTG-3') and Gpa3RSfiI (5'-GTGGGCCGCGTTGGCCCTCAAGATGCCGCTGTCCTTGAGCGCGTTGG-3') by PCR using FB1 genomic DNA as template.

For *rak1*, a 0.9 kb fragment was generated with primer pairs 2048-for (5'-CGCAGTTGCATATGTCTGAGTCTCTCGTCTAC-3') and 2048-rev (5'-CACGTACCGCGGATCCTTACAAAACAGTGAAGACACGGACAATG-3') by PCR using p123P$_{otef}$:rak1 as template.

For *rop1*, a 1.1 kb fragment was generated with primer pairs otef-123 (5'-CGCGGCAGAGACGACCAGATTCG-3') and OTB12 (5'-GGCGATATCGGTAGGTGG-3') by PCR using p123P$_{otef}$:rop1 (Brefort *et al*., 2009) as template.

For *fuz7*, a 1.3 kb fragment was generated with primer pairs fuz7-for1 (5'-GATACTCATATGCTTTCGTCCGGTGCGGGATCTTC-3') and fuz7-rev1 (5'-CGCATATGGATCCTTACTTCATCCCATCGGCCCATGCTTG-3') by PCR using FB1 genomic DNA as template.

For *crk1*, a 0.66 kb fragment was generated with primer pairs crk1XmaI (5'-TCCCCCCGGGATGGCACAGGTTGCTTCCAGCTCGAAGC-3') and crk1m-rev (5'-CGACCAATCCTGCGGCAAGCGGACG-3') by PCR using FB1 genomic DNA as template.

For *adr1*, a 1.3 kb fragment was generated with primer pairs crg1for (5'-AGTCTGGAGGCTCAAGACAAAGC-3') and Adr1RBamHI (5'-GCCGGATCCTCAGAAATCCGGGAAAAG-3') by PCR using plasmid pHEcrg:adr1 (Eichhorn *et al*., 2006) as template.

For *yap1*, a 0.7 kb fragment was amplified with primer pairs um02191NcoI (5'-TACTCCATGGATGTCATCTCCAGCTATGGCACAGA-3') and um02191 rev1 (5'-CATCCTGGGCCAGATCTGTTGC-3') by PCR using FB1 genomic DNA as template.

### 4.6.3 DNA microarray analysis

4.6.3.1 Removal of DNA contamination from RNA

RNA prepared with Trizol reagent was treated with Ambion® TURBO DNA-*free*™ to remove DNA contamination from RNA samples. First 0.1 volume of 10X TURBO DNase buffer and 1 µl TURBO DNase were added to the RNA, mixed gently and incubated at 37°C for 20-30 min. Then resuspended DNase Inactivation Reagent (typically 0.1 volume) was added. After mixing well, the sample was incubated for 5 min at room temperature with occasional mixing. Following centrifugation at 10,000 g for 1.5 min and the RNA was transferred to a 1.5 ml eppendorf tube. Finally, RNA was purified with the RNeasy Kit (QIAGEN) and the RNA quality was determined using Agilent RNA 6000 Nano Kit and Agilent 2100 Bioanalyzer. The concentration of RNA was measured by Nanodrop 2000.

4.6.3.2 One-Cycle Target Labeling

The process was performed as described in the "GeneChip® Expression analysis technical manual" (P/N 702232 Rev. 3).

First-strand cDNA synthesis

2 µg of total RNA and 2 µl of 50 µM T7-oligo(dT) Primer in a 12 µl reaction were incubated at 70ºC for 10 min, the sample was cooled at 4°C for 2 min and spun. Next, 4 µl of 5X first-strand reaction buffer, 2 µl of 0.1 M DTT and 1 µl of 10 mM dNTP mix were added and incubated at 42ºC for 2 min. Afterwards, 1 µl of SuperScript II RT was added to the reaction tube, mixed and incubated for 1 h at 42ºC.

Second-strand cDNA synthesis

91 µl RNase-free $H_2O$, 30 µl of 5X Second-strand reaction mix, 3 µl of 10 mM dNTP mix, 1 µl *E. coli* DNA Ligase, 4 µl *E. coli* DNA Polymerase I and 1 µl RNase H were added to the first strand synthesis sample. After mixing and centrifugation, the sample was incubated for 2 h at 16ºC. Afterwards, 2 µl of T4 DNA Polymerase was added and incubated for 5 min at 16ºC. Finally, the reaction was blocked by the addition of 10 µl of 0.5 M EDTA.

Cleanup of double stranded cDNA

Cleanup of double stranded cDNA was performed using the GeneChip® Sample Cleanup Module (QIAGEN). 600 µl cDNA binding buffer was added to the double stranded cDNA synthesis preparation and mixed by vortexing. The sample was applied to a cDNA cleanup spin column and centrifuged at 10,000 rpm for 1 min. The flow-through was discarded, 750 µl cDNA wash buffer was added and centrifuged at 10,000

rpm for 1 min. The flow-through was discarded, and the column centrifuged at 13,000 rpm for 5 min with an open cap. The column was transferred to a 1.5 ml centrifuge tube, 14 µl elution buffer was applied to the column matrix, incubated for 1 min and centrifuged at 13,000 rpm for 1 min. The quality of the cDNA was analyzed using Agilent RNA 6000 Nano Kit and Agilent 2100 Bioanalyzer. The concentration of cDNA was measured by Nanodrop 2000.

Synthesis of Biotin-Labeled cRNA

12 µl of double strand cDNA, 4 µl of 10X IVT labeling buffer, 12 µl IVT labeling NTP mix, 4 µl IVT labeling enzyme mix were added to a reaction tube and was adjusted the volume to 40 µl with RNase-free $H_2O$. The reaction was gently mixed followed by short centrifugation and incubation in a thermal cycler for 16 h at 37ºC.

Cleanup of cRNA

Cleanup of cRNA was performed with GeneChip® Sample Cleanup Module (QIAGEN). 60 µl of RNase-free $H_2O$ was added to the IVT reaction and mixed by vortexing for 3 sec. Next, 350 µl IVT cRNA binding buffer was added and mixed by vortexing for 3 sec. 250 µl of 100% ethanol was added, mixed gently, applied to the IVT cRNA cleanup spin column and centrifuged at 10,000 rpm for 15 sec. Afterwards, 500 µl of 80% ethanol was loaded to the column and centrifuged at 10,000 rpm for 15 sec. The flow-through was discarded and the column centrifuged for at 13,000 rpm for 5 min with open cap. The column was transferred to a new 1.5 ml centrifuge tube and 11 µl RNase-free $H_2O$ was added to the column matrix and centrifuged at 13,000 rpm for 1 min. Finally, additional 10 µl of RNase-free $H_2O$ was applied to the column membrane and centrifuged at 13,000 rpm for 1 min. The quality of the cRNA was analyzed using Agilent RNA 6000 Nano Kit and Agilent 2100 Bioanalyzer. The concentration of cRNA was measured by Nanodrop 2100.

4.6.3.3 cRNA fragmentation for target preparation

20 µg of cRNA (20 µl) and 8 µl of 5X fragmentation buffer were added to a reaction tube and was adjusted the volume to 40 µl with RNase-free $H_2O$. The reaction was incubated at 94ºC for 35 min and placed on ice. The quality of fragmented cRNA was analyzed using Agilent RNA 6000 Nano Kit and Agilent 2100 Bioanalyzer.

4.6.3.4 Microarray hybridization

For analysis of *U. maydis* transcriptome, Affymetrix Gene Chip *Ustilago* genome arrays were used. For microarray hybridization, 15 μg fragmented cRNAs were mixed with 5 μl of 3 nM control oligonucleotide B2, 15 μl of 20X eukaryotic hybridization controls (heated to 65ºC for 5 min before using), 150 μl of 2X hybridization mix and 30 μl DMSO, and adjusted a total volume to 300 μl with RNase-free $H_2O$. The hybridization cocktail was heated at 99ºC for 5 min, and incubated at 45ºC for 5 min following by centrifugation at 13,000 rpm for 5 min at room temperature. In the mean time, the probe array filled with pre-hybridization mix was incubated at 45ºC for 10 min with rotation. After equilibration, the solution was removed and refilled with 200 μl of the hybridization cocktail. The arrays were placed into the hybridization oven (GeneChip® Hybridization Oven 640) and hybridized at 45ºC with 60 rpm for 16 h.

4.6.3.5 Microarray detection

After 16 h of hybridization, the hybridization cocktail was removed from the array. The GeneChip® hybridization wash and stain kit was used to wash and stain the array using GeneChip Fluidics Station 450 (P/N 702731 Rev. 3). All arrays were scanned on an Affymetrix GSC3000 Microarray Scanner.

4.6.3.6 Microarray data analysis

Affymetrix Gene ChipR *Ustilago* genome arrays were performed in three biological replicates using Affymetrix protocols. The image data produced by the microarray scanner was analyzed using Affymetrix MicroArray Suite 5.1 (MAS 5.1), which normalized the data and generated expression values for each probe set. Further analysis was carried out using R software (http://www.r-project.org/), which adjusts the *P*-value for each probe set using the false discovery rate (fdr) method (Benjamini and Hochberg, 1995). Expression values were converted to $\log_2$ (value +1). Probe sets that were present in three biological replicates were considered expression. Only genes that displayed fold changes of at least twofold with a difference between expression values >50 and a corrected *P*-value <0.01 were considered as significant. Functional enrichment analysis was carried out using FunCatDB (http://mips.helmholtz-muenchen.de/cgi-bin/proj/funcatDB/search_advanced.pl?gene=2).

## 4.7 Biochemical methods

### 4.7.1 Protein preparation

4.7.1.1 Protein preparation from yeast (Lanver *et al.*, 2010)

Yeast cells were grown to an $OD_{600}$ of 1.0 in indicated media. 1.5 ml of culture was collected and centrifuged for 5 min at 7,000 rpm followed by washing once with 1 ml Tris-HCl (50 mM pH 7.5). The pellet was resuspended in 30 µl ESB buffer (2% SDS, 80 mM Tris-HCl pH 8.0, 10% glycerol, 0.1 mg $ml^{-1}$ bromphenol blue, 100 mM DTT) and boiled at 95°C for 3 min. 100 mg glass beads were added following by vortexing for 2 min. Afterwards, 70 µl ESB buffer was added and incuated for 1 min at 95°C. 15-20 µl of sample was loaded on SDS gel.

4.7.1.2 Protein preparation from *U. maydis*

*U. maydis* strains were grown in CM medium with 1% glucose to an $OD_{600}$ of 0.5-1.0. Cultures were collected by centrifugation for 5 min at 3,500 rpm. The pellet was washed once with Tris-HCl (50 mM pH 7.5) following by centrifugation for 5 min at 3,500 rpm. The pellet was resuspended in cold lysis buffer (PBS buffer with Roche Complete Protease Inhibitor Cocktail and 1% Triton X-100) and 100 mg of lysing matrix B (MP Biomedicals) was added following lysis in a FastPrep homogenization system (MP Biomedicals) with 4.5 30 s, 5.5 30 s, 5.5 30 s and centrifugation at 13,000 rpm for 10 min at 4°C. The supernant was transferred to a 1.5 ml eppendorf tube. The sample loading buffer was added following by boiling at 95°C for 3 min and 15-20 µl of sample was subjected to SDS-PAGE.

**PBS buffer (phosphate-buffered saline):** 8 g NaCl, 0.2 g KCl, 1.44 g $Na_2HPO_4$, 0.24 g $KH_2PO_4$ and $ddH_2O$ was added to 1 liter and pH was adjusted to 7.4 with HCl following autoclaving at 121$^{o}$C for 5 min.

4.7.1.3 Cellular fractionation

Cellular fractionation was based on the protocol of Lanver *et al.* (2010) with minor modification**.** Briefly, 100 ml of cells were grown in YEPS light medium to an $OD_{600}$ of 0.8, collected by centrifugation. The pellet was washed twice in PBS buffer, resuspended in 2 ml lysis buffer (50 mM Tris-HCl, 150 mM NaCl, 1% Nonidet P40, 0.5% sodium deoxycholate, pH 7.5) and lysed in a FastPrep homogenization system (MP Biomedicals) with lysing matrix B (MP Biomedicals). Samples were centrifuged at 1,000 g for 5 min; half of the supernatant was precipitated with trichloroacetic acid (TCA; f.c. 25%) on ice for 10 min, centrifuged (20,000 g, 10 min) and resuspended in lysis buffer (whole cell extract). The other half of the supernatant was centrifuged for 30 min at 4°C, 20,000 g and the supernatant was TCA precipitated and resuspended in lysis

buffer (cytoplasmic fraction). The pellet was directly suspended in lysis buffer (membrane fraction). Samples were subjected to SDS-PAGE.

4.7.1.4 *In vitro* translation system

*In vitro* translation was performed using the TNT7 Coupled Reticulocyte Lysate system as described by the manufacturer (Promega). Briefly, 25 µl TNT® Rabbit Reticulocyte Lysate, 2 µl TNT® Reaction Buffer, 1 µl TNT® T7 RNA Polymerase, 0.5 µl of 1mM amino acid mixture minus leucine and 0.5 µl of 1 mM amino acid mixture minus methionine, and 4 µl of 2.5 µg/µl plasmid were added to a 1.5 ml eppendorf tube and were adjusted the volume to 50 µl with RNase-free $H_2O$. After incubation at 30°C for 90 min, 2 µl of sample was subjected to SDS-PAGE and Western blotting analysis was performed.

### 4.7.2 Western blotting

Protein extracts were separated by SDS-PAGE and transferred to a PVDF (polyvinylidene difluoride) membrane. Membrane was blocked with TBST buffer (50 mM Tris-HCl, 150 mM NaCl, 0.1% Tween-20, pH 7.4) containing 5% non-fat dry milk at room temperature for 1 h. The membrane was washed three times with TBST buffer each time for 5 min. Afterwards, the membrane was incubated with respective antibody as the primary antibody diluted in TBST buffer with 3% non-fat dry milk with shaking at 4°C overnight. The membrane was washed with TBST buffer three times each time for 5 min. Next the membrane was incubated with respective secondary antibody in TBST buffer containing 3% non-fat dry milk and incubated for 1 h with shaking at room temperature. Finally, the membrane was washed with TBST buffer three times each time for 5 min. Chemiluminescent detection was performed using an ECL kit (Amersham Biosciences, cat. no. RPN-2106). Immunodetection was carried out using related antibodies (Table 7).

**Table 7 Antibodies used in this study**

| antibody | source | company & catalog no. | Working solution |
|---|---|---|---|
| α-c-myc | mouse | Sigma M5546 | 1:3,000 |
| α-HA | mouse | Sigma H9658 | 1:10,000 |
| α-Flag | mouse | Sigma F3165 | 1:50,000 |
| α-eGFP | mouse | Roche 1181446000 | 1:2,000 |

| | | | |
|---|---|---|---|
| α-Actin | mouse | Calbiochem CP01 | 1:10,000 |
| α-BD | mouse | Santa Crutz biotechnology sc-510 | 1:2,000 |
| α-AD | mouse | Santa Crutz biotechnology sc1663 | 1:2,000 |
| α-mouse IgG, HRP-linked antibody | horse | Cell Signaling Technology #7076 | 1:10,000 |

### 4.7.3 Immunoprecipitation

*U. maydis* cells were incubated in CM medium with 1% glucose to an $OD_{600}$ of 0.5-1.0 and collected by centrifugation at 4,000 rpm for 5 min. The pellet was washed once with 50 ml Tris-HCl (50 mM pH 7.5) followed by centrifugation at 4,000 rpm for 5 min. The pellet was resuspended in 1.5 ml cold lysis buffer (PBS buffer with Roche Complete Protease Inhibitor Cocktail and 1% Triton X-100) and aliqouted to two 2 ml screw cap centrifuge tubes. 100 mg of lysing matrix B (MP Biomedicals) was added followed by lysis in a FastPrep homogenization system (MP Biomedicals) with 4.5 30 s, 5.5 30 s, 5.5 30 s. After centrifugation at 13,000 rpm for 10 min at 4°C, the supernant was transferred to a 1.5 ml eppendorf tube and centrifuged again until the protein lysate was clear.700 µl protein lysate was aliquoted into a spin column with a closed bottom and 70 µl anti-HA affinity matrix (around 0.1 volume of protein lysate) was added and incubated at $4^{o}$C with rotation overnight following by washing 3 times with 500 µl cold lysis buffer, once with salt solution (150 mM NaCl) and centrifugation at 2,000 g for 1min. 70 µl elution solution (0.15 M glycerin-HCl, pH 2.5) was added, incubated in the workbench for 10 min, and centrifuged at 13,000 rpm for 2 min. The pH of elution solution was adjusted to 7.0 with 0.1 volume of 1 M Tris-HCl (pH 9.5). The sample was subjected to SDS-PAGE or LC-MS analysis.

## 4.8 Microscopy

Zeiss Axioplan II microscope with differential interference contrast optics was used for microscopy. The nucleus was stained with DAPI. After fixation with fresh 3.7% (f.c.) formaldehyde solution for 10 min at room temperature with agitation, spun and cells were resuspended in 1 µg/ml DAPI in PBS buffer for 1-5 min. Samples were observed with a standard 4′, 6′-diamidino-2-phenylindole filter set. GFP fluorescence was detected with a specific filter set (band-pass 470/20, beam splitter 493, band-pass 505-530 nm; Zeiss). Fluorescence of mCherry and calcofluor white was observed using TexasRed (HC562/40BP, HC593LP, and HC624/40BP) and 4',6-diamidino-2-

phenylindole (HC375/11BP, HC409BS, and HC447/60BP) filter sets (Semrock). Images were taken with a CoolSNAP-HQ charge-couple device camera (Photometrics). Digital images were processed with MetaMorph software (Universal Imaging).

# 5 References


Abramovitch, R.B., Yang, G. and Kronstad, J.W. (2002) The *ukb1* gene encodes a putative protein kinase required for bud site selection and pathogenicity in *Ustilago maydis*. *Fungal Genet Biol*, **37**, 98-108.

Andrews, D.L., Egan, J.D., Mayorga, M.E. and Gold, S.E. (2000) The *Ustilago maydis ubc4* and *ubc5* genes encode members of a MAP kinase cascade required for filamentous growth. *Mol Plant-Microbe Interact*, **13**, 781-786.

Armache, J.P., Jarasch, A., Anger, A.M., Villa, E., Becker, T., Bhushan, S., Jossinet, F., Habeck, M., Dindar, G., Franckenberg, S., Marquez, V., Mielke, T., Thomm, M., Berninghausen, O., Beatrix, B., Soding, J., Westhof, E., Wilson, D.N. and Beckmann, R. (2010) Cryo-EM structure and rRNA model of a translating eukaryotic 80S ribosome at 5.5-angstrom resolution. *Proc Natl Acad Sci U S A*, **107**, 19748-19753.

Arnold, K., Bordoli, L., Kopp, J. and Schwede, T. (2006) The SWISS-MODEL workspace: a web-based environment for protein structure homology modelling. *Bioinformatics*, **22**, 195-201.

Ausubel, F.M., R. Brent, R.E. Kingston, D.D. Moore, J.G. Seidman, J.A. Smith and Struhl, K. (1987) *Current Protocols in Molecular Biology*. Greene Publishing Associates/Wiley Interscience, New York.

Banuett, F. (1995) Genetics of *Ustilago maydis*, a fungal pathogen that induces tumors in maize. *Annu Rev Genet*, **29**, 179-208.

Banuett, F. and Herskowitz, I. (1989) Different *a* alleles of *Ustilago maydis* are necessary for maintenance of filamentous growth but not for meiosis. *Proc Natl Acad Sci U S A*, **86**, 5878-5882.

Banuett, F. and Herskowitz, I. (1994) Identification of Fuz7, a *Ustilago maydis* MEK/MAPKK homolog required for *a*-locus-dependent and -independent steps in the fungal life cycle. *Genes Dev*, **8**, 1367-1378.

Basse, C.W. and Steinberg, G. (2004) *Ustilago maydis*, model system for analysis of the molecular basis of fungal pathogenicity. *Mol Plant Pathol*, **5**, 83-92.

Baum, S., Bittins, M., Frey, S. and Seedorf, M. (2004) Asc1p, a WD40-domain containing adaptor protein, is required for the interaction of the RNA-binding protein Scp160p with polysomes. *Biochem J*, **380**, 823-830.

Benjamini, Y. and Hochberg, Y. (1995) Controlling the false discovery rate: a practical and powerful approach to multiple testing. *J. R. Stat. Soc. Ser. B Stat. Methodol*, **57**, 289-300.

Berndt, P., Lanver, D. and Kahmann, R. (2010) The AGC Ser/Thr kinase Aga1 is essential for appressorium formation and maintenance of the actin cytoskeleton in the smut fungus *Ustilago maydis*. *Mol Microbiol*, **78**, 1484-1499.

Bolker, M. (2001) *Ustilago maydis* - a valuable model system for the study of fungal dimorphism and virulence. *Microbiology*, **147**, 1395-1401.

Bolker, M., Genin, S., Lehmler, C. and Kahmann, R. (1995) Genetic regulation of mating and dimorphism in *Ustilago maydis*. *Can J Bot*, **73**, S320-S325.

Bolker, M., Urban, M. and Kahmann, R. (1992) The *a* mating type locus of *U. maydis* specifies cell signaling components. *Cell*, **68**, 441-450.

Bottin, A., Kamper, J. and Kahmann, R. (1996) Isolation of a carbon source-regulated gene from *Ustilago maydis*. *Mol Gen Genet*, **253**, 342-352.

Brachmann, A., Konig, J., Julius, C. and Feldbrugge, M. (2004) A reverse genetic approach for generating gene replacement mutants in *Ustilago maydis*. *Mol Genet Genomics*, **272**, 216-226.

Brachmann, A., Schirawski, J., Muller, P. and Kahmann, R. (2003) An unusual MAP kinase is required for efficient penetration of the plant surface by *Ustilago maydis*. *EMBO J*, **22**, 2199-2210.

Brachmann, A., Weinzierl, G., Kamper, J. and Kahmann, R. (2001) Identification of genes in the bW/bE regulatory cascade in *Ustilago maydis*. *Mol Microbiol*, **42**, 1047-1063.

Brefort, T., Doehlemann, G., Mendoza-Mendoza, A., Reissmann, S., Djamei, A. and Kahmann, R. (2009) *Ustilago maydis* as a pathogen. *Annu Rev Phytopathol*, **47**, 423-445.

Brefort, T., Muller, P. and Kahmann, R. (2005) The high-mobility-group domain transcription factor Rop1 is a direct regulator of *prf1* in *Ustilago maydis*. *Eukaryot Cell*, **4**, 379-391.

Burke, D., Dawson, D. and Stearns, T. (2000) *Methods in Yeast Genetics: A Cold Spring Harbor Laboratory Course Manual.* Cold Spring Harbor Laboratory Press, New York.

Ceci, M., Gaviraghi, C., Gorrini, C., Sala, L.A., Offenhauser, N., Marchisio, P.C. and Biffo, S. (2003) Release of eIF6 (p27(BBP)) from the 60S subunit allows 80S ribosome assembly. *Nature*, **426**, 579-584.

Chang, B.Y., Chiang, M.L. and Cartwright, C.A. (2001) The interaction of Src and RACK1 is enhanced by activation of protein kinase C and tyrosine phosphorylation of RACK1. *J Biol Chem*, **276**, 20346-20356.

Chang, B.Y., Conroy, K.B., Machleder, E.M. and Cartwright, C.A. (1998) RACK1, a receptor for activated C kinase and a homolog of the beta subunit of G proteins, inhibits activity of Src tyrosine kinases and growth of NIH 3T3 cells. *Mol Cell Biol*, **18**, 3245-3256.

Chen, D., Toone, W.M., Mata, J., Lyne, R., Burns, G., Kivinen, K., Brazma, A., Jones, N. and Bahler, J. (2003) Global transcriptional responses of fission yeast to environmental stress. *Mol Biol Cell*, **14**, 214-229.

Chen, S.H., Dell, E.J., Lin, F., Sai, J.Q. and Hamm, H.E. (2004) RACK1 regulates specific functions of G beta gamma. *J Biol Chem*, **279**, 17861-17868.

Coyle, S.M., Gilbert, W.V. and Doudna, J.A. (2009) Direct link between RACK1 function and localization at the ribosome in vivo. *Mol Cell Biol*, **29**, 1626-1634.

Croze, E., Usacheva, A., Asarnow, D., Minshall, R.D., Perez, H.D. and Colamonici, O. (2000) Receptor for activated C-kinase (RACK-1), a WD motif-containing protein, specifically associates with the human type IIFN receptor. *J Immunol*, **165**, 5127-5132.

Dell, E.J., Connor, J., Chen, S., Stebbins, E.G., Skiba, N.P., Mochly-Rosen, D. and Hamm, H.E. (2002) The βγ subunit of heterotrimeric G proteins interacts with RACK1 and two other WD repeat proteins. *J Biol Chem*, **277**, 49888-49895.

Di Stasio, M., Brefort, T., Mendoza-Mendoza, A., Munch, K. and Kahmann, R. (2009) The dual specificity phosphatase Rok1 negatively regulates mating and pathogenicity in *Ustilago maydis*. *Mol Microbiol*, **73**, 73-88.

Durrenberger, F., Laidlaw, R.D. and Kronstad, J.W. (2001) The *hgl1* gene is required for dimorphism and teliospore formation in the fungal pathogen *Ustilago maydis*. *Mol Microbiol*, **41**, 337-348.

Durrenberger, F., Wong, K. and Kronstad, J.W. (1998) Identification of a cAMP-dependent protein kinase catalytic subunit required for virulence and morphogenesis in *Ustilago maydis*. *Proc Natl Acad Sci U S A*, **95**, 5684-5689.

Egan, J.D., Garcia-Pedrajas, M.D., Andrews, D.L. and Gold, S.E. (2009) Calcineurin is an antagonist to PKA protein phosphorylation required for postmating

filamentation and virulence, while PP2A is required for viability in *Ustilago maydis*. *Mol Plant-Microbe Interact*, **22**, 1293-1301.

Eichhorn, H., Lessing, F., Winterberg, B., Schirawski, J., Kamper, J., Muller, P. and Kahmann, R. (2006) A ferroxidation/permeation iron uptake system is required for virulence in *Ustilago maydis*. *Plant Cell*, **18**, 3332-3345.

Fedler, M., Luh, K.S., Stelter, K., Nieto-Jacobo, F. and Basse, C.W. (2009) The *a2* mating-type locus genes *lga2* and *rga2* direct uniparental mitochondrial DNA (mtDNA) inheritance and constrain mtDNA recombination during sexual development of *Ustilago maydis*. *Genetics*, **181**, 847-860.

Feldbrugge, M., Kamper, J., Steinberg, G. and Kahmann, R. (2004) Regulation of mating and pathogenic development in *Ustilago maydis*. *Curr Opin Microbiol*, **7**, 666-672.

Fuchs, U., Hause, G., Schuchardt, I. and Steinberg, G. (2006) Endocytosis is essential for pathogenic development in the corn smut fungus *Ustilago maydis*. *Plant Cell*, **18**, 2066-2081.

Garcia-Muse, T., Steinberg, G. and Perez-Martin, J. (2003) Pheromone-induced $G_2$ arrest in the phytopathogenic fungus *Ustilago maydis*. *Eukaryot Cell*, **2**, 494-500.

Garrido, E. and Perez-Martin, J. (2003) The *crk1* gene encodes an Ime2-related protein that is required for morphogenesis in the plant pathogen *Ustilago maydis*. *Mol Microbiol*, **47**, 729-743.

Garrido, E., Voss, U., Muller, P., Castillo-Lluva, S., Kahmann, R. and Perez-Martin, J. (2004) The induction of sexual development and virulence in the smut fungus *Ustilago maydis* depends on Crk1, a novel MAPK protein. *Genes Dev*, **18**, 3117-3130.

Gerbasi, V.R., Weaver, C.M., Hill, S., Friedman, D.B. and Link, A.J. (2004) Yeast Asc1p and mammalian RACK1 are functionally orthologous core 40S ribosomal proteins that repress gene expression. *Mol Cell Biol*, **24**, 8276-8287.

Gillissen, B., Bergemann, J., Sandmann, C., Schroeer, B., Bolker, M. and Kahmann, R. (1992) A two component regulatory system for self non-self recognition in *Ustilago maydis*. *Cell*, **68**, 647-657.

Gold, S., Duncan, G., Barrett, K. and Kronstad, J. (1994) cAMP regulates morphogenesis in the fungal pathogen *Ustilago maydis*. *Genes Dev*, **8**, 2805-2816.

Gold, S.E., Brogdon, S.M., Mayorga, M.E. and Kronstad, J.W. (1997) The *Ustilago maydis* regulatory subunit of a cAMP-dependent protein kinase is required for gall formation in maize. *Plant Cell*, **9**, 1585-1594.

Greilinger, D. (2007) Charakterisierung von frühen Komponenten der Signaltransduktion in *Ustilago maydis*. Ph.D thesis.

Guo, J.J., Wang, S.C., Wang, J.B., Huang, W.D., Liang, J.S. and Chen, J.G. (2009) Dissection of the relationship between RACK1 and heterotrimeric G-proteins in Arabidopsis. *Plant Cell Physiol*, **50**, 1681-1694.

Halic, M., Becker, T., Pool, M.R., Spahn, C.M.T., Grassucci, R.A., Frank, J. and Beckmann, R. (2004) Structure of the signal recognition particle interacting with the elongation-arrested ribosome. *Nature*, **427**, 808-814.

Hanahan, D. (1985) *DNA Cloning: A Practical Approach (Glover, D.M., ed.)*. IRL Press, McLean, Virginia.

Hartmann, H.A., Kahmann, R. and Bolker, M. (1996) The pheromone response factor coordinates filamentous growth and pathogenicity in *Ustilago maydis*. *EMBO J*, **15**, 1632-1641.

Hartmann, H.A., Kruger, J., Lottspeich, F. and Kahmann, R. (1999) Environmental signals controlling sexual development of the corn smut fungus *Ustilago maydis* through the transcriptional regulator Prf1. *Plant Cell*, **11**, 1293-1305.

Heimel, K., Scherer, M., Schuler, D. and Kamper, J. (2010a) The *Ustilago maydis* Clp1 protein orchestrates pheromone and *b*-dependent signaling pathways to coordinate the cell cycle and pathogenic development. *Plant Cell*, **22**, 2908-2922.

Heimel, K., Scherer, M., Vranes, M., Wahl, R., Pothiratana, C., Schuler, D., Vincon, V., Finkernagel, F., Flor-Parra, I. and Kamper, J. (2010b) The transcription factor Rbf1 is the master regulator for *b*-mating type controlled pathogenic development in *Ustilago maydis*. *PLoS Pathog*, **6**, e1001035.

Hermanto, U., Zong, C.S., Li, W.Q. and Wang, L.W. (2002) RACK1, an insulin-like growth factor I (IGF-I) receptor-interacting protein, modulates IGF-I-dependent integrin signaling and promotes cell spreading and contact extracellular matrix. *Mol Cell Biol*, **22**, 2345-2365.

Herzog, F., Primorac, I., Dube, P., Lenart, P., Sander, B., Mechtler, K., Stark, H. and Peters, J.-M. (2009) Structure of the anaphase-promoting complex/cyclosome interacting with a mitoticcheckpoint complex. *Science*, **323**, 1477-1481.

Hoffman, C. and Winston, F. (1987) A ten-minute DNA preparation from yeast efficiently releases autonomous plasmids for transformation of *Escherichia coli*. *Gene*, **57**, 267-272.

Hoffman, C.S. (2007) Propping up our knowledge of G protein signaling pathways: diverse functions of putative noncanonical Gβ subunits in fungi. **2007**, pe3.

Hoffmann, B., Mosch, H.U., Sattlegger, E., Barthelmess, I.B., Hinnebusch, A. and Braus, G.H. (1999) The WD protein Cpc2p is required for repression of Gcn4 protein activity in yeast in the absence of amino-acid starvation. *Mol Microbiol*, **31**, 807-822.

Hoffmann, B., Wanke, C., LaPaglia, S.K. and Braus, G.H. (2000) c-Jun and RACK1 homologues regulate a control point for sexual development in *Aspergillus nidulans*. *Mol Microbiol*, **37**, 28-41.

Holliday, R. (1974) Molecular aspects of genetic exchange and gene conversion. *Genetics*, **78**, 273-287.

Ikebuchi, Y., Takada, T., Ito, K., Yoshikado, T., Anzai, N., Kanai, Y. and Suzuki, H. (2009) Receptor for activated C-kinase 1 regulates the cellular localization and function of ABCB4. *Hepatol Res*, **39**, 1091-1107.

Ikner, A. and Shiozaki, K. (2005) Yeast signaling pathways in the oxidative stress response. *Mutation Research-Fundamental and Molecular Mechanisms of Mutagenesis*, **569**, 13-27.

Isacson, C.K., Lu, Q., Karas, R.H. and Cox, D.H. (2007) RACK1 is a BKCa channel binding protein. *Am J Physiol Cell Physiol*, **292**, C1459-C1466.

Jorgensen, P., Nishikawa, J.L., Breitkreutz, B.-J. and Tyers, M. (2002) Systematic identification of pathways that couple cell growth and division in yeast. *Science*, **297**, 395-400.

Kaffarnik, F., Muller, P., Leibundgut, M., Kahmann, R. and Feldbrugge, M. (2003) PKA and MAPK phosphorylation of Prf1 allows promoter discrimination in *Ustilago maydis*. *EMBO J*, **22**, 5817-5826.

Kahmann, R. and Kamper, J. (2004) *Ustilago maydis*: how its biology relates to pathogenic development. *New Phytol*, **164**, 31-42.

Kamper, J. (2004) A PCR-based system for highly efficient generation of gene replacement mutants in *Ustilago maydis*. *Mol Genet Genomics*, **271**, 103-110.

Kamper, J., Kahmann, R., Bolker, M., Ma, L.J., Brefort, T., Saville, B.J., Banuett, F., Kronstad, J.W., Gold, S.E., Muller, O., Perlin, M.H., Wosten, H.A.B., de Vries, R., Ruiz-Herrera, J., Reynaga-Pena, C.G., Snetselaar, K., McCann, M., Perez-Martin, J., Feldbrugge, M., Basse, C.W., Steinberg, G., Ibeas, J.I., Holloman, W., Guzman, P., Farman, M., Stajich, J.E., Sentandreu, R., Gonzalez-Prieto, J.M., Kennell, J.C., Molina, L., Schirawski, J., Mendoza-Mendoza, A., Greilinger, D., Munch, K., Rossel, N., Scherer, M., Vranes, M., Ladendorf, O., Vincon, V., Fuchs, U., Sandrock, B., Meng, S., Ho, E.C.H., Cahill, M.J., Boyce, K.J., Klose, J., Klosterman, S.J., Deelstra, H.J., Ortiz-Castellanos, L., Li, W.X., Sanchez-Alonso, P., Schreier, P.H., Hauser-Hahn, I., Vaupel, M., Koopmann, E., Friedrich, G., Voss, H., Schluter, T., Margolis, J., Platt, D., Swimmer, C., Gnirke, A., Chen, F., Vysotskaia, V., Mannhaupt, G., Guldener, U., Munsterkotter, M., Haase, D., Oesterheld, M., Mewes, H.W., Mauceli, E.W., DeCaprio, D., Wade, C.M., Butler, J., Young, S., Jaffe, D.B., Calvo, S., Nusbaum, C., Galagan, J. and Birren, B.W. (2006) Insights from the genome of the biotrophic fungal plant pathogen *Ustilago maydis*. *Nature*, **444**, 97-101.

Kamper, J., Reichmann, M., Romeis, T., Bolker, M. and Kahmann, R. (1995) Multiallelic recognition: nonself-dependent dimerization of the bE and bW homeodomain proteins in *Ustilago maydis*. *Cell*, **81**, 73-83.

Khrunyk, Y., Munch, K., Schipper, K., Lupas, A.N. and Kahmann, R. (2010) The use of FLP-mediated recombination for the functional analysis of an effector gene family in the biotrophic smut fungus *Ustilago maydis*. *New Phytol*, **187**, 957-968.

Kiely, P.A., O'Gorman, D., Luong, K., Ron, D. and O'Connor, R. (2006) Insulin-like growth factor I controls a mutually exclusive association of RACK1 with protein phosphatase 2A and beta 1 integrin to promote cell migration. *Mol Cell Biol*, **26**, 4041-4051.

Kim, S.W., Joo, Y.J. and Kim, J. (2010) Asc1p, a ribosomal protein, plays a pivotal role in cellular adhesion and virulence in *Candida albicans*. *Journal of Microbiology*, **48**, 842-848.

Klosterman, S.J., Martinez-Espinoza, A.D., Andrews, D.L., Seay, J.R. and Gold, S.E. (2008) Ubc2, an ortholog of the yeast Ste50p adaptor, possesses a basidiomycete-specific carboxy terminal extension essential for pathogenicity independent of pheromone response. *Mol Plant-Microbe Interact*, **21**, 110-121.

Klosterman, S.J., Perlin, M.H., Garcia-Pedrajas, M., Covert, S.F. and Gold, S.E. (2007) Genetics of morphogenesis and pathogenic development of *Ustilago maydis*. *Fungal Genomics*, **57**, 1-47.

Koehler, J.A. and Moran, M.F. (2001) RACK1, a protein kinase C scaffolding protein, interacts with the PH domain of p120(GAP). *Biochem Biophys Res Commun*, **283**, 888-895.

Kronstad, J.W. and Leong, S.A. (1990) The *b*-mating-type locus of *Ustilago maydis* contains variable and constant regions. *Genes Dev*, **4**, 1384-1395.

Kruger, J., Loubradou, G., Regenfelder, E., Hartmann, A. and Kahmann, R. (1998) Crosstalk between cAMP and pheromone signalling pathways in *Ustilago maydis*. *Mol Gen Genet*, **260**, 193-198.

Kuroha, K., Akamatsu, M., Dimitrova, L., Ito, T., Kato, Y., Shirahige, K. and Inada, T. (2010) Receptor for activated C kinase 1 stimulates nascent polypeptide-dependent translation arrest. *EMBO Rep*, **11**, 956-961.

Laity, C., Giasson, L., Campbell, R. and Kronstad, J. (1995) Heterozygosity at the *b*-mating-type locus attenuates fusion in *Ustilago maydis*. *Curr Genet*, **27**, 451-459.

Lanver, D., Mendoza-Mendoza, A., Brachmann, A. and Kahmann, R. (2010) Sho1 and Msb2-related proteins regulate appressorium development in the smut fungus *Ustilago maydis*. *Plant Cell*, **22**, 2085-2101.

Lesage, G., Shapiro, J., Specht, C.A., Sdicu, A.M., Menard, P., Hussein, S., Tong, A.H.Y., Boone, C. and Bussey, H. (2005) An interactional network of genes involved in chitin synthesis in Saccharomyces cerevisiae. *BMC Genet*, **6**, -.

Letourneux, C., Rocher, G. and Porteu, F. (2006) B56-containing PP2A dephosphorylate ERK and their activity is controlled by the early gene IEX-1 and ERK. *EMBO J*, **25**, 727-738.

Liliental, J. and Chang, D.D. (1998) Rack1, a receptor for activated protein kinase C, interacts with integrin beta subunit. *J Biol Chem*, **273**, 2379-2383.

Link, A.J., Eng, J., Schieltz, D.M., Carmack, E., Mize, G.J., Morris, D.R., Garvik, B.M. and Yates, J.R. (1999) Direct analysis of protein complexes using mass spectrometry. *Nat Biotechnol*, **17**, 676-682.

Liu, Q.H. and Hofmann, P.A. (2003) Modulation of protein phosphatase 2a by adenosine A(1) receptors in cardiomyocytes: role for p38 MAPK. *American Journal of Physiology-Heart and Circulatory Physiology*, **285**, H97-H103.

Liu, X., Nie, X., Ding, Y. and Chen, J. (2010) Asc1, a WD-repeat protein, is required for hyphal development and virulence in *Candida albicans*. *Acta Biochim Biophys Sin*, **42**, 793-800.

Liu, Y.V., Baek, J.H., Zhang, H., Diez, R., Cole, R.N. and Semenza, G.L. (2007) RACK1 competes with HSP90 for binding to HIF-1 alpha and is required for O-2-independent and HSP90 inhibitor-induced degradation of HIF-1 alpha. *Mol Cell*, **25**, 207-217.

Lopez-Bergami, P., Habelhah, H., Bhoumik, A., Zhang, W.Z., Wang, L.H. and Ronai, Z. (2005) Receptor for RACK1 mediates activation of JNK by protein kinase C. *Mol Cell*, **19**, 578-579.

Ludin, K., Hilti, N. and Schweingruber, M. (1995) *Schizosaccharomyces pombe rds1*, an adenine-repressible gene regulated by glucose, ammonium, phosphate, carbon dioxide and temperature. *Molecular and General Genetics MGG*, **248**, 439-445.

Müller, F., Krüger, D., Sattlegger, E., Hoffmann, B., Ballario, P., Kanaan, M. and Barthelmess, I. (1995) The cpc-2 gene of *Neurospora crassa* encodes a protein entirely composed of WD-repeat segments that is involved in general amino acid control and female fertility. *Molecular and General Genetics MGG*, **248**, 162-173.

Mamidipudi, V. and Cartwright, C. (2006) Rack1 induces apoptosis of human colon cells by suppressing SRC tyrosine kinase activity in the intrinsic and Akt pathways. *Gastroenterology*, **130**, A131-A131.

Martinez-Espinoza, A.D., Garcia-Pedrajas, M.D. and Gold, S.E. (2002) The Ustilaginales as plant pests and model systems. *Fungal Genet Biol*, **35**, 1-20.

Matyskiela, M.E. and Morgan, D.O. (2009) Analysis of activator-binding sites on the APC/C supports a cooperative substrate-binding mechanism. *Mol Cell*, **34**, 68-80.

Mayorga, M.E. and Gold, S.E. (1999) A MAP kinase encoded by the *ubc3* gene of *Ustilago maydis* is required for filamentous growth and full virulence. *Mol Microbiol*, **34**, 485-497.

Mayorga, M.E. and Gold, S.E. (2001) The *ubc2* gene of *Ustilago maydis* encodes a putative novel adaptor protein required for filamentous growth, pheromone response and virulence. *Mol Microbiol*, **41**, 1365-1379.

McCahill, A., Warwicker, J., Bolger, G.B., Houslay, M.D. and Yarwood, S.J. (2002) The RACK1 scaffold protein: A dynamic cog in cell response mechanisms. *Mol Pharmacol*, **62**, 1261-1273.

McLeod, M., Shor, B., Caporaso, A., Wang, W., Chen, H. and Hu, L. (2000) Cpc2, a fission yeast homologue of mammalian RACK1 protein, interacts with Ran1 (Pat1) kinase to regulate cell cycle progression and meiotic development. *Mol Cell Biol*, **20**, 4016-4027.

Mendoza-Mendoza, A., Berndt, P., Djamei, A., Weise, C., Linne, U., Marahiel, M., Vranes, M., Kamper, J. and Kahmann, R. (2009a) Physical-chemical plant-derived signals induce differentiation in *Ustilago maydis*. *Mol Microbiol*, **71**, 895-911.

Mendoza-Mendoza, A., Eskova, A., Weise, C., Czajkowski, R. and Kahmann, R. (2009b) Hap2 regulates the pheromone response transcription factor *prf1* in *Ustilago maydis*. *Mol Microbiol*, **72**, 683-698.

Molina, L. and Kahmann, R. (2007) An *Ustilago maydis* gene involved in $H_2O_2$ detoxification is required for virulence. *Plant Cell*, **19**, 2293-2309.

Muller, P., Aichinger, C., Feldbrugge, M. and Kahmann, R. (1999) The MAP kinase Kpp2 regulates mating and pathogenic development in *Ustilago maydis*. *Mol Microbiol*, **34**, 1007-1017.

Muller, P., Katzenberger, J.D., Loubradou, G. and Kahmann, R. (2003a) Guanyl nucleotide exchange factor Sql2 and Ras2 regulate filamentous growth in *Ustilago maydis*. *Eukaryot Cell*, **2**, 609-617.

Muller, P., Leibbrandt, A., Teunissen, H., Cubasch, S., Aichinger, C. and Kahmann, R. (2004) The G β-subunit-encoding gene *bpp1* controls cyclic-AMP signaling in *Ustilago maydis*. *Eukaryot Cell*, **3**, 806-814.

Muller, P., Weinzierl, G., Brachmann, A., Feldbrugge, M. and Kahmann, R. (2003b) Mating and pathogenic development of the smut fungus *Ustilago maydis* are regulated by one mitogen-activated protein kinase cascade. *Eukaryot Cell*, **2**, 1187-1199.

Nilsson, J., Sengupta, J., Frank, J. and Nissen, P. (2004) Regulation of eukaryotic translation by the RACK1 protein: a platform for signalling molecules on the ribosome. *EMBO Rep*, **5**, 1137-1141.

Nunez, A., Franco, A., Madrid, M., Soto, T., Vicente, J., Gacto, M. and Cansado, J. (2009) Role for RACK1 orthologue Cpc2 in the modulation of stress response in fission yeast. *Mol Biol Cell*, **20**, 3996-4009.

Okano, K., Schnaper, H.W., Bomsztyk, K. and Hayashida, T. (2006) RACK1 binds to Smad3 to modulate transforming growth factor-beta 1-stimulated alpha 2(I) collagen transcription in renal tubular epithelial cells. *J Biol Chem*, **281**, 26196-26204.

Onishi, I., Lin, P.J.C., Diering, G.H., Williams, W.P. and Numata, M. (2007) RACK1 associates with NHE5 in focal adhesions and positively regulates the transporter activity. *Cell Signal*, **19**, 194-203.

Palmer, D.A., Thompson, J.K., Li, L., Prat, A. and Wang, P. (2006) Gib2, a novel Gβ-like/RACK1 homolog, functions as a Gβ subunit in cAMP signaling and is essential in *Cryptococcus neoformans*. *J Biol Chem*, **281**, 32596-32605.

Pass, J.M., Gao, J.M., Jones, W.K., Wead, W.B., Wu, X., Zhang, J., Baines, C.P., Bolli, R., Zheng, Y.T., Joshua, I.G. and Ping, P.P. (2001) Enhanced PKC beta II

translocation and PKC beta II-RACK1 interactions in PKC epsilon-induced heart failure: a role for RACK1. *Am J Physiol Heart Circ Physiol*, **281**, H2500-H2510.

Patterson, R.L., van Rossum, D.B., Barrow, R.K. and Snyder, S.H. (2004) RACK1 binds to inositol 1,4,5-trisphosphate receptors and mediates $Ca^{2+}$ release. *Proceedings of the National Academy of Sciences of the United States of America*, **101**, 2328-2332.

Paul, S.K., Oowatari, Y. and Kawamukai, M. (2009) A large complex mediated by Moc1, Moc2 and Cpc2 regulates sexual differentiation in fission yeast. *FEBS J*, **276**, 5076-5093.

Perez-Martin, J., Castillo-Lluva, S., Sgarlata, C., Flor-Parra, I., Mielnichuk, N., Torreblanca, J. and Carbo, N. (2006) Pathocycles: *Ustilago maydis* as a model to study the relationships between cell cycle and virulence in pathogenic fungi. *Mol Genet Genomics*, **276**, 211-229.

Regenfelder, E., Spellig, T., Hartmann, A., Lauenstein, S., Bolker, M. and Kahmann, R. (1997) G proteins in *Ustilago maydis*: Transmission of multiple signals? *EMBO J*, **16**, 1934-1942.

Regmi, S., Rothberg, K.G., Hubbard, J.G. and Ruben, L. (2008) The RACK1 signal anchor protein from *Trypanosoma brucei* associates with eukaryotic elongation factor 1A: a role for translational control in cytokinesis. *Mol Microbiol*, **70**, 724-745.

Reiner, C.L., McCullar, J.S., Kow, R.L., Le, J.H., Goodlett, D.R. and Nathanson, N.M. (2010) RACK1 Associates with Muscarinic Receptors and Regulates M-2 Receptor Trafficking. *PLoS ONE*, **5**, e13517.

Rigas, A.C., Ozanne, D.M., Neal, D.E. and Robson, C.N. (2003) The scaffolding protein RACK1 interacts with androgen receptor and promotes cross-talk through a protein kinase C signaling pathway. *J Biol Chem*, **278**, 46087-46093.

Rodriguez, M.M., Ron, D., Touhara, K., Chen, C.H. and Mochly-Rosen, D. (1999) RACK1, a protein kinase C anchoring protein, coordinates the binding of activated protein kinase C and select pleckstrin homology domains in vitro. *Biochemistry*, **38**, 13787-13794.

Ron, D., Chen, C.H., Caldwell, J., Jamieson, L., Orr, E. and Mochlyrosen, D. (1994) Cloning of an intracellular receptor for protein kinase C: A homolog of the β subunit of G proteins. *Proc Natl Acad Sci U S A*, **91**, 839-843.

Ron, D., Jiang, Z., Yao, L.N., Vagts, A., Diamond, I. and Gordon, A. (1999) Coordinated movement of RACK1 with activated beta IIPKC. *J Biol Chem*, **274**, 27039-27046.

Rosdahl, J.A., Mourton, T.L. and Brady-Kalnay, S.M. (2002) Protein kinase C delta (PKC delta) is required for protein tyrosine phosphatase mu (PTP mu)-dependent neurite outgrowth. *Mol Cell Neurosci*, **19**, 292-306.

Rothberg, K.G., Burdette, D.L., Pfannstiel, J., Jetton, N., Singh, R. and Ruben, L. (2006) The RACK1 homologue from *Trypanosoma brucei* is required for the onset and progression of cytokinesis. *J Biol Chem*, **281**, 9781-9790.

Ruepp, A., Zollner, A., Maier, D., Albermann, K., Hani, J., Mokrejs, M., Tetko, I., Guldener, U., Mannhaupt, G., Munsterkotter, M. and Mewes, H.W. (2004) The FunCat, a functional annotation scheme for systematic classification of proteins from whole genomes. *Nucleic Acids Res*, **32**, 5539-5545.

Sambrook, J., Fritsch, E.F. and Maniatis., T. (1989) *Molecular cloning: a laboratory manual*. Cold Spring Harbor Laboratory Press, New York, USA.

Scherer, M., Heimel, K., Starke, V. and Kamper, J. (2006) The Clp1 protein is required for clamp formation and pathogenic development of *Ustilago maydis*. *Plant Cell*, **18**, 2388-2401.

Schulz, B., Banuett, F., Dahl, M., Schlesinger, R., Schafer, W., Martin, T., Herskowitz, I. and Kahmann, R. (1990) The *b*-alleles of *U. maydis*, whose combinations program pathogenic development, code for polypeptides containing a homeodomain-related motif. *Cell*, **60**, 295-306.

Sengupta, J., Nilsson, J., Gursky, R., Spahn, C.M.T., Nissen, P. and Frank, J. (2004) Identification of the versatile scaffold protein RACK1 on the eukaryotic ribosome by cryo-EM. *Nat Struct Mol Biol*, **11**, 957-962.

Shor, B., Calaycay, J., Rushbrook, J. and McLeod, M. (2003) Cpc2/RACK1 is a ribosome-associated protein that promotes efficient translation in *Schizosaccharomyces pombe*. *J Biol Chem*, **278**, 49119-49128.

Silverstein, A.M., Barrow, C.A., Davis, A.J. and Mumby, M.C. (2002) Actions of PP2A on the MAP kinase pathway and apoptosis are mediated by distinct regulatory subunits. *Proc Natl Acad Sci U S A*, **99**, 4221-4226.

Spellig, T., Bolker, M., Lottspeich, F., Frank, R.W. and Kahmann, R. (1994) Pheromones trigger filamentous growth in *Ustilago maydis*. *EMBO J*, **13**, 1620-1627.

Spellig, T., Bottin, A. and Kahmann, R. (1996) Green fluorescent protein (GFP) as a new vital marker in the phytopathogenic fungus *Ustilago maydis*. *Mol Gen Genet*, **252**, 503-509.

Steele, M.R., McCahill, A., Thompson, D.S., MacKenzie, C., Isaacs, N.W., Houslay, M.D. and Bolger, G.B. (2001) Identification of a surface on the beta-propeller protein RACK1 that interacts with the cAMP-specific phosphodiesterase PDE4D5. *Cell Signal*, **13**, 507-513.

Steinberg, G. and Perez-Martin, J. (2008) *Ustilago maydis*, a new fungal model system for cell biology. *Trends Cell Biol*, **18**, 61-67.

Tsukuda, T., Carleton, S., Fotheringham, S. and Holloman, W.K. (1988) Isolation and characterization of an autonomously replicating sequence from *Ustilago maydis*. *Mol Cell Biol*, **8**, 3703-3709.

Ullah, H., Scappini, E.L., Moon, A.F., Williams, L.V., Armstrong, D.L. and Pedersen, L.C. (2008) Structure of a signal transduction regulator, RACK1, from Arabidopsis thaliana. *Protein Sci*, **17**, 1771-1780.

Urban, M., Kahmann, R. and Bolker, M. (1996) Identification of the pheromone response element in *Ustilago maydis*. *Mol Gen Genet*, **251**, 31-37.

Usacheva, A., Tian, X.Y., Sandoval, R., Salvi, D., Levy, D. and Colamonici, O.R. (2003) The WD motif-containing protein RACK-1 functions as a scaffold protein within the type IIFN receptor-signalling complex. *J Immunol*, **171**, 2989-2994.

Vomastek, T., Iwanicki, M.P., Schaeffer, H.J., Tarcsafalvi, A., Parsons, J.T. and Weber, M.J. (2007) RACK1 targets the extracellular signal-regulated kinase/mitogen-activated protein kinase pathway to link integrin engagement with focal adhesion disassembly and cell motility. *Mol Cell Biol*, **27**, 8296-8305.

Wahl, R., Zahiri, A. and Kamper, J. (2010) The *Ustilago maydis b* mating type locus controls hyphal proliferation and expression of secreted virulence factors in planta. *Mol Microbiol*, **75**, 208-220.

Weinzierl, G., Leveleki, L., Hassel, A., Kost, G., Wanner, G. and Bolker, M. (2002) Regulation of cell separation in the dimorphic fungus *Ustilago maydis*. *Mol Microbiol*, **45**, 219-231.

Xu, Y.Z., Wang, N.F., Ling, F., Li, P.Z. and Gao, Y. (2009) Receptor for activated C-kinase 1, a novel binding partner of adiponectin receptor 1. *Biochem Biophys Res Commun*, **378**, 95-98.

Yaka, R., Thornton, C., Vagts, A.J., Phamluong, K., Bonci, A. and Ron, D. (2002) NMDA receptor function is regulated by the inhibitory scaffolding protein, RACK1. *Proc Natl Acad Sci U S A*, **99**, 5710-5715.

Yarwood, S.J., Steele, M.R., Scotland, G., Houslay, M.D. and Bolger, G.B. (1999) The RACK1 signaling scaffold protein selectively interacts with the cAMP-specific phosphodiesterase PDE4D5 isoform. *J Biol Chem*, **274**, 14909-14917.

Zahiri, A., Heimel, K., Wahl, R., Rath, M. and Kamper, J. (2010) The *Ustilago maydis* forkhead transcription factor Fox1 is involved in the regulation of genes required for the attenuation of plant defenses during pathogenic development. *Mol Plant-Microbe Interact*, **23**, 1118-1129.

Zarnack, K., Eichhorn, H., Kahmann, R. and Feldbrugge, M. (2008) Pheromone-regulated target genes respond differentially to MAPK phosphorylation of transcription factor Prf1. *Mol Microbiol*, **69**, 1041-1053.

Zeller, C.E., Parnell, S.C. and Dohlman, H.G. (2007) The RACK1 ortholog Asc1 functions as a G-protein β subunit coupled to glucose responsiveness in yeast. *J Biol Chem*, **282**, 25168-25176.

Zhang, W.Z., Cheng, G.Z., Gong, J.L., Hermanto, U., Zong, C.S., Chan, J., Cheng, J.Q. and Wang, L.H. (2008) RACK1 and CIS mediate the degradation of BimEL in cancer cells. *J Biol Chem*, **283**, 16416-16426.

Zhang, W.Z., Zong, C.S., Hermanto, U., Lopez-Bergami, P., Ronai, Z. and Wang, L.H. (2006) RACK1 recruits STAT3 specifically to insulin and insulin-like growth factor 1 receptors for activation, which is important for regulating anchorage-independent growth. *Mol Cell Biol*, **26**, 413-424.

# 6 Supplementary data

Data CD: The data CD contains the following two files:

Supplementary Table 1 Functional enrichment of genes up-regulated in FB1Δrak1.

Supplementary Table 2 Functional enrichment of genes down-regulated in FB1Δrak1.

# 7 Acknowledgement

My most sincere thanks go to my supervisor Prof. Dr. Regine Kahmann. I thank her for giving me the opportunity to study in her lab. I thank her for her suggestions, support and encouragement during the development of my PhD project, which will lay the solid foundation for my future career in scientific research. I am very grateful to the members of my PhD thesis committee Prof. Dr. Michael Bölker, Prof. Dr. MD. Lotte Sogaard-Andersen and Prof. Dr. Hans-Ulrich Mösch for their insight and guidance.

I want to express sincere gratitude to Dr. Patrick Berndt for helping me to perform DNA microarray and data analysis as well as to translate the German summary. I thank Daniel Lanver for generously providing the Sho1-Flag strain and mCherry-harboring plasmid and his kind help. I appreciate the help from Dr. Artemio Mendoza-Mendoza, Dr. Maurizio Di Stasio and Dr Thomas Brefort for inspiring discussions and valulabe suggestions. I also would like to thank the suggestions from Dr. Armin Djamei, Dr. Stefanie Reißmann about immunoprecipitation as well as Jörg Kahnt for LC-MS analysis. I also want to thank Karin Münch, Nicole Rössel and Ria Faber for their great technical support. I am obliged to all of colleagues in the Department of Organismic Interactions, especially the people in our lab including the former colleagues, who gave me much assistance and enjoyable time during my study here.

It is a pleasure to convey many thanks to the EU consortium Signalpath and MPI für terrestrische Mikrobiologie for providing financial supporting and Prof. Dr. Dohlman HG. (University of North Carolina, USA) for generously providing yeast *asc1* deletion strains. I am grateful to Ms. Susanne Rommel and Mr. Christian Bengelsdorff for taking care of the documents for my daily life and Rolf Rösser for the computational support.

I would like to express my gratitude to my wife Xiaojuan Xia, who is my truly best partner for both my scientific and personal life.

Finally, I feel indebted to my parents and parents-in-law for their understanding everlasting encouragement and love as well as all of my friends for their moral supports.

# 8 Curriculum Vitae

**Personal information**

Name Lei Wang

Date of birth Oct. 1982

Place of birth Shandong, China

**Education**

09/2000-06/2004 Bachelor of Science

Shandong Normal University, Jinan, China

09/2004-06/2007 Master of Science

Institute of Botany, Chinese Academy of Sciences, Beijing, China.

Thesis Title: The preliminary study of the influence of near null magnetic field on the growth and development of *Arabidopsis thaliana* and functional analysis of ferric reductase gene *MmFre* of *Magnetospirillum magneticum*

10/2007-02/2011 PhD (Dr. rer. nat.)

Philipps-Universität Marburg

Max-Planck-Institute for Terrestrial Microbiology, Germany

PhD thesis: Functional characterization of a seven-WD40 repeat protein Rak1 in *Ustilago maydis*